

# POLITECNICO DI TORINO

Collegio di Ingegneria Chimica e dei Materiali

**Master of Science Course  
in Materials Engineering**

Master of Science Thesis

## **Polymeric hydrogels containing polyphenols for wastewater treatment**



### **Tutors**

*Signature of the Tutors*

Marco Sangermano, Maria Silvia Spriano

.....

.....

**Candidate**

.....

Vincenzo Metrangolo

March 2022



## Sommario

RIASSUNTO .....	5
1 – POLYMERIC HYDROGELS.....	16
1.1 – INTRODUCTION.....	16
1.2 – PHYSICAL HYDROGELS .....	18
1.2 – CHEMICAL HYDROGELS.....	19
1.3 – PHOTOCURABLE HYDROGELS .....	20
2 – EXPLOITATION OF POLYMERIC HYDROGELS IN WASTEWATER TREATMENT.....	21
2.1 – AN INTRODUCTION.....	21
2.2 – USE OF CHITOSAN HYDROGELS FOR THE REMOVAL OF HEAVY METAL IONS IN WASTEWATER TREATMENT .....	23
2.2.1 – REMOVAL OF MERCURY .....	25
2.2.2 – CHEMICAL MODIFICATION OF CHITOSAN FOR THE REMOVAL OF MERCURY .....	27
2.2.3 – REMOVAL OF ARSENIC.....	30
2.2.4 – REMOVAL OF LEAD – INFLUENCE OF PH .....	33
2.2.5 – REMOVAL OF CHROMIUM – XPS ANALYSIS.....	35
2.2.6 – COPPER REMOVAL – SORPTION KINETICS AND EQUILIBRIA .....	37
3 – EXPLOITATION OF POLYPHENOLS IN HEAVY METAL IONS’ COMPLEXATION .....	41
3.1 – AN INTRODUCTION.....	41
3.2 – PRECIPITATION OF COPPER(II) IONS BY PLANT POLYPHENOLS.....	42
3.3 – COMPLEXATION OF GALLIC ACID BY FE(II) .....	46
3.4 – ALUMINUM-POLYPHENOL COMPLEXES .....	48
4 – MATERIALS AND METHODS.....	51
4.1 – MATERIALS.....	51
4.2 – METHACRYLATION OF CHITOSAN.....	51
4.3 – HYDROGEL PREPARATION AND FUNCTIONALIZATION WITH TANNIC ACID.....	53
4.4 – CHARACTERIZATION .....	55
Swelling Test.....	55
FTIR – Fourier transform Infrared Spectroscopy.....	55
TGA – Thermogravimetric analysis.....	56
DSC – Differential Scanning Calorimetry .....	57
UV-Vis Spectroscopy.....	58
EDS-SEM (Energy Dispersive spectroscopy – Scanning electron microscopy) .....	59
5 – RESULTS AND DISCUSSION .....	60
5.1 – FUNCTIONALIZATION OF CHITOSAN .....	60
5.2 – PREPARATION AND CHARACTERIZATION OF CHITOSAN HYDROGELS .....	63

Methacrylation process.....	63
FTIR – Fourier transform Infrared Spectroscopy.....	64
TGA – Thermogravimetric analysis.....	66
DSC – Differential Scanning Calorimetry.....	67
UV-Vis Spectroscopy.....	68
EDS-SEM (Energy Dispersive spectroscopy – Scanning electron microscopy).....	69
5.3 – STUDY ON COPPER REMOVAL.....	71
Kinetic study.....	71
Isothermal study.....	72
6 – CONCLUSIONS.....	76
7 – BIBLIOGRAPHY.....	83
8 – RINGRAZIAMENTI.....	88

## RIASSUNTO

Il lavoro svolto nell'ambito di questa Tesi ha come obiettivo la sintesi di un hydrogel di Chitosano, bio-based e fotoreticolabile alla luce UV, la sua funzionalizzazione con un polifenolo (nel caso in esame, si è usato Acido Tannico), la caratterizzazione del materiale e la valutazione della sua capacità nel catturare ioni metallici da una soluzione di acqua contaminata, in particolare una soluzione di ioni rameici Cu(II) ottenuti sciogliendo in acqua bi-distillata del solfato rameico anidro CuSO<sub>4</sub>.

Gli hydrogel polimerici sono da qualche tempo impiegati nella depurazione di acque (e anche dei terreni) dai metalli pesanti, e il Chitosano (*Figura 6*) è tra i più famosi: è stato impiegato nella rimozione di ioni metallici quali ioni di Cromo, Mercurio, Arsenico, Piombo, Rame e altri ancora. L'efficacia del Chitosano nel catturare gli ioni metallici (tipicamente cationi) risiede nella natura dei suoi gruppi funzionali: gruppi ossidrilici (-OH) e gruppi amminici (-NH<sub>2</sub>), che a seconda del pH della soluzione possono protonarsi o deprotonarsi, e favorire dunque la cattura di specie cariche, come appunto gli ioni.

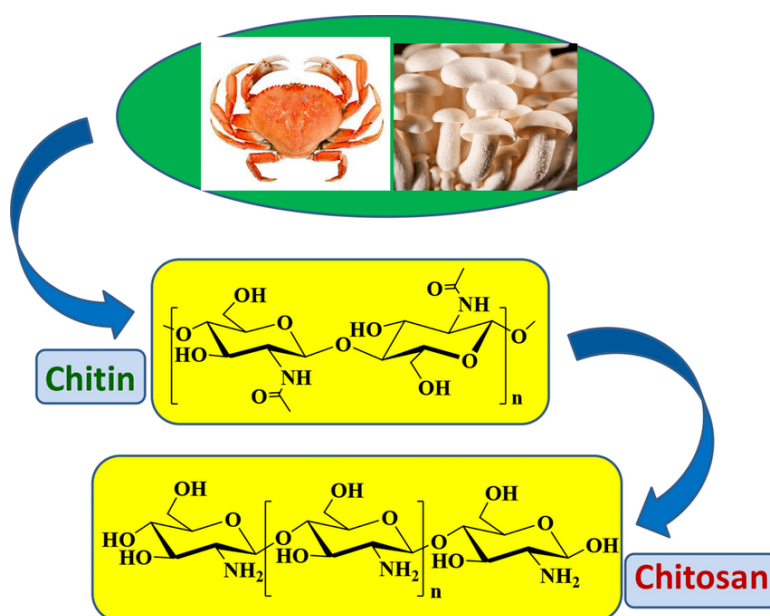


*Figura 6*

Nell'ambito della depurazione di acque e suoli, non meno famosi e utilizzati sono i polifenoli, complesse molecole organiche derivanti, per la maggior parte, da piante e vegetali in genere. Tra i più utilizzati si possono sicuramente citare l'acido tannico, l'acido gallico e il penta-galloil-glucosio (*Figura 32*). Come il chitosano, anche queste macromolecole sono dotate di gruppi funzionali quali gruppi ossidrilici e gruppi amminici, che si protonano o deprotonano a seconda del pH, e quindi possono legarsi con determinate specie ioniche; in aggiunta, i cationi metallici vengono tipicamente catturati da queste sostanze grazie alla presenza di "code" cariche negativamente, capaci di legarsi a cationi metallici in modi differenti: tipicamente, due terminazioni negative generano un legame pontato con un catione bivalente (*Figura 28*).

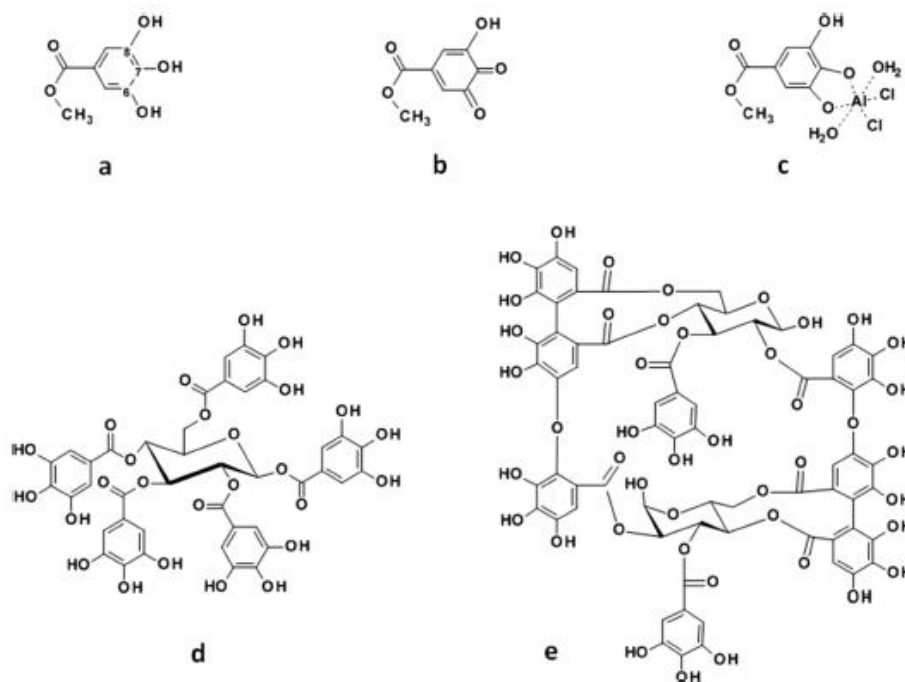


Figura 32

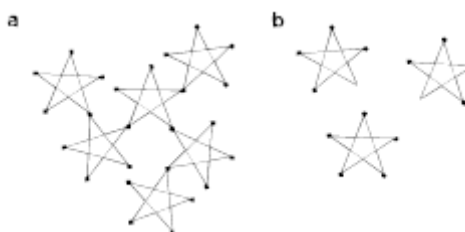
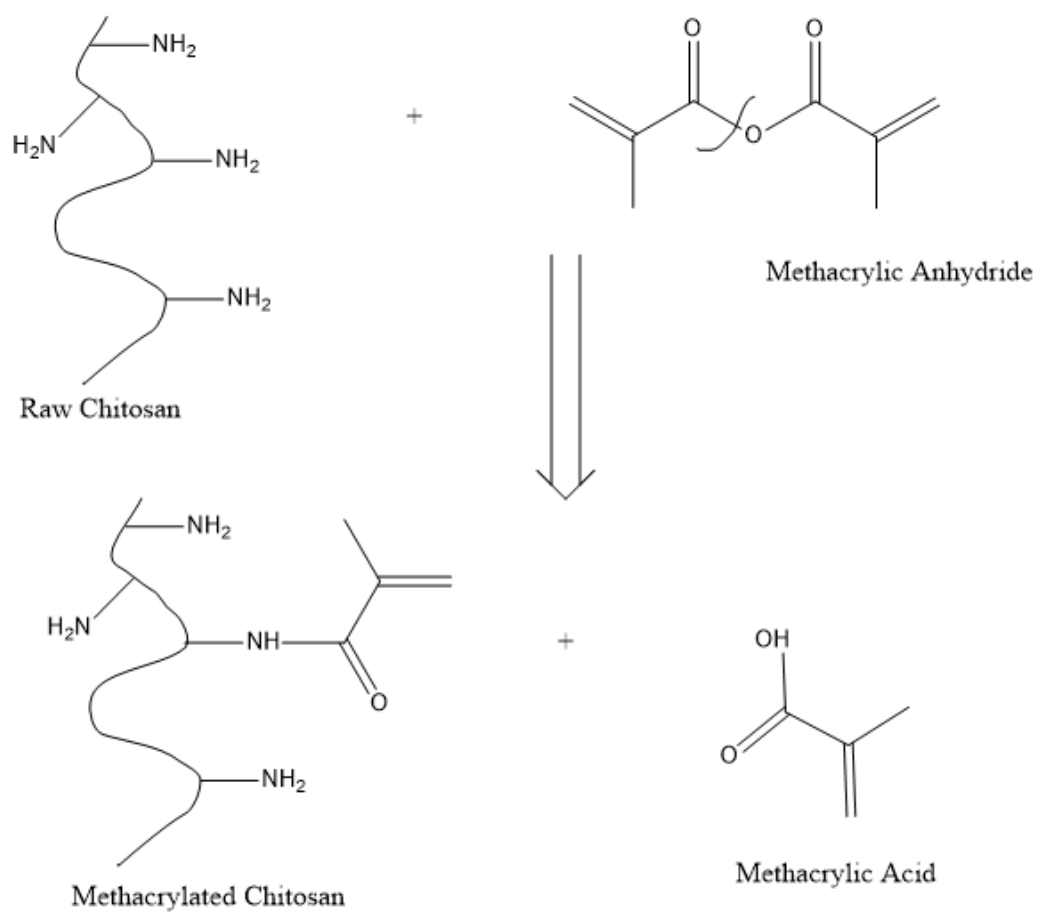


Figura 28

Nell'attività di Tesi Magistrale si è partiti dalla Metacrilazione del chitosano: il chitosano grezzo è stato solubilizzato in acqua acida (una soluzione di acqua distillata e acido acetico) con Anidride Metacrilica: i prodotti di reazione sono Chitosano Metacrilato e Acido Metacrilico (Figura 50). Il Chitosano Metacrilato così ottenuto, in forma di liquido dall'aspetto lattiginoso, è stato depurato in sottili membrane di cellulosa immerse in acqua distillata per circa sette giorni: il chitosano coagula e, grazie ad un processo osmotico, perde la frazione acida residua. Dopo purificazione, il chitosano è stato liofilizzato, e questo è l'ultimo step necessario alla sintesi dell'hydrogel (Figura 36).



*Figura 50*



*Figura 36*

Il chitosano liofilizzato è stato solubilizzato in acqua acida (una soluzione di acqua distillata al 2% in peso di acido acetico), a cui poi si è aggiunto il fotoiniziatore (Irgacure 2959) per permettere la reticolazione. Questa soluzione è stata versata in piccoli stampi cilindrici, prelevandola tramite una pipetta Pasteur, e reticolata tramite una lampada a luce UV. Un corretto processo di reticolazione si è ottenuto irraggiando ogni campione per 6 minuti e imponendo una distanza di 4 cm tra campione e sorgente luminosa: questa distanza corrisponde ad una potenza di  $114 \text{ mW/cm}^2$ . Gli hydrogel così ottenuti (*Figura 38*) sono stati immersi in acqua distillata al fine di perdere la frazione acida residua (la miglior purificazione si ottiene per un tempo in bagno di circa due giorni, cambiando l'acqua dalle due alle tre volte al giorno). Dopo la purificazione, gli hydrogel sono posti a seccare in aria (sotto cappa) a temperatura ambiente.



*Figura 38*

All'essiccazione degli hydrogel è seguita a funzionalizzazione con acido tannico. Alcuni hydrogel sono stati immersi in piccole multiwell in una soluzione di acqua e acido tannico, in concentrazione pari a  $15 \text{ mg/mL}$ . Queste multiwell sono state poste in forno ad una temperatura di  $37 \text{ }^\circ\text{C}$  per un tempo di 3 ore. terminate le 3 ore, i campioni (che hanno rigonfiato durante la permanenza in soluzione) sono stati nuovamente posti a seccare in aria e a temperatura ambiente.

Prima di procedere allo studio del processo di cattura degli ioni  $\text{Cu(II)}$ , i campioni sono stati caratterizzati. Tramite l'analisi FTIR, si sono confrontati dapprima il chitosano grezzo e il chitosano metacrilato: la presenza di doppi legami  $\text{C=O}$  e  $\text{C=C}$  nel chitosano metacrilato ha rivelato il successo del processo di metacrilazione. Successivamente, si sono confrontati gli spettri di acido tannico e chitosano funzionalizzato con acido tannico: in questo caso, la parziale sovrapposibilità degli spettri e la presenza (nel chitosano) di gruppi funzionali riconducibili alla struttura chimica dell'acido tannico, hanno rivelato il successo nella funzionalizzazione degli hydrogel. La riuscita del processo, empiricamente, è stata testimoniata dal cambio nella colorazione dei campioni dopo la funzionalizzazione: dal tipico giallo chiaro ad un colore arancio/bruno, tipico dell'acido tannico (*Figura 40*).

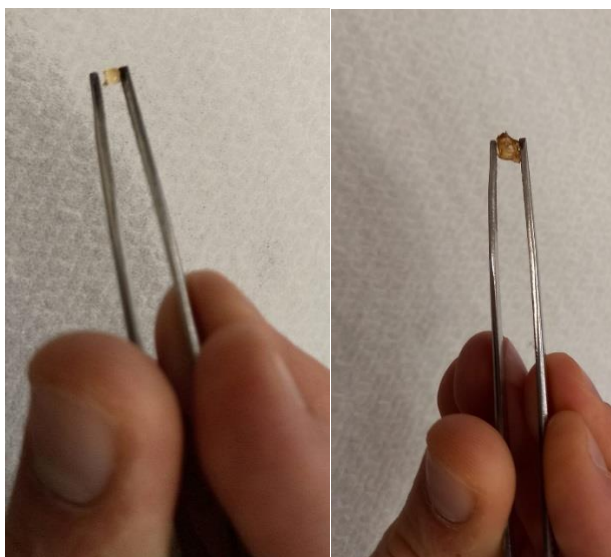


*Figura 40*

L'analisi TGA sui campioni essiccati ha rivelato una buona corrispondenza con risultati ottenuti da altri ricercatori: la curva, per entrambi i campioni (chitosano originale e chitosano funzionalizzato), rivela una degradazione termica "one-step" vicino ai 200 °C, e la differenza nel residuo dei due campioni (maggiore per il campione funzionalizzato) è riconducibile alla presenza di acido tannico (*Figura 66*). L'analisi DSC ha rivelato due flessi principali: il primo, intorno ai 73 °C, può essere riconducibile (secondo altri autori) ad una degradazione del chitosano, mentre il secondo flesso intorno ai 110 °C può essere riconducibile alla  $T_g$ .

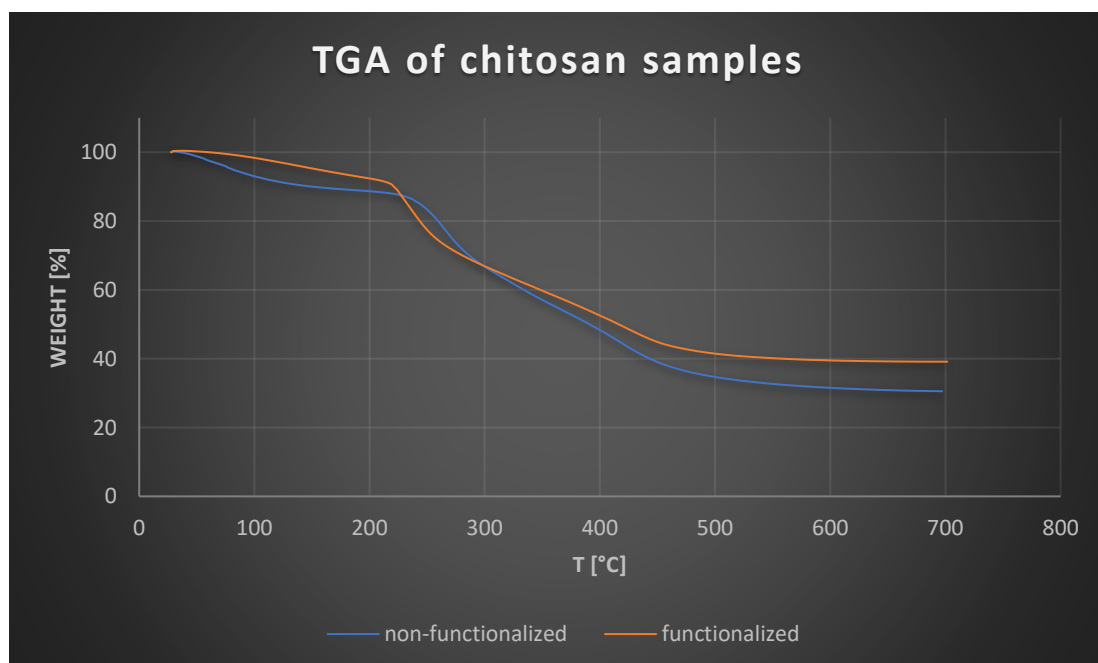


*Figura 66*

Dopo questa prima caratterizzazione, si è proceduto con lo studio nella rimozione degli ioni Cu(II) da soluzione. Una soluzione di ioni Cu(II) è stata ottenuta sciogliendo solfato rameico ( $\text{CuSO}_4$ ) in acqua ultrapura (milliQ): la scelta dell'acqua ultrapura (bi-distillata), anziché l'acqua distillata, risiede

nella necessità di evitare la presenza di qualsivoglia specie ionica che possa in qualche modo alterare la misura della Concentrazione di ioni rameici. Si è inoltre scelto di utilizzare un rapporto fisso “peso hydrogel : volume di soluzione” pari a 7 mg per 10 mL: non potendo controllare il peso degli hydrogel essiccati (compreso tuttavia tra 5 mg e 10 mg), per ogni hydrogel è stato calcolato il volume di soluzione opportuno a mantenere il rapporto 7:10.

E’ stata dapprima effettuata una prova *Cinetica*: un hydrogel viene immerso in una soluzione a concentrazione iniziale nota di ioni Cu(II), pari a 10 mg/L (ovvero 10 ppm), e si valuta l’evoluzione nella concentrazione di ioni in soluzione nel tempo (effettuando la misura della concentrazione ad intervalli stabiliti). Tale prova è stata effettuata sia su hydrogel di chitosano tal quali che su campioni di chitosano funzionalizzati con acido tannico, a temperatura ambiente e mantenendo il pH della soluzione tra 6 e 8 per rispettare le istruzioni indicate nell’utilizzo dello Spettrofotometro per Rame, strumento utilizzato per la misura della concentrazione di ioni Rame in soluzione. I risultati sono visibili nelle *Figure 59 e 60*.

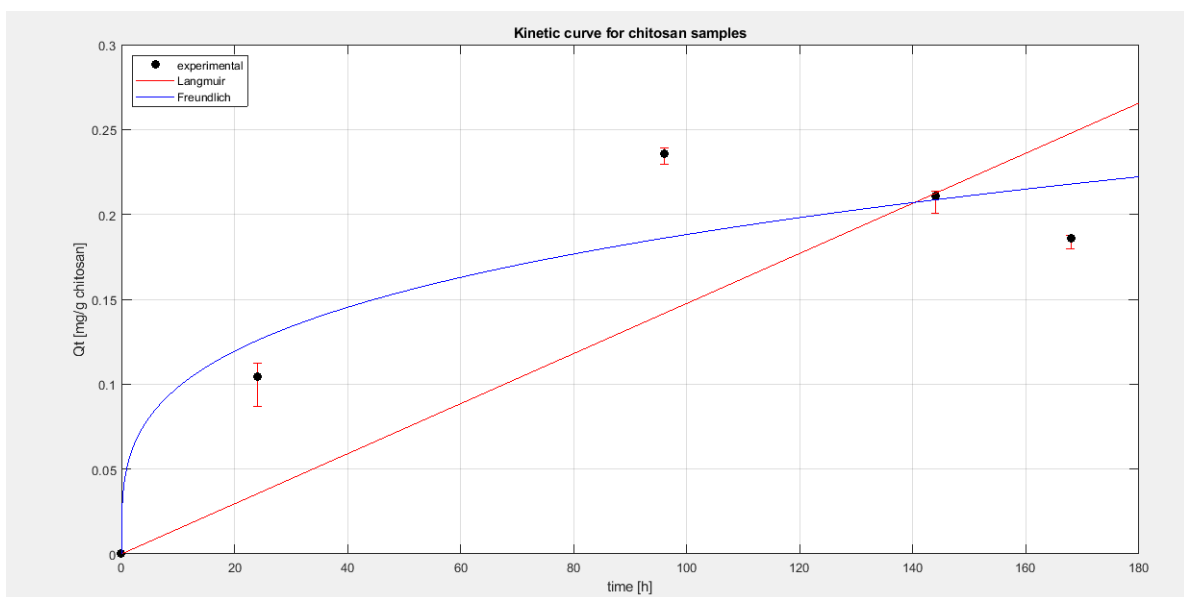


Figura 59

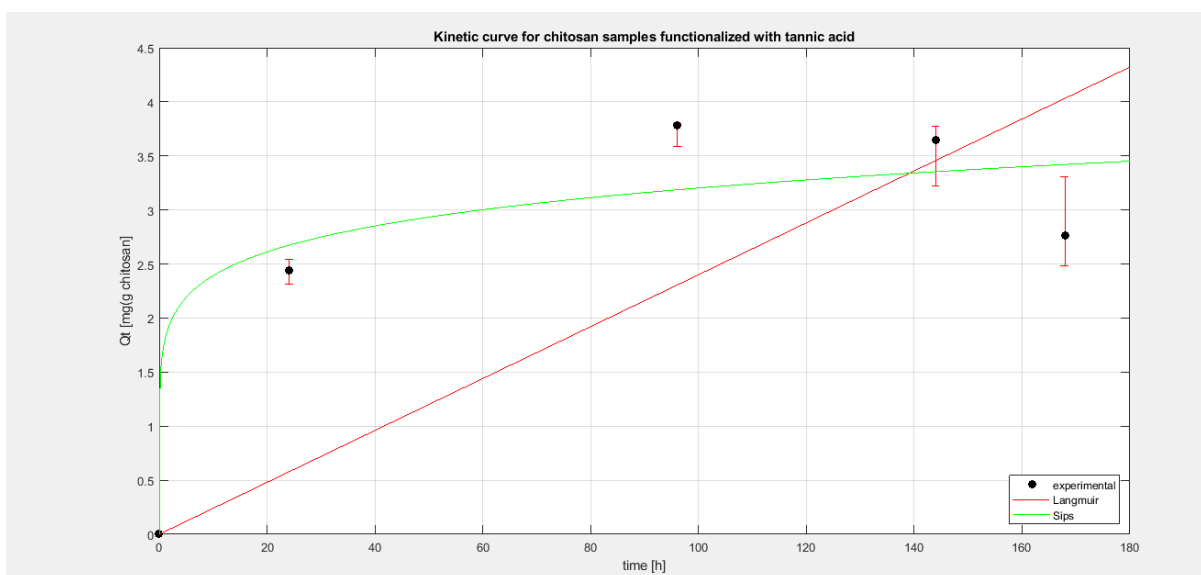
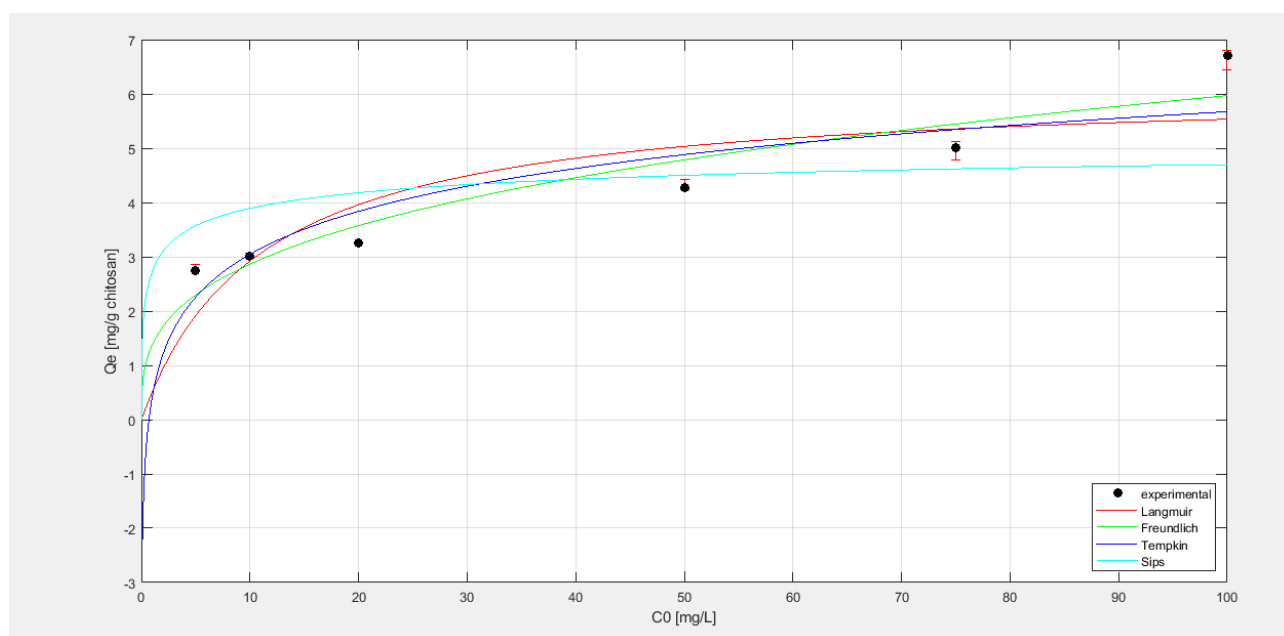


Figura 60

Successivamente è stata effettuata una prova in *Isotherma*: sei campioni di hydrogel di chitosano funzionalizzato con acido tannico sono stati testati, ognuno su una soluzione a determinata concentrazione iniziale di ioni Cu(II), con sei diverse concentrazioni (5 mg/L, 10 mg/L, 20 mg/L, 50 mg/L, 75 mg/L e 100 mg/L). E' stato mantenuto il rapporto 7:10 per quanto concerne il peso del campione e il volume di soluzione in cui il medesimo è immerso.

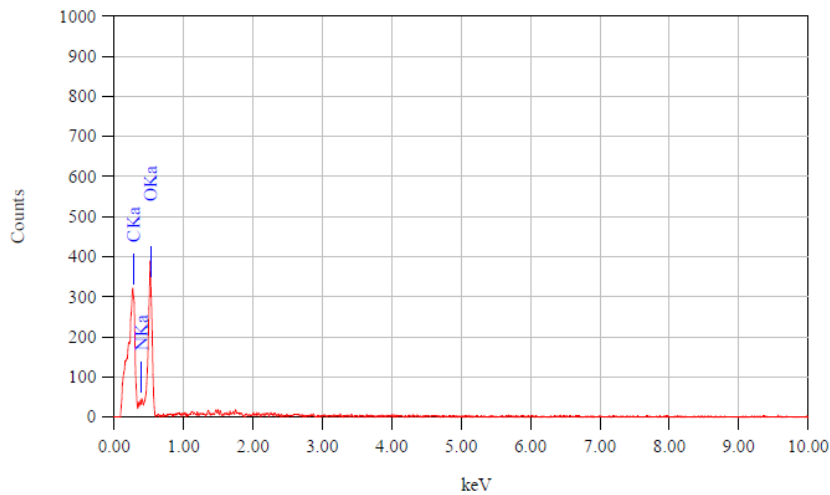
Ogni soluzione è lasciata in agitazione, a temperatura ambiente e sotto la cappa per 96 ore (quattro giorni), trascorse le quali una aliquota di soluzione viene prelevata e analizzata per verificare una diminuzione della concentrazione di ioni Cu(II). Lo spettrofotometro per il Rame può rilevare una massima quantità di sostanza pari a 1,5 mg/L, pertanto tutte le soluzioni preparate e analizzate in questa Tesi sono state opportunamente diluite (con acqua ultrapura), a volte con multiple diluizioni per soluzioni ad elevata concentrazione (quali ad esempio quelle a concentrazione iniziale pari a 75 mg/L e 100 mg/L). I risultati della prova in *Isotherma* sono visibili in *Figura 61*.



*Figura 61*

La seconda parte della caratterizzazione del materiale è stata effettuata dopo le prove di cattura degli ioni rameici.

L'analisi EDS-SEM sui campioni essiccati, prima e dopo immersione in soluzione di ioni Cu(II), evidenzia la differenza composizionale dei campioni trattati in soluzione che presentano, oltre a Carbonio, Ossigeno e Azoto, anche Rame in piccola percentuale (è presente anche Alluminio, e si è ipotizzato che possa derivare da un qualche tipo di contaminazione nel processo di preparazione degli hydrogel). Uno spettro EDS di un campione immerso in soluzione 10 mg/L di ioni rameici è mostrata nelle *Figure 56 e 57*.

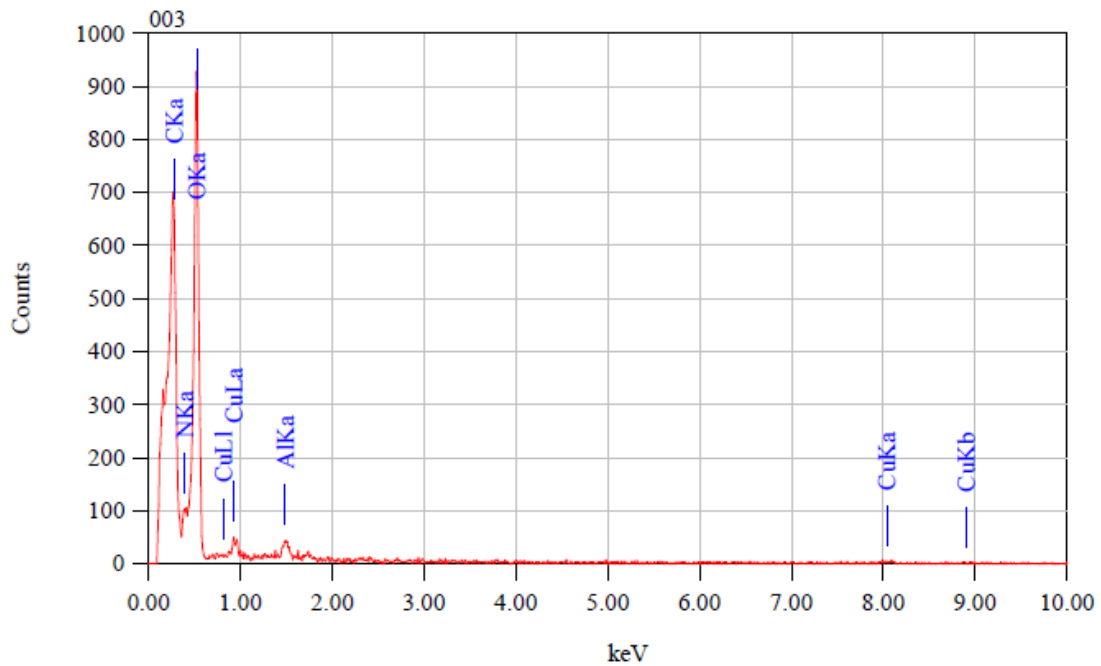


Acquisition Parameter  
 Instrument : JCM-6000PLUS  
 Acc. Voltage : 15.0 kV  
 Probe Current: 7.47500 nA  
 PHA mode : T3  
 Real Time : 50.28 sec  
 Live Time : 50.00 sec  
 Dead Time : 0 %  
 Counting Rate: 213 cps  
 Energy Range : 0 - 20 keV

ZAF Method Standardless Quantitative Analysis  
 Fitting Coefficient : 0.2919

Element	(keV)	Mass%	Sigma	Atom%	Compound	Mass%	Cation	K
C K	0.277	29.62	0.51	35.53				26.1615
N K	0.392	8.44	1.12	8.68				10.3141
O K	0.525	61.94	1.48	55.79				63.5244
Total		100.00		100.00				

Figura 56



ZAF Method Standardless Quantitative Analysis  
 Fitting Coefficient : 0.2388

Element	(keV)	Mass%	Sigma	Atom%	Compound	Mass%	Cation	K
C K	0.277	28.00	0.33	34.27				22.4907
N K	0.392	7.60	0.70	7.98				9.4380
O K	0.525	61.99	0.94	56.97				65.3760
Al K	1.486	0.71	0.07	0.39				0.7707
Cu K	8.040	1.70	0.33	0.39				1.9245
Total		100.00		100.00				

Figura 57

L'analisi spettroscopica UV-Vis è stata effettuata sulla restante parte di liquido presente nelle provette alla fine delle prove di rimozione degli ioni Cu(II): si tenga conto che parte del liquido contenuto viene prelevata come aliquota da analizzare allo spettrofotometro del Rame, e parte viene persa nell'estrazione del campione (posto a essiccare per l'analisi EDS). L'analisi spettroscopica UV-Vis è stata effettuata su quattro campioni di liquido: acqua ultrapura dove era stato immerso chitosano tal quale, acqua ultrapura dove era stato immerso chitosano funzionalizzato con acido tannico, soluzione 10 mg/L di ioni rameici dove era stato immerso chitosano tal quale e soluzione 10 mg/L di ioni rameici dove era stato immerso chitosano funzionalizzato con acido tannico. L'analisi della prima soluzione non ha evidenziato la presenza di elementi. L'analisi delle due soluzioni che avevano contenuto i campioni funzionalizzati con acido tannico (sia la sola acqua ultrapura che acqua ultrapura e ioni rameici) mostra un picco comune intorno a 280 nm, picco riconducibile all'acido tannico. Questa analisi indica che gli hydrogel di chitosano funzionalizzati rilasciano parte dell'acido tannico in soluzione. L'analisi della terza soluzione (chitosano tal quale immerso in una soluzione 10 mg/L di ioni rameici) evidenzia un picco intorno ai 282 nm (quasi sovrapponibile ai picchi presenti a 280nm): altri autori riportano come il picco del complesso Chitosano-Rame sia situato (utilizzando la stessa tecnica di analisi) tra i 200 nm e i 300 nm, ma non si menziona nulla di più specifico. E' tuttavia plausibile, dunque, che tale picco rilevato a 282 nm sia attribuibile alla formazione di un complesso tra Chitosano e Rame (*Figura 68*).

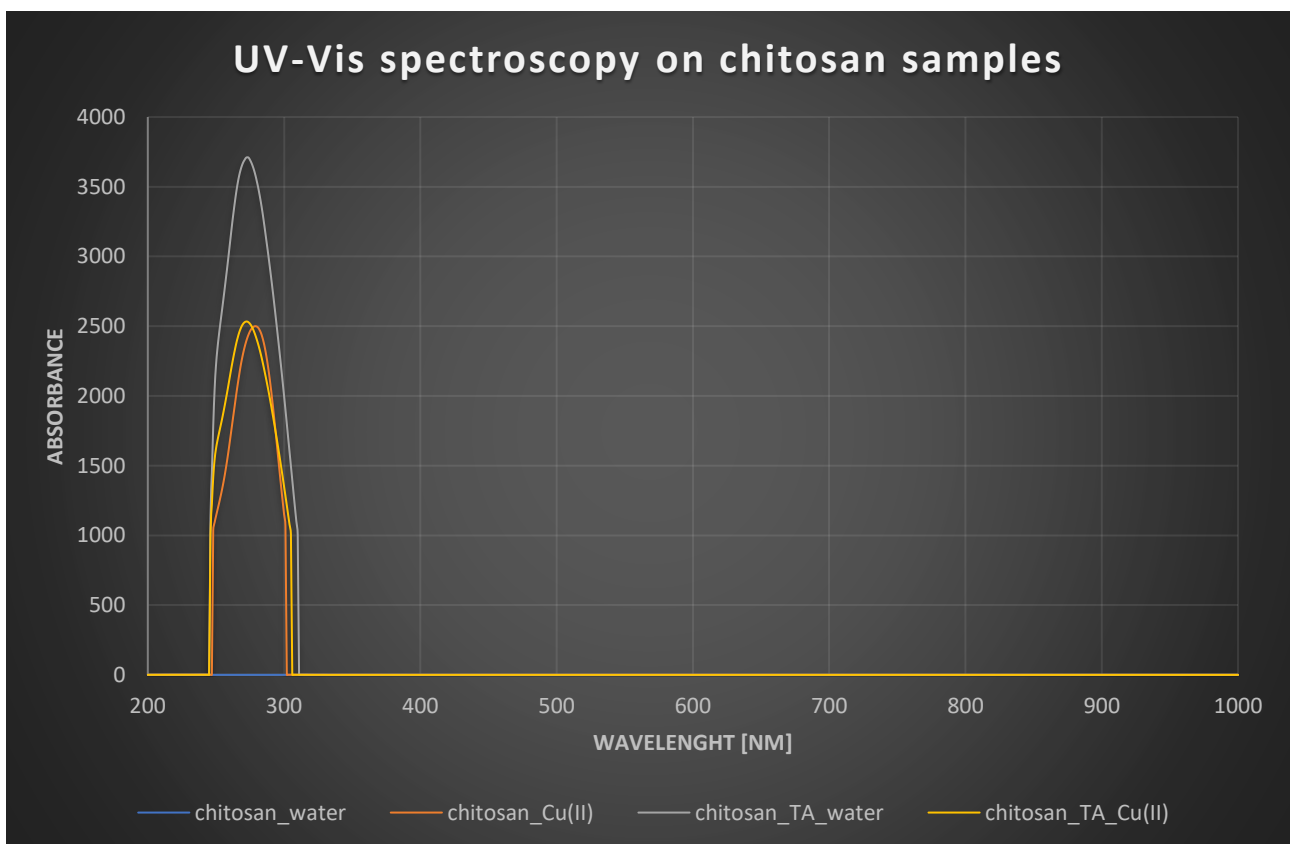


*Figura 68*

Lo studio dell'utilizzo di hydrogel di chitosano funzionalizzati con acido tannico rileva la capacità di tali hydrogel di catturare ioni Cu(II) da soluzione. Il valore massimo raggiunto nella prova Cinetica per gli hydrogel funzionalizzati è pari ad un  $Q_t$  (ovvero la quantità adsorbita all'istante di tempo generico " $t$ " e riferita alla massa del campione) di 3,75 mg/g dopo 96 ore. Nella prova in Isoterma, invece, la quantità " $Q_e$ " (ovvero la quantità adsorbita all'equilibrio) cresce al crescere della concentrazione iniziale di ioni rameici in soluzione. Per quanto riguarda le due prove, però, l'andamento dei punti sperimentali non è riconducibile a nessun andamento noto (sia esso interpolato tramite l'equazione di Languir, Freundlich, Sips o Tempkin), perché in nessuno dei due casi si raggiunge un plateau di adsorbimento: nella prova Cinetica, la quantità adsorbita decresce dopo aver raggiunto un massimo (dopo 96 ore), mentre nella prova in Isoterma i valori di " $Q_e$ " aumentano all'aumentare della concentrazione iniziale di ioni rameici " $C_0$ ", pertanto è possibile supporre che un plateau possa essere raggiunto per concentrazioni iniziali superiori a 100 mg/L.

Ulteriori analisi potranno chiarire il meccanismo di adsorbimento e il comportamento complessivo di questi hydrogel nella cattura di ioni metallici: variazioni di temperatura e pH della soluzione, variazione della dimensione degli stessi hydrogel, così come della concentrazione di acido tannico nel processo di funzionalizzazione dei campioni; questi, e altri parametri, potrebbero essere modificati il loro effetto analizzato, per il completamento di questo lavoro.



# 1 – POLYMERIC HYDROGELS

## 1.1 – INTRODUCTION

A hydrogel is a crosslinked polymer, hydrophilic, which does not dissolve in water. Hydrogels are highly adsorbent, but at the same time they maintain a defined structure. Many hydrogels are synthetic, but some are derived from nature. Hydrogels can be divided in two main categories: chemical hydrogels and physical hydrogels. Chemical hydrogels present covalent cross-linking bonds, while physical hydrogels present non-covalent bonds.

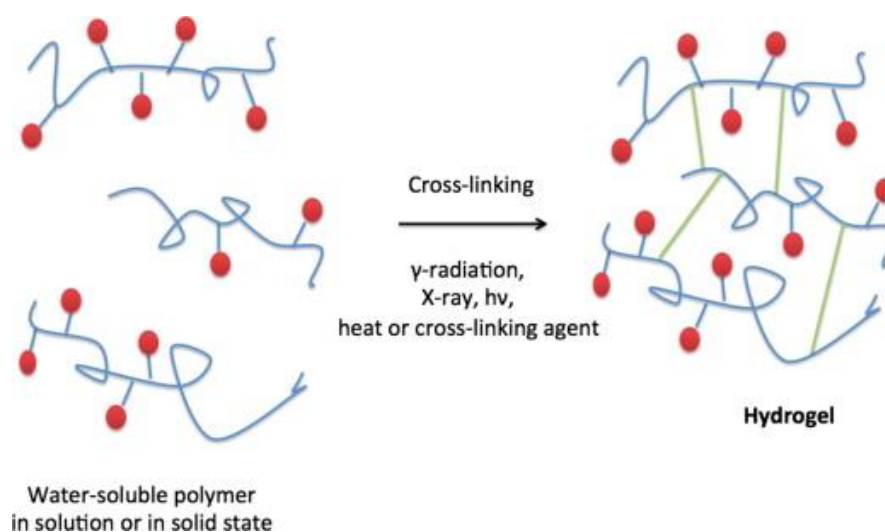


*Fig 1. The formation of a hydrogel*

Chemical hydrogels result in strong, irreversible gels, and this is due to the covalent bonding and, generally, they are not suitable for biomedical applications, because some of their main constituents may result harmful. Physical hydrogels, instead, have high biocompatibility, they are generally considered non-toxic, and are reversible by changing an external stimulus (pH or temperature, for instance). Physical crosslinks consist of, among others: hydrogen bonds, hydrophobic interactions, chain entanglements. Chemical crosslinks consist of covalent bonds between polymer strands. For this reason, Chemical hydrogels are sometimes called “permanent” hydrogels, while Physical hydrogels are sometimes called “reversible” hydrogels.

Hydrogels are prepared by use of a variety of materials, but the main distinction can be made between natural or synthetic polymers. Natural polymers include hyaluronic acid, chitosan, heparin, alginate, and fibrin. Synthetic polymers include polyvinyl alcohol (PVA), polyethylene glycol (PEG), sodium polyacrylate, acrylate polymers.

Two mechanisms exist for physical hydrogel formation. The first one is the so called gelation of nanofibrous peptide assemblies, observed for oligopeptide precursors. Precursors self-assemble into fibers, tapes, tubes, or ribbons, and these latter entangle to form non-covalent cross-links. The second one involves non-covalent interactions of cross-linked domains: these domains are separated by water-soluble linkers, and this mechanism is observed in longer multi-domain structures.

Another method widely used to start a polymerization reaction involves the use of light as a stimulus. In this method, photoinitiators are used. Photoinitiators are compounds which cleave from the absorption of photons, and they are added to the precursor solution to become the hydrogel. The precursor solution is exposed to a source of light, and photoinitiators cleave and form free radicals, and these latter begin a polymerization reaction, generating crosslinks between polymer strands. It's easy to understand that the reaction will cease if the light source is removed, so that the amount of crosslinks forming in the hydrogel can be controlled. Properties of a hydrogel are highly influenced by the type and quantity of its crosslinks.

## 1.2 – PHYSICAL HYDROGELS

Hydrogels can be cross-linked through physical networks, which hold them together by physicochemical interactions like hydrogen bonds, hydrophobic interactions, charge condensation, supramolecular chemistry. These are weak interactions, but they are numerous and responsible for the presence of complex behaviors. Interactions depend on external stimuli (pH, ionic strength, composition of the solvent, or temperature), and this fact allows hydrogels to be highly versatile concerning the environment, unlike covalently bonded materials.

One example of Physical Hydrogels can be seen in Amphiphilic Hydrogels. Amphiphilic copolymers contain both hydrophilic and hydrophobic units and can aggregate in water to form micelles and hydrogels in which the hydrophobic segments self-assemble. Copolymers usually form hydrogels with fragments of different nature. Considering for instance the PEG biocompatibility and PLA biodegradability, the hydrogels formed by these copolymer blocks have been widely studied. Multiple triblock polymer systems, which present hydrophobic segments in between, have been investigated. As an example, PEG-PLGA-PEG form micelles in water, at low concentration, while for higher concentrations they form thermo-reversible hydrogels. The critical gelation concentration, as for the sol-gel transition temperature, depend on the blocks' molecular weights and composition (in the case of PEG-PLGA-PEG copolymers, they gel when temperature changes from room temperature to 37°C, and the concentration is high enough. Cross-linking is due to hydrophobic interactions).

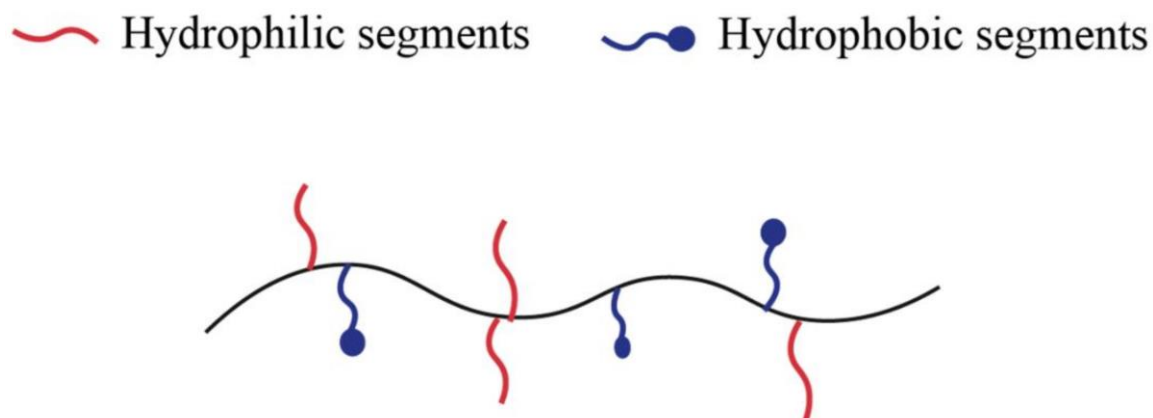


*Fig 2. Schematic illustration of an Amphiphilic polymer*

## 1.2 – CHEMICAL HYDROGELS

Chemical hydrogels consist of covalently crosslinked networks. Chemical hydrogels are not homogeneous, similarly to physical ones. It contains regions of high cross-linking density and low swelling degree (clusters), dispersed in other regions of low cross-linking density and high swelling degree. The presence of these clusters is attributed to hydrophobic aggregation of the cross-linking agent.

An interesting example of Chemical Hydrogels can be represented by Graft Copolymerization and Irradiation Crosslinking. Gamma radiation has been successfully used to graft polymers onto polymeric materials. This technique does not require any kind of initiators or additives. The polymerization reaction, as the cross-linking, can start at room temperature. This radiation acts as initiator of the copolymerization between the polymer matrix (the material) and the monomer to be grafted on. Radiation acts on the polymer matrix and reactive sites form, which then interact with a molecule to be grafted, through a free radical polymerization process [1].

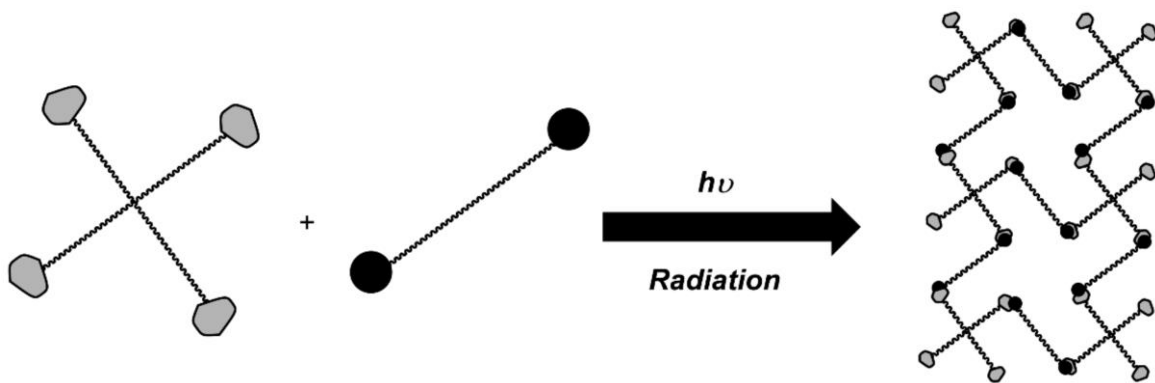


*Fig 3. Representation of graft polymerization*

### 1.3 – PHOTOCURABLE HYDROGELS

A hydrogel is a network of polymers that retain water. In most cases, nothing in the hydrogel structure is photo-reactive. The most common way to make a hydrogel photocurable is to modify its polymers and introduce a photoinitiator. In this case, the photoinitiator is a reagent that releases free radicals from its structure when exposed to a certain wavelength. Typically, the hydrogel is modified by adding acryl or tyrosine functional groups to the polymer chains. These functional groups react to the free radicals released by the photoinitiator. This causes the polymers in the hydrogel to form more interlinking bonds, in a process referred to as crosslinking (as shown in Fig 4). A higher degree of crosslinking gives the hydrogel enhanced physical properties.

The extent of crosslinking (and therefore stiffness) is controlled primarily by the concentration of photoinitiator in the hydrogel, the intensity of the light source, and the duration of the curing. In general, the entire hydrogel will be composed of photoinitiator-compatible polymers. This ensures that the photoinitiator is the limiting reagent in the crosslinking process. In general, more concentrated photoinitiators have the capacity to release more free radicals, causing more crosslinking and therefore a firmer gel. Similarly, using a higher intensity light source over longer periods provides more energy to release free radicals, leading to a firmer gel again.

Bioprinting commonly uses hydrogels which encapsulate cells, but often present poor mechanical properties for building constructs. Photocuring is an excellent technique for adding some needed firmness. It offers an optimal flexibility: the amount of light exposure and the chemical composition of the hydrogel can be modified to fine-tune the stiffness. This can be especially helpful when working with cells that are outside of their native environment during a print. Photocuring also provides an alternative to thermal or chemical crosslinking for experiments that cannot tolerate them [2].

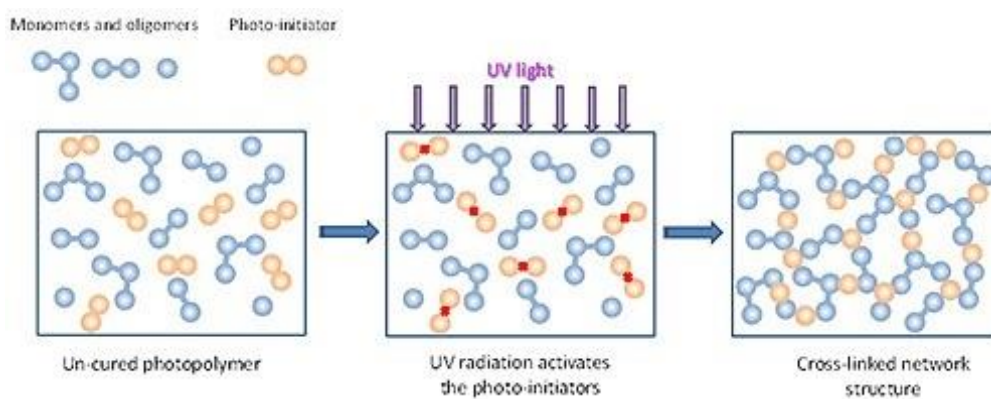


*Fig 4. Photocuring mechanism*

## 2 – EXPLOITATION OF POLYMERIC HYDROGELS IN WASTEWATER TREATMENT

### 2.1 – AN INTRODUCTION

Urbanization, development of facilities, mining operation and pesticides industries (among others) result in a huge discharge of the effluents containing toxic substances, such as heavy metal ions, dyes and organic pollutants. These toxic substances go into the environment and water. Speaking of toxic and carcinogenic nature of effluents, the release of toxic waste in the environment should be controlled as finely as possible.

Different and numerous techniques are used for the removal of toxic pollutants from water, such as chemical precipitation, ion exchange, adsorption, electrochemical treatment and more. Above others, adsorption is the most effective (and, nonetheless, non-destructive) technique used for the removal of metal ions from water and aqueous solutions. The researchers have studied to find a cheaper and more efficient way to remove pollutants from water. Material as Zeolite, Clay, Lignin, Chitosan and more are found to be ideal for the wastewater application and in particular Adsorption, because of many factors: their natural abundance, the flexibility in synthesis and the capability to regenerate for a multiple usage (*Table1*).

Biopolymer	Source	Characteristics
Chitosan	crustaceans and fungi	biocompatible, biodegradable, antimicrobial activity, antistatic activity, nontoxic, chelating property, deodorizing property, film forming ability, chemical reactivity, polyelectrolyte nature, dyeing improvement ability, cost-effectiveness, thickening property, wound healing activity.
Alginate	Brown Algae	Biocompatibility, biodegradable, drug delivery, wound healing, tissue engineering , adsorbent for heavy metals
Cellulose	Green plants, Algae and oomycetes	Tasteless, odourless, hydrophilic , biodegradable, insoluble in water and most organic solvents, adsorbent
Lignin	Vascular green plants	Antioxidant, Antifungal, Extraction of heavy metals in various methods.

*Tab 1. biopolymers and their source and main characteristics*

In the last years, researchers focused on the Hydrogels, which are found to be suitable for applications such as agriculture, biomedical and, most of all speaking about the main focus of this Thesis, in wastewater treatment (*Figure 5*). Hydrogels are hydrophilic, they present a well-defined 3D porous structure, and possess functional groups chemically responsible for the capture of ions of metals or dyes (changing the conditions of the aqueous solution, these ions can be released). They present a flexible network, thanks to the hydrophilic character, in which the solutes can easily penetrate and bind to the functional groups which are present, forming complexes. The functional groups which make this possible are group such as carboxylic acid, amine, hydroxyl and sulfonic acid groups; these functional groups act as complexing agents and make possible the removal of metal ions from the solution.

Hydrogels capture metal ions in water after they swell and “open up” in water, which means that the polymer chain are accessible (hydrogels can swell up to 400 times their original weight). Hydrogels can be regenerated because they’re insoluble in water, and this is due to crosslinking. Crosslink percentage increases the mechanical strength but decreases the swelling ratio, so, to get the optimal Hydrogels, the optimal amount of crosslinking must be pursued. Hydrogels commonly derive from polar monomers, and can be either natural hydrogels or organic hydrogels, or a combination of the two (and, in this case, we speak about hybrid hydrogels), and can be divided in two main categories: physical and chemical hydrogels, as mentioned before.

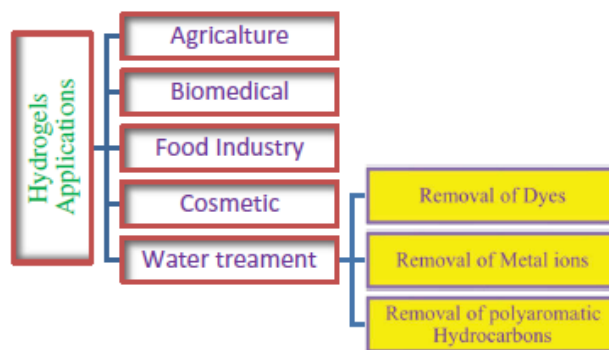


*Fig 5. Hydrogels applications*

## 2.2 – USE OF CHITOSAN HYDROGELS FOR THE REMOVAL OF HEAVY METAL IONS IN WASTEWATER TREATMENT

Many industries, such as mining operations industries and metal plating, generate wastes in which heavy metals are present, like Chromium (Cr), Cadmium (Cd), Lead (Pb) and Mercury (Hg). These metals (and their ions) are particularly dangerous for the majority of life forms, and even at low concentrations. Pollution of waters, for instance, leads to the pollution of marine environment, and generating in the end a dangerous impact on the seafood industry.

Different methods have been developed to treat and decontaminate polluted waters. Among these ones, the main are precipitation, solvent extraction, reverse osmosis, and adsorption. This latter is nowadays considered as the most efficient method, for many reasons: low cost, availability of different adsorbents, efficiency and ease of handling (as shown in *Table 1*).

Adsorption process depends on different parameters such as particle size, temperature, pH of the solution, species of adsorbent used, metal ion concentration, and more. As seen before, a variety of natural adsorbents is present and available in nature.

However, this work is focused on the study of Chitosan and Chitosan Hydrogels for the removal of heavy metal ions in wastewater treatment.

Chitosan is a polyaminosaccharide, deriving by alkaline N-deacetylation of chitin involving deproteination and deacetylation. Chitosan possesses a variety of interesting properties: hydrophilicity, biodegradability, biocompatibility, non-toxicity, presence of reactive amino(-NH<sub>2</sub>) and hydroxyl(-OH) groups located in its backbone. The ability of binding heavy metal ions, in Chitosan, is very dependent on pH, and the capability to bind metal ions is increased if Chitosan undergoes a crosslinking process involving the following materials: ethylene, formaldehyde, epichlorohydrin, and isocyanates (and more). These crosslinking agents have two main positive effects on Chitosan: they increase its mechanical properties and, most of all, make it insoluble in acidic medium.

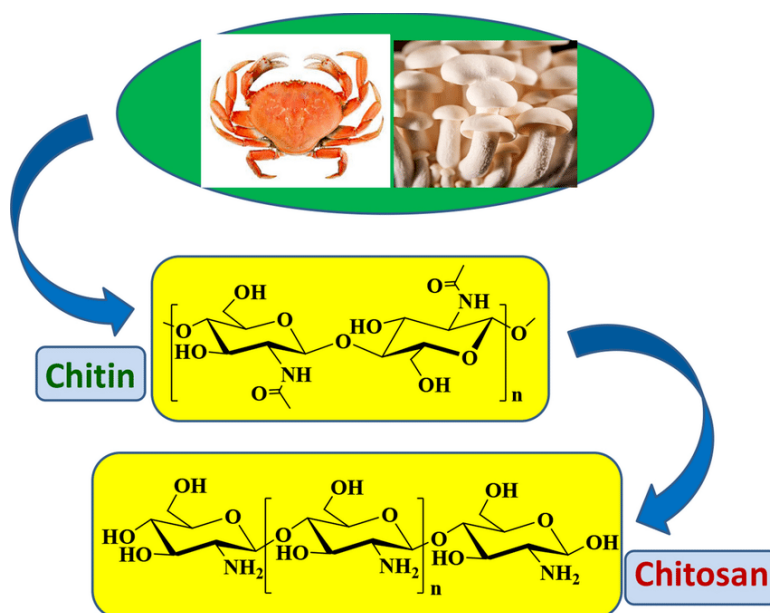


Fig 6. Chitin and Chitosan

Adsorbent	Adsorbate	Adsorption capacity (mg/g)	Temp . (oC)	pH	Kinetic model	Isotherm
Polyelectrolyte complex pectin/chitosan	lead (II)	30.1	-	5	-	-
Chitosan	Lead(II)	-	-	-	Ist order Kinetics	-
Magnetic chitosan resin (EMCMCR)	Copper (II)	-	25	6	-	Langmuir adsorption
Chitosan blended with Cellulose	Copper (II)	-	-	-	-	Langmuir, Freundlich
Chitosan coated carbon	Cr (IV) Cd(II)	-	-	5.0, 5.5	Pseudo second-order	Langmuir adsorption
Chitosan CS/PEG	Cr (VI) Fe	11.6 -	25 -	5 -	- -	- Freundlich
Semi-IPN hydrogels/CS	Cu (II)	261.3	-	-	-	-
Bromine pretreated chitosan	Pb(II)	0.001755	-	-	-	Freundlich
Chitosan-magnetite microparticles	Ni,CO	588.24,833.34 resp.	-	-	-	Langmuir, Freundlich
Chitosan produced from shrimp shell waste	Cu(II), Hg(II), Pb(II) and Zn(II)	79.94, 109.55, 58.71, 47.15	-	6	-	Langmuir, Freundlich, Redlich-Peterson and SIPS
Chitosan-silica hybrid	Co (II), Ni (II), Cd (II), Pb(II)	0.63mmol/g	-	-	-	Langmuir and Sips
Grafted chitosan of polyacrylonitrile	Cr (VI) and Cu(II)	-	-	-	-	Langmuir

Tab 2. Chitosan composites and their effect on adsorption of some heavy metal ions

## 2.2.1 – REMOVAL OF MERCURY

Mercury (Hg) is known as one of the most toxic heavy metals and its impact on the environment is highly dangerous, mostly due to its ability to accumulate into living organisms and then to bio-magnify itself through the food chain.

Among adsorbents, Chitosan is the most widely used to remove Mercury ions from wastewater; its ability to achieve this purpose depends on several factors, like its degree of deacetylation, pH of the solution and selectivity for the metal species. Chemical modifications of Chitosan, with glutaraldehyde or epichlorohydrin or using the grafting method to introduce new functional groups, have been used in the research field of Hg(II) adsorption. Changing the pH range makes possible to enhance selectivity for a specific metal species. The adsorption of Hg(II) on Chitosan is known to occur through different mechanisms: coordination and chelation (on both hydroxyl and amino groups), electrostatic attraction and ion exchange.

As previously said, the removal of Hg(II) by Chitosan depends on many actors such as pH of the solution, temperature, particle size etc. In *Table 3* are summarized the results of many researchers as far as regarding Hg(II) adsorption by use of Chitosan.

Chitosan origin	Maximum adsorption capacity (mg.g <sup>-1</sup> )	Physical form	Type of study	Chitosan characterization	pH	Isotherm
Lobster shell	815 430	Particles	Equilibrium studies Equilibrium and dynamic studies		4.0	L L
Crab shell	51.6 (C = 5.22 × 10 <sup>-6</sup> M)	Powder	Equilibrium and kinetic studies		5.0	L
Shrimps shells		Surface membranes	Kinetic studies	IR, 13C RMN	6.0	
Red lobster shells	361.1 (pH 2.5), 461.4 (pH 4.5)	Flakes	Equilibrium studies	FTIR	2.5; 4.5	L; F
Commercial chitosan	520	Solid state (flakes) / dissolved state	Equilibrium and kinetic studies		4.0–6.0	
Commercial chitosan		Solid/dissolved state	Equilibrium and kinetic studies	FTIR, SEC	2.0–6.0	
Crab discards		Particles	Dynamic studies		5.0–7.0	
Commercial chitosan	754.3 (PS= 1.19 mm), 1095.5 (PS= 0.5 mm), 1127.4 (PS= 0.177 mm)	Particles	Equilibrium studies		3.0; 4.5; 6.0	L; F, R-P
Shrimps shells	106.4	Particles	Equilibrium and kinetic studies		4.0–10.0	L

*Tab 3. Removal of Mercury in aqueous solution using Chitosan*

*Peniche-Covas et al.* [3] studied the kinetics of mercuric ions' sequestration by use of Chitosan deriving from lobster. Adsorption data were found to follow the Langmuir isotherm ( $Q_m = 429.3$  mg/g).

As far as regarding the study of influence of temperature, [4], Chitosan membranes were prepared by stirring a Chitosan powder in acetic medium; it was observed that a rise in temperature was responsible for causing an acceleration in Hg(II) uptake by the membrane: in this case, Avrami equation was the best fit.

As far as regarding the study of influence of pH range, Chitosan flakes deriving from red lobster were used. The pH range of investigation was from 2.5 to 4.5, and it was observed that the uptake capacity of Hg(II) ions by Chitosan flakes raised from pH 2.5 to pH 4.5 (from 361 mg/g to 461 mg/g) [5].

*Guibal et al.* [6] dealt with the Hg(II) recovery on chitosan, through the PEUF process (“polymer enhanced ultrafiltration process”), which comes to be necessary when the chitosan is saturated with Hg(II). The maximum adsorption capacity was found to be equal to 519 mg/g. Diffusion properties were found to be poor and this was attributed to the particle size of the flakes, so HCl was added to maintain Chitosan soluble. HCl and Hg(II) caused chloride species to form and bind onto protonated amino groups: in this case, kinetics were improved.

*Kunkoro et al.* [7] studied again the PEUF technique; they focused on the molar ratio “metal/protonated amino groups” which are present at saturation level, both in the dissolved and in the solid state, and they found that the adsorption capacity was improved in the dissolved state. Again, as the previous work by *Guibal et al.* [6], chloride species bind to protonated amino groups, so this influenced the uptake of Hg(II) ions.

*Gamage and Shahidi* [8] studied the effect of the degree of deacetylation. They used three different deacetylation degrees (91%, 89% and 86%), and found that in all these three cases, the Hg(II) uptake is high (from 90% to 97%, at pH 3).

*M. Benavente* [9] studied the kinetics of adsorption and desorption of Hg(II) ions on Chitosan deriving from shrimp shells, and these kinetics were found to be well fitted by a pseudo-II order equation. Desorption was studied by use of NaCl, which caused the formation of chloride species with Mercury, and desorption was obtained due to the fact that these species are negatively charged, so a repulsive phenomenon occurs.

Chitosan possesses a quite low specific area (from 2 to 30 m<sup>2</sup>/g), if we compare it to activated carbons (from 800 to 1500 m<sup>2</sup>/g); anyway, it shows a great uptake capacity (from 430 to 1127 mg/g) and near to pH neutral, and this fact has to be attributed to the numerous reactive functional groups.

As far as regarding the regeneration of Chitosan, some disadvantages have to be considered: first of all, being Chitosan soluble in acidic medium, it cannot accomplish its adsorbent function under acidic conditions, unless it is chemically modified; one more problem is related to the degree of deacetylation, which impacts on the uptake capacity of this material, and it must be considered that the deacetylation degree is difficult to control; in the end, the wastes produced in the process are alkaline wastes and not environmental friendly.

## 2.2.2 – CHEMICAL MODIFICATION OF CHITOSAN FOR THE REMOVAL OF MERCURY

The uptake capacity for Hg(II) ions for Chitosan can be enhanced through chemical modification. Particularly, a reaction occurs between chitosan and ethylenediamine or glutaraldehyde, and the uptake capacity was calculated to be equal to 2.26 mmol/g dry mass and at pH 7 (shown in *Table 4*). Analyzing the uptake capacity for aminated beads, it was discovered an increase of about 47% would respect to the control, and the reason for this higher uptake has to be attributed to the affinity showed by Hg(II) ions towards the amine groups, if compared to other functional groups. HSAB theory defines Hg(II) as a soft ion, and these kind of ions form strong bonds with R-S<sup>-</sup>, -SH<sup>-</sup>, CN<sup>-</sup> and, most of all, NH<sub>2</sub><sup>-</sup> (binding to this latter, the highest uptake was observed) [10].

Several chemical modification methods	Adsorption capacity (mmol g <sup>-1</sup> dry mass)
Aminated chitosan bead	2.26
Xanthated chitosan bead	1.84
Phosphorylated chitosan bead	1.55
Carboxylated chitosan bead	1.51
Crosslinked chitosan bead (control)	1.47

*Tab 4. uptake capacities of modified chitosan beads*

In Figure 7 the IR spectra of different chitosan beads samples is presented. It can be observed that, in the case of crosslinked chitosan with glutaraldehyde, the peak of the C=O bond is visible at 1600-1650 cm<sup>-1</sup>, and this peak represents the carbonyl group, showing that the crosslinking reaction occurred successfully. It is also visible a narrower peak at 3000-3500 cm<sup>-1</sup> for the aminated beads respect to the natural ones, relatively; this indicates that the hydroxyl groups from natural beads became aminated ones. Relatively to the interval of 1600-1650 cm<sup>-1</sup> mentioned above, the peak at 1630 cm<sup>-1</sup> may be indicative that the number of amide groups (-NHCO) increased. As ulterior proof of the increase of amide groups, the concentration rose about 0.76mmol/g would respect to the control.

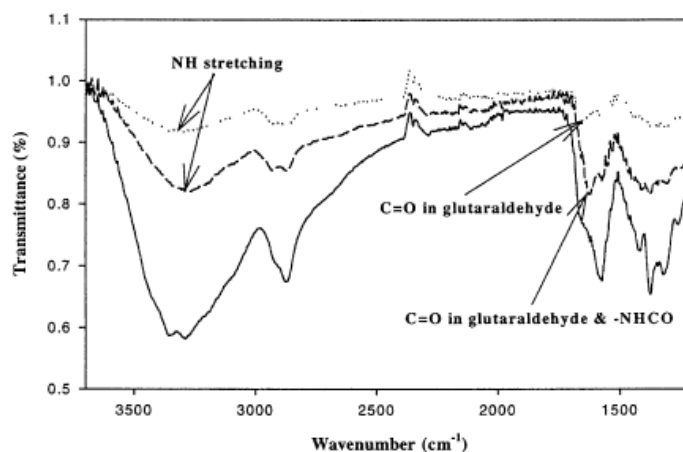
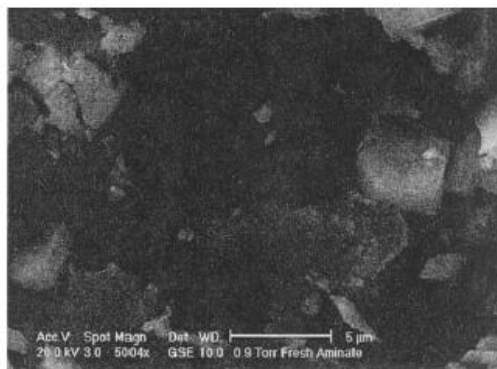
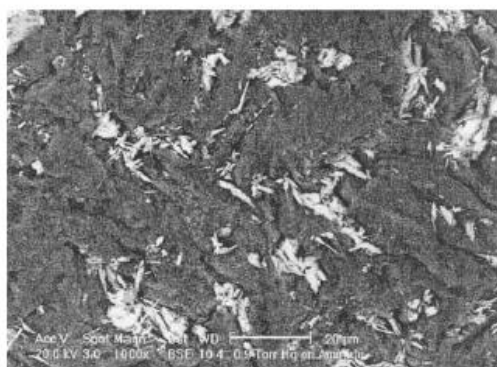


*Fig 7. IR spectrum of various chitosan beads*

In addition, ESEM photographs were analyzed before and after adsorption of Hg(II) ions; the pores observed are attributed to amine groups. In Figure 8b it can be observed that the pore reduction can surely be attributed to the adsorption of Hg(II) ions, and samples result to be swollen.



(a)



(b)

*Fig 8. ESEM photographs of aminated beads before (a) and after (b) adsorption of Hg(II) ions*

In the end, through a EDX analysis it is clearly shown (*Figure 9b*) that the electron dense part is due to the presence of Hg. In the EDX spectrum taken after adsorption, the peak of Hg is clearly visible.

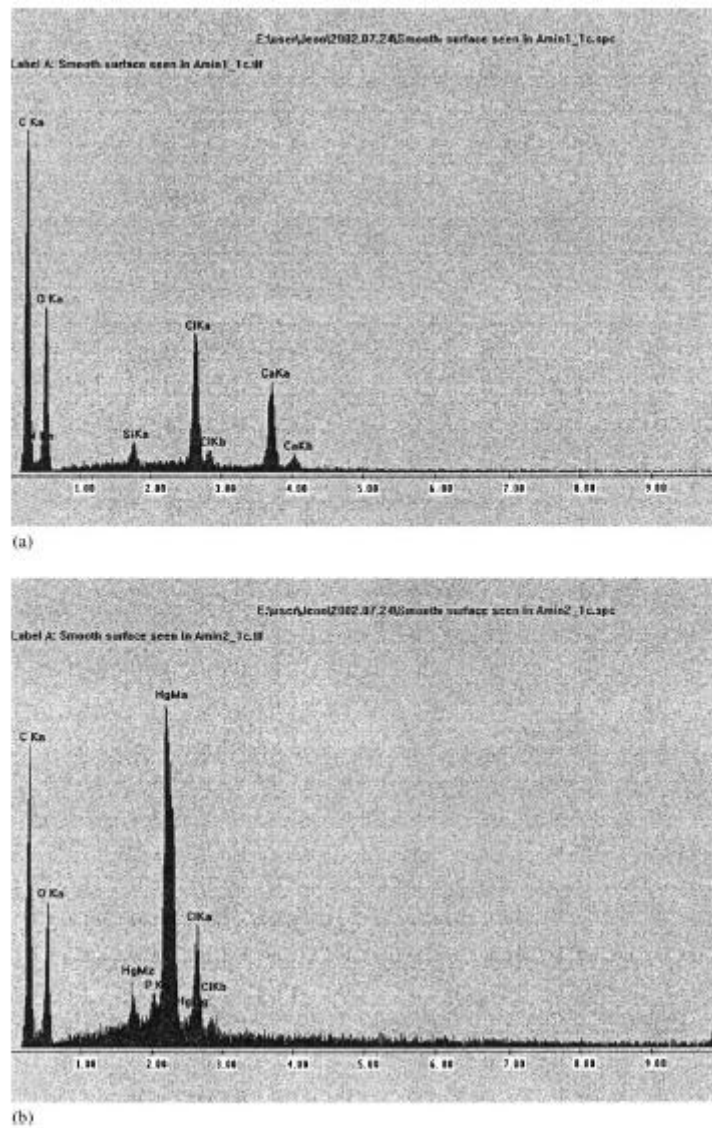


*Fig 9. EDX spectra of aminated chitosan beads before (a) and after (b) adsorption of Hg(II) ions*

### 2.2.3 – REMOVAL OF ARSENIC

Arsenic figures among dangerous and toxic metals. Arsenic is known for its carcinogenic chronic effect on humans and for the contamination of water and soil.

The accumulation of Arsenic in human body leads to chronic damage to respiratory tracts, liver, skin, nervous and cardiovascular system. As(V) and As(III) are the most common Arsenic ions found in waters. Also, species like MMAA (monomethylarsonic acid) and DMAA (dimethylarsonic acid) are dangerous pollutants and derive from agriculture and industrial facilities.

The uptake of As is usually carried out by use of modified chitosan (through processes like chemical/physical modification or crosslinking), instead of using crude chitosan, and this is due to different reasons: crude chitosan presents heterogeneities related to the difficulty in controlling its deacetylation degree, it presents also a quite low sorptive capacity towards As(III) ions and results to be unstable at the usual pH at which As is removed.

The capability of chitosan to retain anions is due to the protonation of amine groups. These groups are important also in terms of solubility: a low solubility makes chitosan usable in acidic media. As already seen in the previous chapter about Hg(II) adsorption, chitosan is often treated to crosslink by use of glutaraldehyde (in detail, hydroxyl and amino groups react with the coupling agent to form a Schiff base). After crosslinking, stability of chitosan is increased.

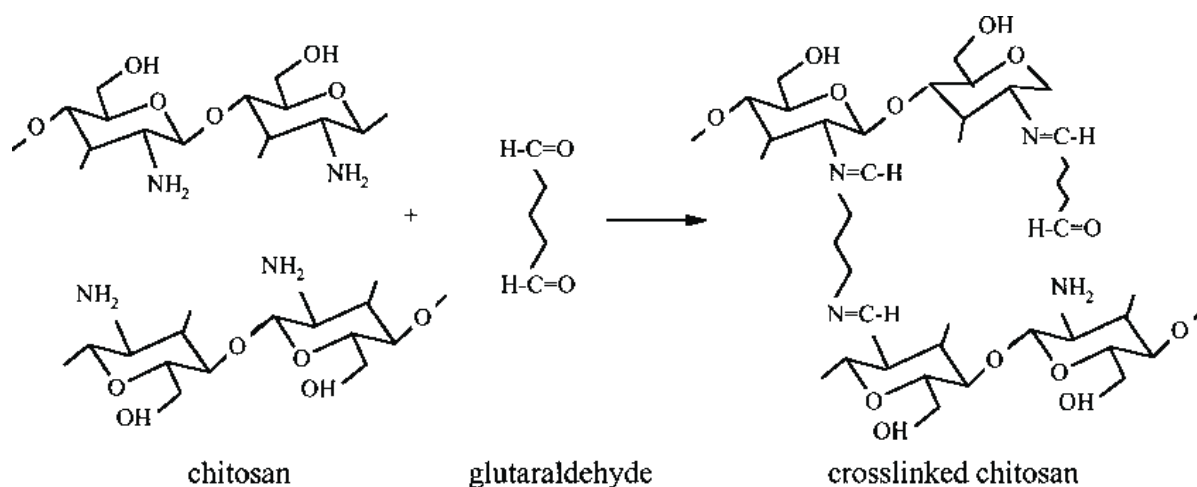


*Fig 10. Crosslinking of chitosan with glutaraldehyde*

Diffusion is the main mechanism in adsorption processes, so diffusion has to be as high as possible; in order to do so, two fundamental aspects have to be considered: reduction of crystallinity and increase of porosity. This is achieved by both gel beads manufacturing and crosslinking (although crosslinking has a little countereffect, because it reduces the access to internal sites).

One way to increase the access sites without compromising mobility is to immobilize chitosan onto a support structure.

The uptake capacity of chitosan towards As ions can be increased by use of metal impregnation: metals used for this purpose are Mo and Fe, because they form complexes with As(III) and As(V); nonetheless, they possess a high affinity for chitosan. Removal efficiency of As(V) is higher than the one of As(III), in fact TiO<sub>2</sub> is often used to oxidize the species As(III) to the species As(V).

In *Table 5* are showed the maximum values of uptake of ions species As(III) and As(V) obtained using different chitosan and chitosan derivative products; the model used is the Langmuir (monolayer).

It is visible that the uptake of arsenic is widely variable (from 40% to 96%); this variability is due to the process temperature, the quality of the water and the characteristics of the polymer used. The uptake process has to be attributed to electrostatic attraction (As ions are negatively charged, while protonated amino groups are positively charged), and in part due to ion exchange.

Interesting features in the As uptake can be reconducted to the use Molybdenum. As previously said, a certain affinity exists between arsenate and molybdate species, but this affinity has a countereffect: is molybdate species release from the beads, they go into the solution and bind the arsenate species. This means that a certain amount of arsenate will remain in the bath, bond to molybdate. Increasing the concentration of the adsorbent has a positive effect because it increases the presence of molybdate species, while, if the As concentration in the bath increases, the effect is negative because a higher percentage of molybdate will be released from the beads and go into the bath. One way to reduce the labile fraction of molybdate (in order to avoid the release of molybdate) is treating the beads with H<sub>3</sub>PO<sub>4</sub>, which washes away the labile molybdate, or, alternatively, to functionalize chitosan with molybdate using a coagulation bath: in this way, all the sites of molybdate species result to be strong. It must be observed that uptake behavior is optimal between pH 2 and pH 5. Beyond pH 5 molybdate species are released from the beads, and so the uptake capacity rapidly decreases, until pH 9, where 100% of molybdate species are released.

An efficient way to remove a higher percentage of As is the use of both TiO<sub>2</sub> and UV light: TiO<sub>2</sub>, as previously said, TiO<sub>2</sub> promotes the oxidation of As(III) to As(V), more easily removed, and so does UV light too (it was observed that TiO<sub>2</sub> effect is responsible for the excellent 100% removal of As(III), and for the 85% removal of As(V)).

As(V) removal by use of TiO<sub>2</sub> is maximum between pH 4 and 5, until 7.2 (in this pH range we have the presence of H<sub>2</sub>AsO<sub>4</sub><sup>-</sup>, the beads are positively charged, so the electrostatic attraction is favored). Between pH 7.3 and 9.2 As(III) removal is higher than the removal of As(V), because As(III) charge is zero, so no electrostatic repulsion occurs. Between pH 9.3 and 11.6, the opposite behavior occurs: As(III) uptake is higher.

Another metal responsible for the removal of As ionic species is Fe, and even better performances are obtained if chitosan is crosslinked with glutaraldehyde (removal can get to 95%). The mechanism involved in uptake is due to both H bonding and the formation of complexes with Fe. The uptake can even increase of 30% by using imprinted Fe beads. Fe can also be used as metallic Fe encapsulated in chitosan nanospheres; the mechanism proceeds as follows:

- removal of As(V) - Fe(0) is oxidized by As(V), which reduces to As(III)
- removal of As(III) – by formation of complexes with oxidized Fe

For Fe impregnated chitosan beads, the As uptake does not depend on pH until pH 9, and, taking in consideration that under pH 9.2 the As(III) ions are neutral, the uptake must be due to Lewis acid-base interactions.

Composites can be used for the removal of As. For instance, chitosan coated sand is used (preparing it with gangetic sand, or with Al<sub>2</sub>O<sub>3</sub>). The uptake mechanism is due to the interaction of As ions with the polymeric part of the material and, which cannot be excluded, by sorbate diffusion through the composite.

In the previous pages, it was said that the use of raw chitosan is quite limited. It is actually used below its PZC (around pH 6.5), and the uptake capacity towards As ions increases as the pH decreases (because, decreasing pH, the majority of As ions is charged negatively), and the interaction with protonated amino groups is favored. Instead, for chitosan beads from shrimp shells, the PZC is around pH 5.6, and the optimal pH for As(III) removal is between 5 and 6, while for As(V) a broad range of pH is optimal for uptake (between pH 4 and pH 9).

Speaking about As(III)-imprinted chitosan resin, uptake capacity is increased until pH 5 is reached, then it levels off from 5 to 9. Below pH 5, there is a competition in adsorption regarding As(III) and H<sup>+</sup>, because the amino groups are ionized below this value of pH. Above pH 9 the uptake increases, but it is not efficient as it is at pH 5 [11].

## 2.2.4 – REMOVAL OF LEAD – INFLUENCE OF PH

Removal of Pb(II) ions was studied by using chitosan/PVA beads. It may be remarkable remind that in this study, as many others, an optimal pH has been identified for the uptake of that precise metal ion species.

In the case of this study, considering the structure of chitosan/PVA beads, it is supposed that the sites where metal ions can bind are the ones of hydroxyl groups, present both in PVA and chitosan, and amino groups (chitosan). Nitrogen and Oxygen possess a lone pair of electrons, so they can share them to make a complex, with a metal ion or a proton, but it must be noted that, in the case of an O atom, this lone pair undergoes a greater attraction by the nucleus, so it is reasonable to think that N atoms are the major responsible for the Lead uptake. To explain the previous hypothesis, the chemical reaction that follow are proposed to explain the uptake behavior of chitosan/PVA beads:

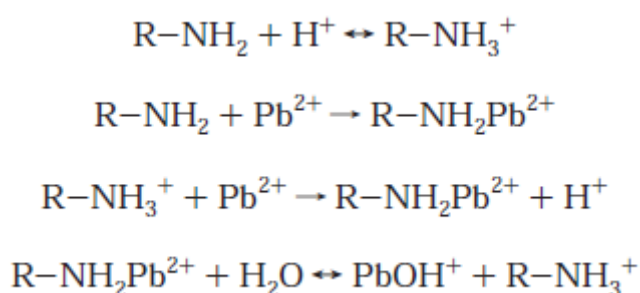


*Fig 11. eq.1 protonation of amino groups, eq.2 binding of a Lead ion to an amino group, eq.3 competitive adsorption between a Lead ion and a proton, eq.4 exchange mechanism of a Lead ion from an amino group to a OH group*

As previously said, N atom shares the lone pair of electrons and bind Pb(II) ions, and this mechanism starts as Pb is added to the solution, and is represented by equation 2, but the mechanism showed in equation 3 is non to be excluded, because the binding of a proton is weaker would respect to the binding of a Pb(II) ion; this reaction (eq.3) is anyway expected to be slower. In the end, it should be taken into account that, due to the greater affinity to OH<sup>-</sup> group, eq.4 is very probable to occur.

Considering the effect of pH, at lower pH (respect to the PZC of chitosan), the number of protonate amino groups increases at the expense of the -NH<sub>2</sub>, so it's easy to understand that the reaction in eq.3 would be more probable to occur in low pH conditions.

Another phenomena to be taken into account is the transport, from bulk to surface, of Pb(II) ions; in fact, at very low pH's, this transport can be inhibited by the electrostatic repulsion present between the ion themselves and the majority of amino groups which are protonated (in Figure 13 this may be the explanation of the diminishing in uptake from pH 4 to pH 2). The following decrease until the minimum is reached at pH 6.5 can be explained by use of the eq.4, where it is shown that Lead ions dissociate from amino groups in favor of OH<sup>-</sup> groups. In the end, the rise in uptake after pH 6.5 can be reconducted to non-specific interactions (eq. 5 and eq. 6) [12].

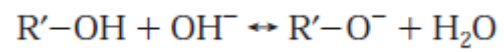


Fig 12. eq.5 hydrogen bonding, eq.6 deprotonation of R'-OH sites

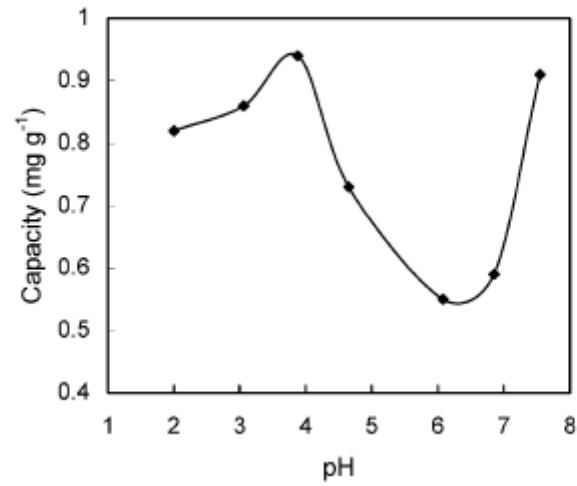


Fig 13. influence of pH on Pb(II) ions removal by chitosan/PVA beads

## 2.2.5 – REMOVAL OF CHROMIUM – XPS ANALYSIS

XPS analysis were conducted on chitosan hydrogels, natural and crosslinked (with glutaraldehyde and epichlorohydrin) to investigate the uptake of Cr(III) and Cr(VI) from wastewater. Comparing the values of BE's before and after Cr ions adsorption (see *Tables 5 and 6*, respectively), it can be noticed that C1s atomic concentration is lower in epichlorohydrin crosslinked and natural chitosan, while is higher in glutaraldehyde crosslinked chitosan. Particularly, the decrease observed for C-N and C=N bonds is indicative of the fact that Cr adsorbed onto imino groups, unreacted amino groups, and hydroxyl groups. In *Figure 14*, XPS spectra for Cr adsorption, on chitosan samples (both natural and crosslinked) is shown [13].

Element	Natural chitosan		GLA-chitosan		ECH-chitosan		Assignments
	BE (eV)	AC (%)	BE (eV)	AC (%)	BE (eV)	AC (%)	
C 1s	284.6	36.2	284.7	44.0	284.8	41.3	C-C or adventitious carbon
C 1s	286.2	25.9	286.3	20.7	286.4	24.0	C-N, C=N, C-O or C-O-C
C 1s	288.0	7.3	287.9	7.8	288.0	7.1	C=O or O-C-O
Total C		69.4		72.5		73.4	
O 1s	532.4	22.4	532.6	20.8	532.6	21.2	-C-O or O-H or bound water
N 1s	399.4	6.2	399.5	4.0	399.4	4.9	N
					401.0	0.4	NH <sub>3</sub> <sup>+</sup>
Total N		6.2		4.0		5.3	
Si 2p	103.3	2.0	102.5	2.7	102.0	1.1	SiO <sub>2</sub> contamination

Element	Natural chitosan		GLA-chitosan		ECH-chitosan		Assignments
	BE (eV)	AC (%)	BE (eV)	AC (%)	BE (eV)	AC (%)	
C 1s	284.7	40.3	284.8	60.1	284.7	41.6	C- or adventitious carbon
C 1s	286.3	18.9	286.4	12.6	286.3	19.3	C-, C=N, C-O or C-O-C
C 1s	288.0	7.1	288.0	5.6	288.0	7.7	C=O or O-C-O
Total C		66.3		78.3		68.6	
O 1s	532.6	23.9	532.5	16.5	532.3	25.7	-C-O or O-H or bound water
N 1s	399.9	4.1	399.5	2.1	399.7	2.8	N
N 1s					401.0	0.7	NH <sub>3</sub> <sup>+</sup>
Total N		4.1		2.1		3.5	
Si 2p		3.4	102.5	2.1	1.8	2.5	
Cr 2p <sub>3/2</sub>	577.0	1.8	577.0	1.1	576.9	2.3	Cr(III)

Tab 5-6. spectral bands, based on BEs, and AC (atomic concentration), for crosslinked and natural chitosan, before (upper Table) and after (lower Table) Cr ions adsorption

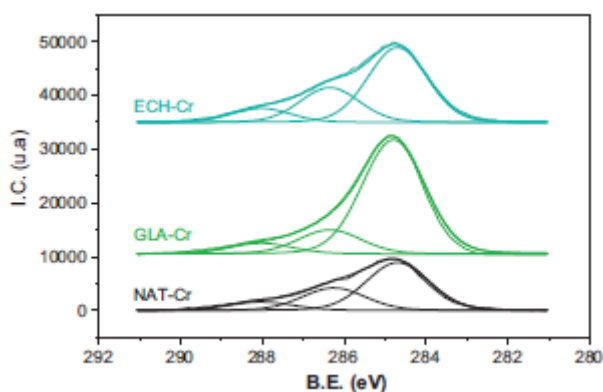
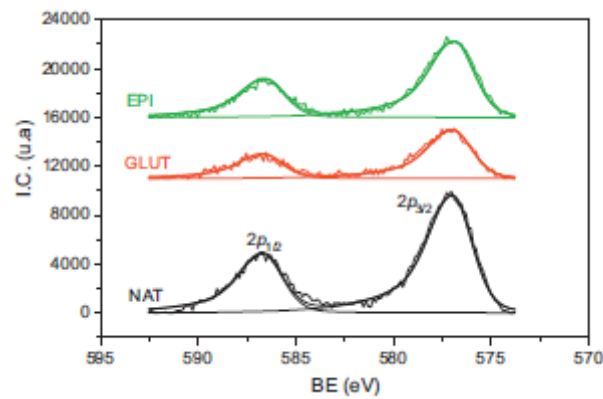


Fig 14. C1s for chitosan samples (NAT is natural chitosan, ECH is epichlorohydrin crosslinked, GLA is glutaraldehyde crosslinked chitosan) after Cr adsorption

The XPS spectrum, regarding Cr 2p core regions, is showed in Figure 15. The Bes assigned to Cr 2p<sub>3/2</sub> reveal the presence of CrCl<sub>3</sub>, Cr<sub>2</sub>O<sub>3</sub>, Cr(OH)<sub>3</sub>, assigned to Cr(III). As far as regarding Cr(VI), K<sub>2</sub>Cr<sub>2</sub>O<sub>7</sub> and CrO<sub>3</sub> were detected: this suggests that all Cr(VI) was reduced.



*Fig 15. Cr 2p for chitosan samples (NAT is natural chitosan, ECH is epichlorohydrin crosslinked, GLA is glutaraldehyde crosslinked chitosan) after Cr adsorption*

*Dambies et al.* [14] observed the total reduction of Cr(VI). Cr(VI) was observed to bind easier to chitosan films, would respect to copper ions. This may be due to the multivalent nature of Cr and may indicate that a multi group interaction is needed to uptake Cr ions.

## 2.2.6 – COPPER REMOVAL – SORPTION KINETICS AND EQUILIBRIA

The uptake of Cr(II) ions was studied using chitosan hydrogels, starting by a solution of CuSO<sub>4</sub> a varying the concentration of metal. Equilibria have been described by equations of Langmuir, Langmuir-Freundlich, Freundlich, Redlich-Peterson, Dubinin-Raduszkiewicz and Toth. The model used to describe the adsorption combines both interparticle diffusion and chemical reaction on the surface of the sorbent.

Sorption kinetics are found to be well described by both first-order reaction model and second-order reaction model (the latter is well fitting when dealing with high concentrations, used for diagrams in *Figures 16a and 16b*) [13].

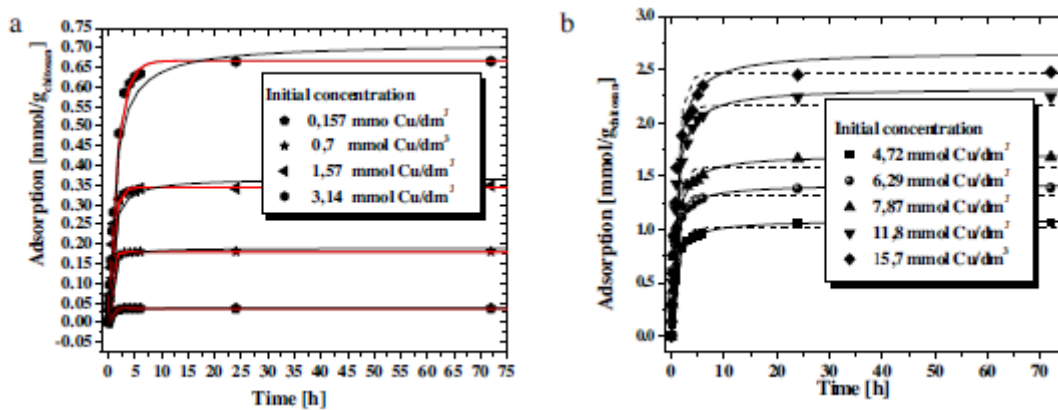


*Fig 16. Sorption kinetics, pH<sub>0</sub>=5 (dashed line is second-order type, continuous line is first-order type)*

The diffusion model used to describe sorption kinetics is shown in *Figure 17* and in *Table 7*. Coefficient  $k_i$  is obtained by linearizing  $q$  as function of time and by dividing the process of adsorption in three stages (1h, 1-5h, exceeding 5h), but the first stage was seen to be the most relevant.

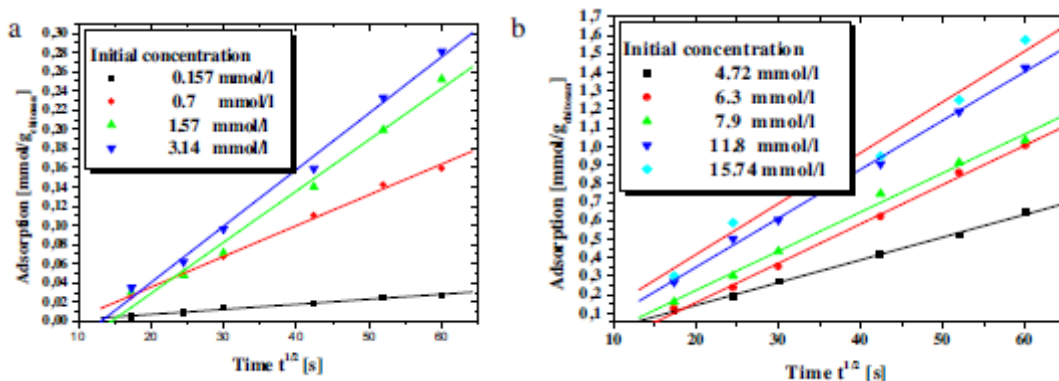


*Fig 17. process linearization (stage I)*

Initial concentration mmol/dm <sup>3</sup>	$k_t$ mmol/g s <sup>0.5</sup>	Diffusion coefficient $D_{As} = \frac{\pi k_t^2 a^2}{36 q_0}$ $\times 10^{10}$ [m <sup>2</sup> /s]
0.157	0.000527	0.71
0.785	0.00321	1.9
1.57	0.0054	1.89
3.15	0.0069	1.92
4.72	0.0122	1.3
6.3	0.020	1.14
7.9	0.021	1.3
11.8	0.026	1.1
15.7	0.02749	0.95

Tab 7. diffusion coefficients at stage I

In stage II, coefficients of diffusion are quite lower would respect to stage I (about two orders of magnitude), and it seems that, if concentration of adsorber is very low, the sorption process occurs on the surface of the adsorbent. In general, it can be stated that the coefficient of diffusion decreases if initial concentration increases.

Examples of experimental data, concerning the behavior at different concentrations, are shown in Figures from 18 to 20, which present curves obtained by use of the model; the description is quite good fitting and the error does not exceed 3%. Two parameters describe the process: the diffusion coefficient and the so called “surface process constant”, and this latter does not depend on concentration.  $16.9 \cdot 10^{-4}$  [1/s] is the mean value found for the kinetic constant regarding the surface process. Also, the Thiele modulus was calculated, as  $R^*(k_v/D_{ab})^{1/2} = 3$ . This is the maximum Thiele modulus value for the average reaction’s rate; when the Thiele modulus exceeds the value of 3, quick reactions are occurring, and this means that both processes play a crucial role for Cu(II) adsorption. In the end, it must be noted that, in the case of Cu(II) ions uptake by chitosan hydrogels, the diffusion process slows down the chemical surface reaction one.

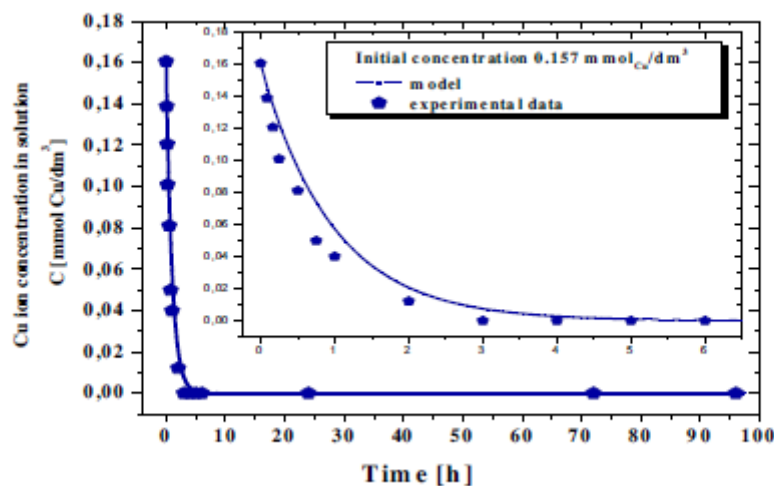


Fig 18. change in Cu(II) ions concentration,  $C_0 = 0,157$ mmol/L

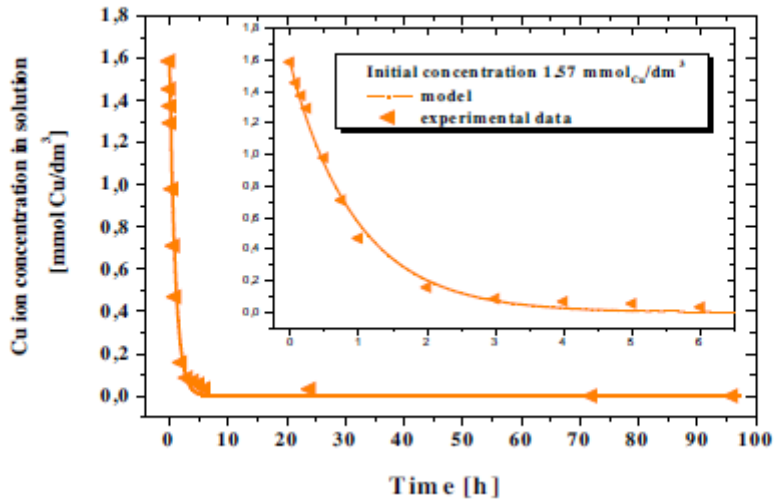


Fig 19. change in Cu(II) ions concentration,  $C_0 = 1,57 \text{ mmol/L}$

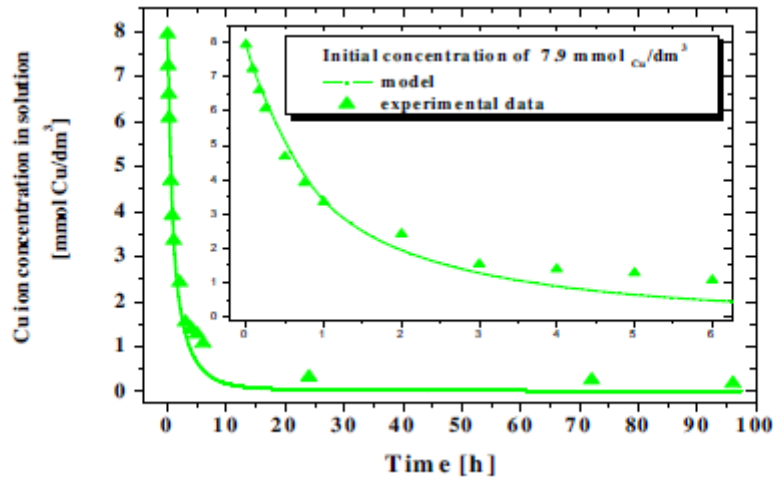


Fig 20. change in Cu(II) ions concentration,  $C_0 = 7,9 \text{ mmol/L}$

After 96h of process the equilibria were determined. Two cases are considered: varying ( $\text{pH}_0$ ) and constant ( $\text{pH}_k$ ) pHs. In the graphs, the fits of the models are shown (L, F, R-P), shown in Figures 21 and 22. The constant value of  $\text{pH}_k = 3.5$  is responsible for causing a partial desorption of copper ions, which adsorbed on chitosan.

This desorption may be caused by competition between Cu(II) ions and protons, protonating the amino groups. In both cases of constant and growing pH, the Langmuir-Freundlich fit is the best one, because it assumes symmetric and quasi-Gaussian distribution.

The Dubinin-Raduszkiewicz theory, which concerns the volume filling of micropores, justifies the diffusion as one of the processes occurring in the adsorption mechanism. The Langmuir isotherm presents a quite large error, but anyway its useful to estimate the strength of Cu(II) ions, related to the binding to amino groups. At  $\text{pH} = 3.5$ ,  $K$  value of Langmuir is the lowest: in this case the presence of protonated amino groups is dominant, so it's reasonable to think that the chelation mechanism is driven by non-protonated amino groups. In almost all cases very good correlation was obtained using the Redlich-Peterson isotherm in the description of equilibrium [13].

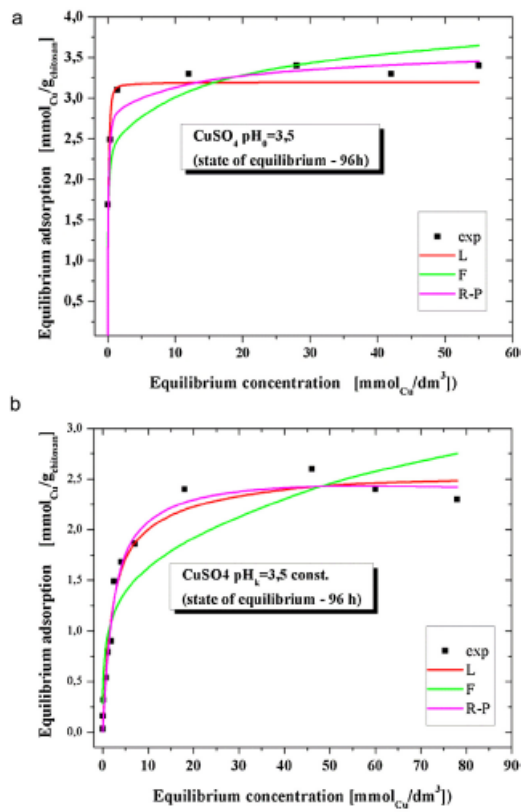


Fig 21.  $\text{pH} = 3.5$ , equilibria after 96h, a) growing  $\text{pH}$ , b) constant  $\text{pH}$

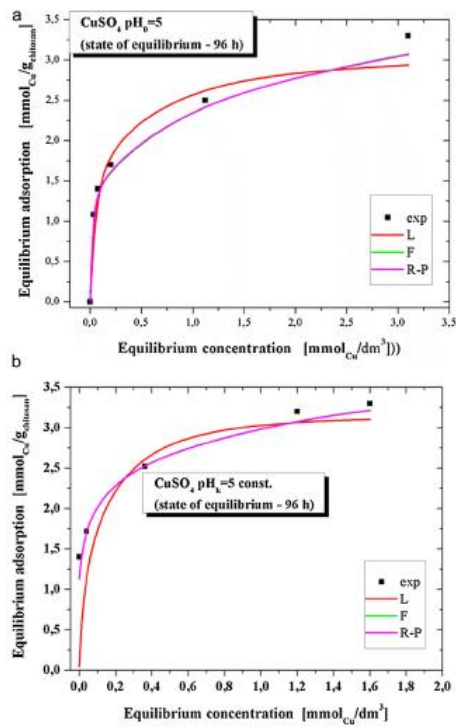


Fig 22.  $\text{pH} = 5$ , equilibria after 96h, a) growing  $\text{pH}$ , b) constant  $\text{pH}$

## 3 – EXPLOITATION OF POLYPHENOLS IN HEAVY METAL IONS' COMPLEXATION

### 3.1 – AN INTRODUCTION

In recent years, new possibilities have opened would respect to the use of conventional methods for the removal of heavy metal ions from wastewaters. Particularly, low cost and green adsorbents have increasingly been used, deriving from plant wastes, cellulosic wastes and more. These wastes can be chemically treated, and it was seen that chemical modifications improve the performances of these materials in the removal of heavy metals from wastewaters.

Chemicals used to remove heavy metal ions are numerous: oxidizing agents, bases, organic compounds, organic and mineral acids, and more., Cu, Zn, Pb, Ni are among the heavy metal which were successfully removed by use of these chemically treated plant wastes.

The industrialization is responsible for plenty of dangerous heavy metals to be released into the environment; industries like battery manufacture, mining, petroleum refineries, pesticides and more, are the cause for the presence in the environment of heavy metal like Zn, Ni, Cd. Pb, Cr and Hg [15, 16].

Heavy metals aren't biodegradable, so their accumulation constitutes a real danger for environment, public health and food chain. Methods used to uptake ions of these heavy metals are different: chemical precipitation, electro-flotation, ion exchange, solvent extraction, reverse osmosis and more [17].

Among all of these techniques, adsorption was found to be one of the most efficient methods. Low-cost adsorbents are those which are found to be very abundant in nature, easy to treat and originated from wastes of industries. Particularly, plants satisfy all of these requirements, [18]

However, there are pros and cons in the use of plants. The advantages are the following: low-cost, free availability, selectivity for specific metals, good adsorption capacity and possibility of regeneration. The disadvantages are the following (if chemically untreated): high TOC (total carbon organic carbon), as well as high BOD (biological chemical demand) and COD (chemical oxygen demand), [19, 20]. If too high, these three parameters can have a negative impact on aquatic life.

### 3.2 – PRECIPITATION OF COPPER(II) IONS BY PLANT POLYPHENOLS

*Proanthocyanidins* (condensed tannins), as for *ellagitannins*, are the most famous polyphenols deriving from plants [21]. It is common for them to accumulate into fruits, vegetables, bark, wood, and they play a crucial role in plants protection against dangers as pathogens and herbivores [22, 23]. Functional groups as *o*-dihydroxyphenyl are contained in these polyphenols, and this groups are capable of chelating ions of heavy metals [24, 25, 26, 27]. Nonetheless, this property is useful in terms of adsorbing the essential ions for plant growth, like Fe(III) [28, 29].

Tannins, and tannins-containing materials, are capable of chelating metal ions as preciously said, and this aspect has made them often used in several industries: anticorrosive primers for both non-ferrous metals and steels [30, 31], rheological modifiers in the field of mineral clays [32], anti-pollution agents for wastewaters [33], leather dying [34], writing inks [35] and more. It is important to remind that, in water, the complexes tannins make with metals precipitate [27].

Complexation of Cu(II) by tannins is studied in the field of treatments for wood preservation. Since most of the woods are acid between pH 4 and 5, pH 5 was chosen for these experiments to be carried out [36].

Precipitation of Cu depends on concentration of tannin and concentration of metal. It was found that, at a given Cu concentration, an optimal tannin concentration exists at which the maximum precipitation occurs (*Figure 23*). It is easy to understand that, if initial Cu concentration increases, then the concentration of tannins requested for precipitation increases as well. In fact, as Cu concentration increases, the concentration of tannins is no more sufficient and must be increased because the concentration of the buffer becomes not enough high to balance the acidification which follows to complexation.

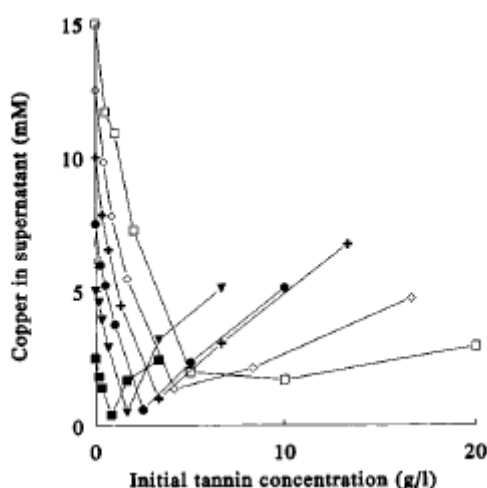


*Fig 23. chestnut tannin operating precipitation of Cu, at different initial Cu concentrations*

If buffer is not present, the solution pH reflects the typical acidity of the tannins. When acetate buffer is added, the pH increases to the one of the buffer, and the more the concentration of buffer is high, the more Cu precipitates (*Figure 24*). Pyridine buffer has the same effects of the acetate one. The difference between acetate and pyridine buffers can find explanation in the pKa of pyridine (5.23), higher than the one of acetic acid (4.76): particularly, pyridine buffering capacity is lower than the one of acetic acid.

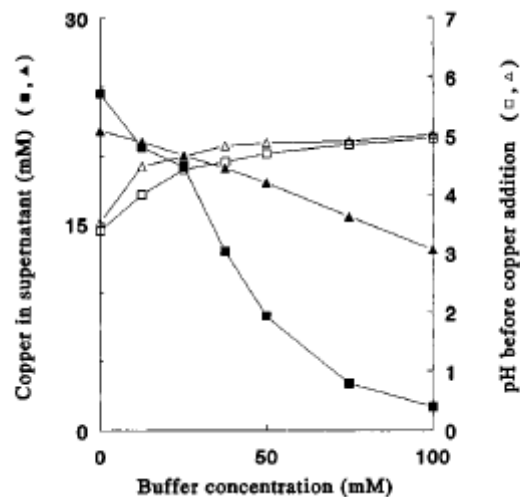


Fig 24. buffer concentration effect on initial pH of the solution, before Cu addition, and on Cu precipitation

Chestnut and tannic acid (hydrolyzable) and Pecan and Quebrancho tannins (condensed) were compared in Cu precipitation. All of these tannins have a maximum in Cu precipitation, while excess tannin concentration brings to some Cu and tannins to remain in the solution (Figure 25 a and b). Pecan tannins show the maximum precipitation capacity, while Quebrancho tannins show the minimum precipitation capacity.

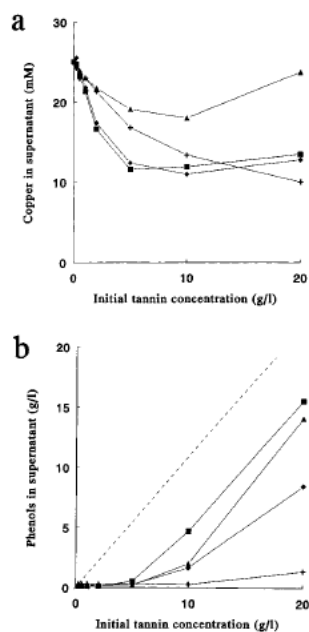


Fig 25. Cu/tannins precipitation by use of different tannins a) Cu in supernatant b) phenols in supernatant

Penta-*O*-galloyl- $\beta$ -D-glucose (Figure 26), as other various polyphenols of low molecular weight, was used to determine the mechanism of Cu complexation. Penta-*O*-galloyl- $\beta$ -D-glucose (Figure 27) gave the best results concerning Cu complexation while, for instance, it was observed no precipitation by *p*-hydroxybenzoic acid.

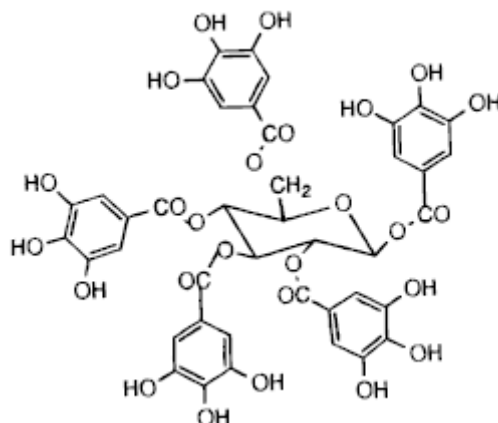


Fig 26. Penta-O-galloyl- $\beta$ -D-glucose

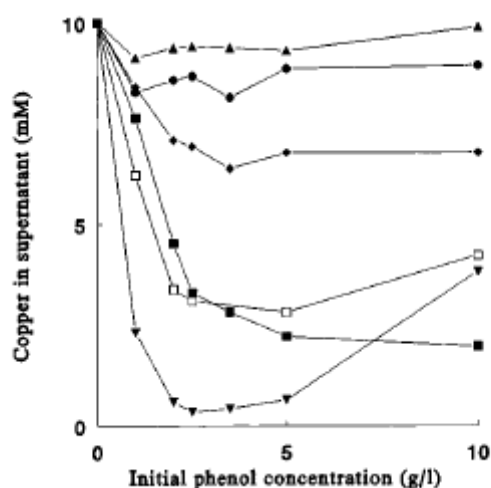


Fig 27. Cu complexation by different polyphenols: best results obtained by Penta-O-galloyl- $\beta$ -D-glucose (▼), no complexation by *p*-hydroxybenzoic acid (▲)

When the metal ion and the phenol form a complex, the solubility can change (both for Cu and the phenol itself), due mainly to three reasons: polarity of tannin's molecule decreases; an uncharged complex is formed; high MW complexes are formed. The latter one, which is the formation of high MW complexes, can be attributed to two reasons:

- Cu(II) catalyzes the oxidation of *o*-dihydroxybenzene (pH of 4.5-5.5) which occurs by molecular Oxygen; in this pH range, autoxidation does not take place, so that the resulting semiquinones or quinones first polymerize and then precipitate with Cu(II).
- Tannins like polyfunctional ones, which possess several *o*-dihydroxyphenyl functional groups, may form high MW complexes even without oxidation. Each molecule of the tannin can bind two or more ions, and each Cu(II) can form chelates, binding to *o*-dihydroxyphenyl groups, and these groups belong to two tannin molecules.

The complex formed can be investigated by the proportion between the metal ion ( $M^{2+}$ ) and Ligand (L) (Table 8). For instance, copper/catechol stoichiometry suggests that is possible the formation of a complex made by one Cu atom and two catechol molecules, but surely not the bis(catecholato) ( $L_2MH_4^{2-}$ ) [37], because it would have not precipitated due to its negative charge. Penta-*O*-galloyl- $\beta$ -D-glucose (Figure 26) has, as already seen, five *o*-dihydroxyphenyl functional groups. There are two possibilities: the formation of a high MW complex like  $M[(LH_{-10}M_3)-M]_n^{(2n-2)-}$  (Figure 28a); the formation of a neutral complex,  $LH_8M_4$  (Figure 28b).

ligand (L)	precipitation		precipitate			
	initial L concn (g/L)	initial Cu/L molar ratio	elemental analysis (% dry wt)		Cu/L molar ratio	Cu/ <i>o</i> -dihydroxyphenyl group
			C	Cu		
catechol	1.00	2.8	39.6	19.4	0.6	0.6
	5.00	0.6	42.1	16.9	0.5	0.5
	10.00	0.3	45.2	13.9	0.4	0.4
(+)-catechin	1.25	5.8	44.5	7.7	0.5	0.5
gallic acid	2.50	1.9	29.0	31.0	1.4	1.4
penta- <i>O</i> -galloyl- $\beta$ -D-glucose	1.25	18.8	28.5	15.0	3.9	0.8
chestnut tannin	2.50	9.3 <sup>a</sup>	30.5	18.0	4.6 <sup>a</sup>	0.9 <sup>a</sup>
	5.00	4.7 <sup>a</sup>	32.6	16.2	3.9 <sup>a</sup>	0.8 <sup>a</sup>
	15.00	1.6 <sup>a</sup>	38.2	9.1	1.8 <sup>a</sup>	0.4 <sup>a</sup>
pine tannin	4.0	1.8 <sup>b</sup>	43.3	5.1	0.9 <sup>b</sup>	0.9 <sup>b</sup>

<sup>a</sup> L as castalagin (M = 934) for calculation. <sup>b</sup> L as procyanidin unit (M = 288) for calculation.

Tab 8. elemental analysis for Cu/polyphenol precipitates

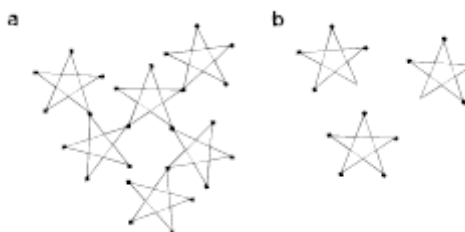
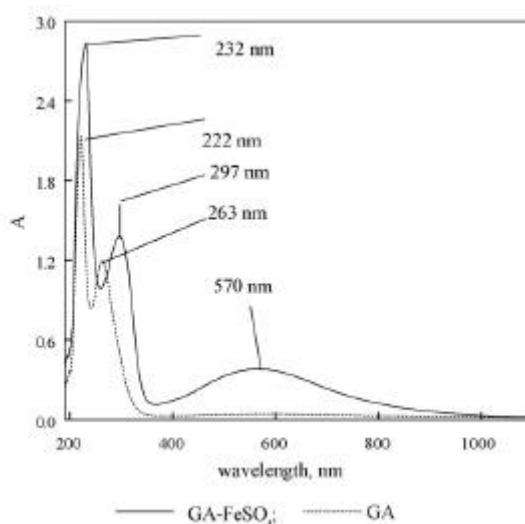


Fig 28. proposed structures for Cu/polyphenol precipitates, where (●) is the metal and (Δ) is the tannin molecule

### 3.3 – COMPLEXATION OF GALLIC ACID BY FE(II)

Gallic acid (3,4,5-trihydroxybenzoic acid) is a chemical widely used in several industries, like food, pharmaceutical and organic synthesis. Catechol (1,2-dihydroxybenzene) has been recently replaced by gallic acid (ultrapure) in the field of electronics as far as regarding the removal of photoresists and polymeric residues from a substrate, because GA is more environmentally friendly [38, 39]. Nonetheless, the fast development of integrated circuit industry made the demand of ultra-pure GA's quality to increase. Gallic acid is the raw material and becomes to be ultra-pure by processes such as filtration, resin adsorption and crystallization, and all of these processes share a common base as far as regarding the removal of the metal ion to be accomplished. The researchers [39, 40] have discovered that ions such as Ca(II) and Fe(II) are difficult to be removed. The complexation of GA with Fe(II) has been studied [41, 42, 43].

A complex between Fe(II) and GA is formed, and it is proved by the UV-VIS spectroscopy. GA has an adsorption band at wavelength equal to 263 nm, but this one undergoes a shift of 34nm when the complex is formed. The wavelength peak of the complex is at 570 nm (*Figure 29*)



*Fig 29. UV-Vis spectroscopy of GA and the complex of GA-Fe(II)*

The stoichiometry of the complex was determined by Job's method and was found to be 1:1, and in the pH range investigated (from pH 3,5 to pH 5,5), pH was seen to lightly influence stoichiometry itself. The complex GA-Fe(II) forms through a three-step process, involving opposite charged species [41, 42].

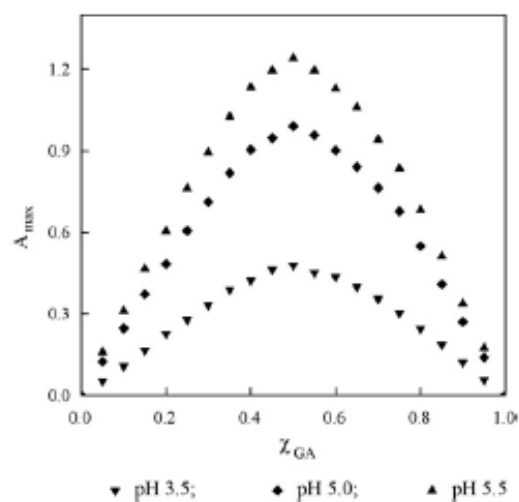
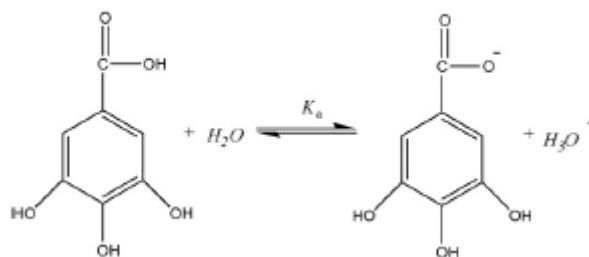


Fig 30. stoichiometry of the complex

Step 1: Acid–base dissociation of GA.



Step 2: Ionization of  $\text{FeSO}_4$ .



Step 3: Ionic reaction between the GA anion and metal cation.

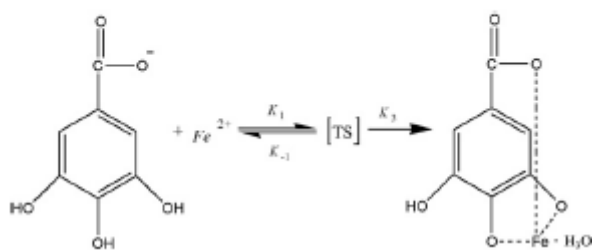


Fig 31. complex formation steps

The free activation energy (in water) was determined through kinetic experiments at different temperatures, and it was found to be equal to  $71.64 \text{ kJ mol}^{-1}$ . The hypothesis of a reaction between two opposite charged species is supported by the fact that, increasing the permittivity of the medium, the reaction rate increases. The mechanism proposed is the one represented in *Figure 31*, and the third step is found to be the rate-determining step.

### 3.4 – ALUMINUM-POLYPHENOL COMPLEXES

The presence of Al in fields can be dangerous to plants because it inhibits the growth of the roots. [44] Most of world's soils (about 50%) are acidic, especially in tropical regions. [45] Crops like rubber or tea easily grow in these fields, but the cultivation of other crops such as grain and legumes results to be difficult in acidic soils because of the presence of Al. [44, 45, 46] Some Al-resistant plants exist and they secrete a chelating agent, preventing Al adsorption, and this ability is called "exclusion", while another ability of plants, called "tolerance", consists in the chelation of Al to fix this metal into the cells, or chemically turning it into a non-toxic form.

[44] Polyphenols have been studied and became famous as Al-chelating agents. [47] Some polyphenols, like catechin and rutin, are found to be not exudated by the plant, yet they remain in the root and work as Al-detoxifying agents. [48] High MW polyphenols such as tannins have been identified to be Al-detoxifying agents in plants such as Camphora. [49] Eucalyptus camaldulensis is a plant which uses oenothein B (a gallate-derived polyphenol) to chelate Al. Oenothein B (OeB) derives from GA metabolism: particularly, it derives from the core metabolite PGG. [50, 51] PGG or MeG are cheaper than OeB, but OeB is more used because it shows a higher stoichiometric ratio, in terms of Al binding. Purified polyphenols such as MeG, PGG, and OeB (*Figure 32*) have been used to characterize the interaction between Al and polyphenols in acidic medium.

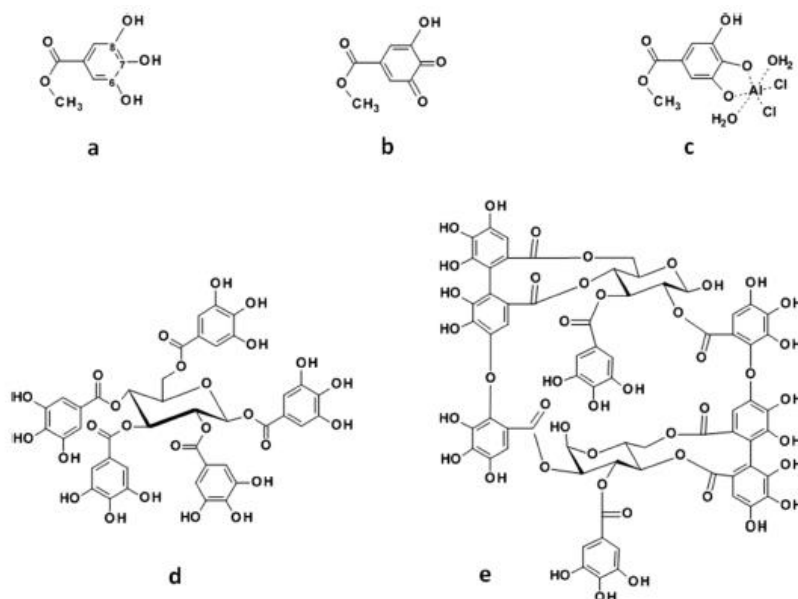


*Fig 32. a) MeG (methyl-gallate), b) MeG's quinone, c) the complex Al-MeG (based on simulation), d) PGG (penta-galloyl glucose), e) OeB (oenothein B)*

Reaction of complexation between polyphenols and Al occurred at pH 6. Titration with  $\text{AlCl}_3$  was made in a buffered solution (at pH 6), and this showed the spectral changes for polyphenols. Products were red-shifted but, as far as regarding Al complexes, the shifts were smaller would respect to the deprotonated polyphenols (*Table 9*). Spectra of Al-MeG complexes were examined, but only one possible complex resulted to be corresponding to the experimental spectrum (*Figure 33b*). For PGG, the titration with Al is dependent on Al:polyphenol ratio and it is seen through one isosbestic point at 298 nm (low ratio) and one more at 292 nm (ratio > 1.5) (*Figure 33d*).

	$\lambda_{max}$ (nm $\pm$ 1 nm)		
	methyl gallate	pentagalloyl glucose	oenothein B
Protonation State			
L	270	280	267
L <sup>-</sup>	318	325	316
L <sup>-2</sup>	279		
Aluminum Complex pH 6			
AlL	304		
Al <sub>3</sub> L <sub>2</sub>		305	307
Al <sub>2</sub> L		315	
Aluminum Complex pH 4			
AlL		281	270

Tab 9. spectral features of complexes ( $Al_mL_n$ ) and polyphenols (L) at pH 6 and pH 4

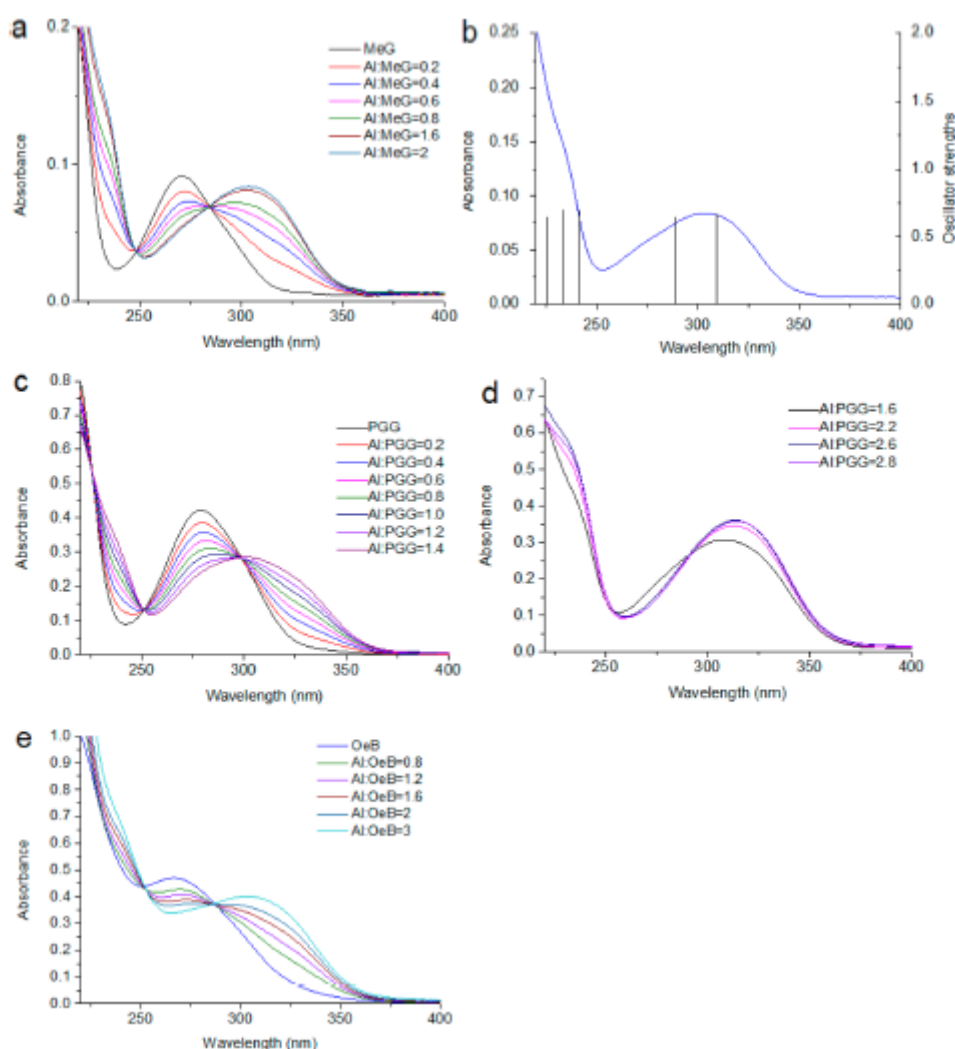


Fig 33. spectra of  $Al^{3+}$  titrated polyphenols a) MeG b) Al-MeG complex c) PGG d) PGG for a ratio  $Al:PGG > 1.5$  e) OeB

For OeB, titration shows a spectral change by a single isosbestic point (at 287 nm) (Figure 33e), then the product was red-shifted would respect to the parent compound (Table 9, Figure 33e). The stoichiometric ratios were analyzed by Job's method (the complex is indicated by  $Al_mL_n$ , while the ligand is indicated by L) by continuous variations except for PGG at pH 6, because a mixture with two or more complexes cannot be analyzed by this method. [52] At pH 6, MeG formed a 1:1 complex, while OeB formed a  $Al_3L_2$  complex (Figure 34 a,b).

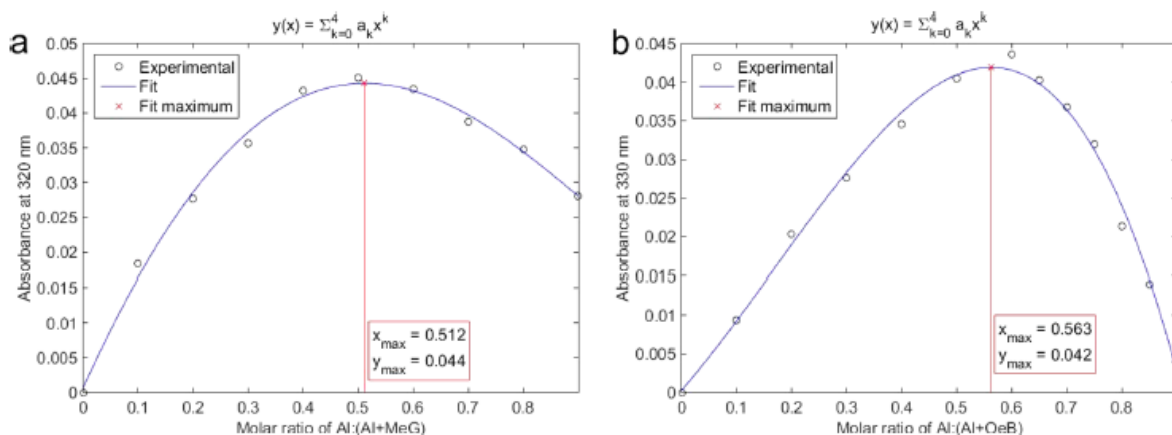


Fig 34. Job's method for a) MeG and b) OeB

Tahare et al. [53] noticed that OeB forms insoluble complexes with Al at pH 4 and hypothesized that OeB is able to detoxify Al by precipitating it into the vacuoles of the plant. All of the analyzed polyphenols (MeG, OeB, PGG) form, at pH 4, non-soluble complexes with Al (Table 10), and the results obtained in Job's plots have been confirmed by the chemometric software: MeG forms 1:1 complexes, while OeB forms 3:2 complexes; in the end, PGG forms  $Al_3L_2$  complexes or  $Al_2L$  complexes, respectively for high or low Al concentrations.

Al:L (mole:mole)	visual precipitation		
	methyl gallate	pentagalloyl glucose	oenothain B
0	no	no	no
0.5	no	yes	no
1	no	yes	yes
2	no	yes	yes
4	no	no	no

Tab 10. Solubility of Al:polyphenol complexes

## 4 – MATERIALS AND METHODS

### 4.1 – MATERIALS

All chemicals were purchased by Sigma-Aldrich, except when differently specified: low molecular weight chitosan, whose molecular weight ranges from 50.000 to 190.000 Da, based on viscosity, and the degree of Deacetylation lies between 75% and 85%, while viscosity lies between 20 cP and 300 cP; Tannic Acid (Tannin, Gallotannin); Irgacure 2959 (2-Hydroxy-4'-(2-hydroxyethoxy)-2-methylpropiophenone); Acetic Acid (CH<sub>3</sub>COOH) 96% pure was used to dissolve chitosan; Methacrylic Anhydride (CH<sub>2</sub>=C(CH<sub>3</sub>)CO)<sub>2</sub>O; CuSO<sub>4</sub> anhydrous powder 99% pure. Aqueous solutions for chitosan hydrogels were prepared using distilled water, while aqueous solutions added with CuSO<sub>4</sub> were prepared using ultrapure water (milliQ).

### 4.2 – METHACRYLATION OF CHITOSAN

Raw chitosan must undergo methacrylation to get methacrylated chitosan, which will then be UV-cured into chitosan hydrogels. The molecular weight of one repetitive unit of chitosan is equal to 322 g/mol so, for a given initial amount of raw chitosan (i.e. 1 g), the amount of Methacrylic Anhydride is calculated, and then a molar excess of 20 times is applied. Particularly, to methacrylate 1g of raw chitosan, 9,7 g of Methacrylic Anhydride are needed.

The solution used to methacrylate chitosan is an acidic aqueous solution at 2%wt Acetic Acid, and chitosan must be at 1,5%wt of this solution. The following quantities are used:

- 1 g chitosan
- 64,68 g distilled water
- 1,32 g acetic acid

This solution is put to stir at 700 rpm, at 50 °C, for 4 hours. When the solution reaches 50°C, methacrylic anhydride is added. After 4 hours passed, the solution obtained (white and lightly viscous, reminding milk) is poured into thin cellulose balloons, to undergo a purification (dialysis) process: these balloons are put in distilled water for a period of 4-7 days. The chitosan solution coagulates and after the purification process it is transferred to a freeze-dryer to be lyophilized. After being lyophilized, methacrylated chitosan assumes a soft, cloudy form, like a piece of cotton or wool.

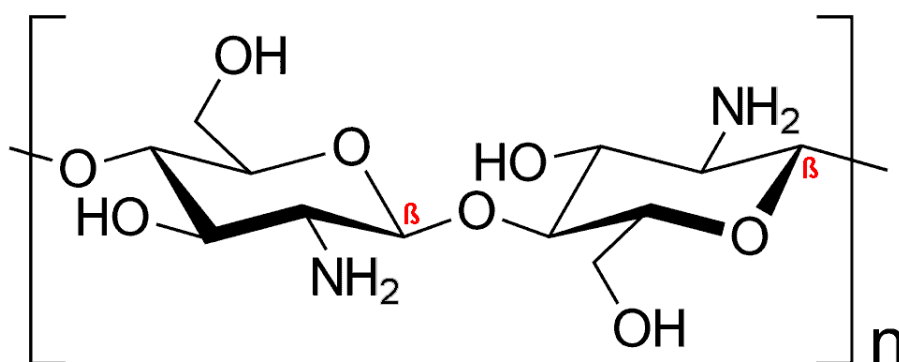
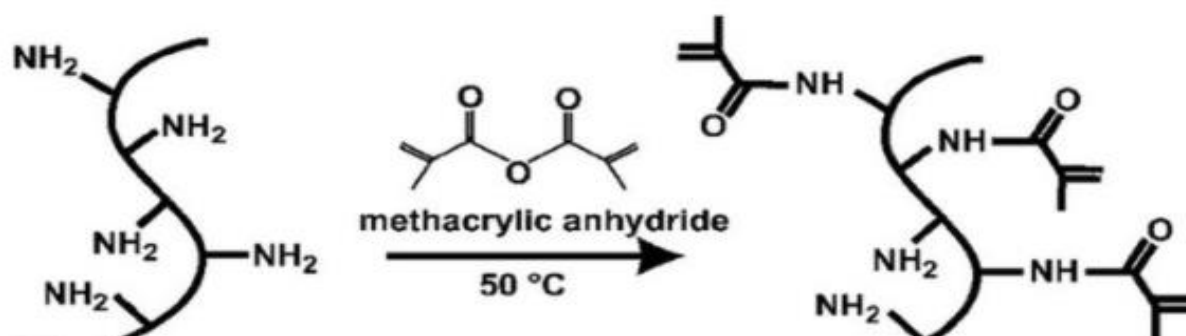


Fig 35. Chitosan's repetitive unite



*Fig 36. Raw chitosan (left) and methacrylated chitosan after lyophilization (right)*



*Fig 37. Schematic representation of methacrylation of raw chitosan*

### 4.3 – HYDROGEL PREPARATION AND FUNCTIONALIZATION WITH TANNIC ACID

The solution prepared to UV-cure chitosan presents the same proportions of the solution used to methacrylate chitosan. This means that a solution at 2%wt of Acetic Acid in distilled water is prepared, and this solution must be at 1,5%wt of methacrylated chitosan.

To make chitosan hydrogels, no more than 300 mg of chitosan are solubilized each time, because it is not recommended for excess solution to remain (it could undergo a degradation process which would negatively influence hydrogel's properties, or it could undergo an initial curing if exposed to light). The following quantities are used:

- 300 mg methacrylated chitosan
- 394 mg acetic acid
- 19,3 g distilled water

This solution is put to stir at room temperature and, after a good solubilization is reached, the photoinitiator is added (Irgacure 2959). Quantity of photoinitiator must be 2%wt of the weight of chitosan (so in this case, 6 mg must be added to the solution).

After adding the photoinitiator, stirring is carried out until a good solubilization is reached, but this time the glass must be covered in tinfoil, to avoid incipient curing due to sunlight or illumination of the laboratory.

The solution is ready to be UV-cured. Little quantities of liquid (about 1 mL for each sample) are taken by use of a Pasteur pipe. The liquid is poured into cylindrical molds and cured using a UV-lamp. The distance between the mold and the source of UV light is chosen to be 4 cm, and the Energy at this height is equal to 114,05 mW/cm<sup>2</sup>. Curing time needed for each sample is equal to 6 minutes.

After UV-curing process, hydrogels are put into distilled water to be purified from acetic acid, and this step requires 3 days (the solution in which samples are immersed is replaced with fresh water twice per day). After purification, the hydrogels are dried out under the Adsorption Hood.



*Fig 38. A chitosan hydrogel as just UV-cured*



*Fig 39. UV-lamp used to UV-cure chitosan samples*

The hydrogels are allowed to dry and then are functionalized with Tannic Acid (TA). Samples are immersed in a solution 15 mg/mL of TA, and these samples are placed in oven at 37°C for 3h. After 3h, they are taken out of the oven and allowed to dry under the Adsorption Hood.

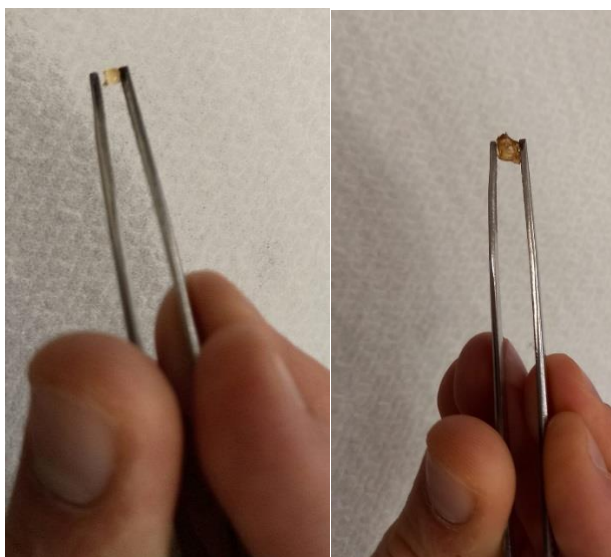


*Fig 40. dried hydrogels before (left) and after (right) functionalization with TA*

## 4.4 – CHARACTERIZATION

### Swelling Test

Chitosan hydrogels were immersed in distilled water and their weight was scaled at precise time intervals to evaluate the amount of time required for samples to be completely swollen. Each time, the samples are taken out of the bath, gently dried by dabbing them on a paper towel, scaled and then immersed again.

### FTIR – Fourier transform Infrared Spectroscopy

Fourier transform infrared spectrometer (FTIR) was used to investigate the functional groups of samples of chitosan, functionalized chitosan (with TA) and samples of chitosan after chelation of Cu(II) ions from CuSO<sub>4</sub> solutions. FTIR is among the most famous instruments used in infrared spectroscopy. The reasons why it is preferred among other techniques are many: non-destructiveness for the sample, ease of use, speed, high sensitivity. The working principle of FTIR analysis is based on the fact that a molecule only absorbs specific energies/frequencies of infrared radiation: different molecules will have different spectra, so FTIR can be used to identify specific molecules or functional groups.

A FTIR spectrometer uses an interferometer for the measurement of the energy transmitted to the sample, and radiation is emitted by a black body. In the end, through the sample's surface, the interferogram is transmitted.

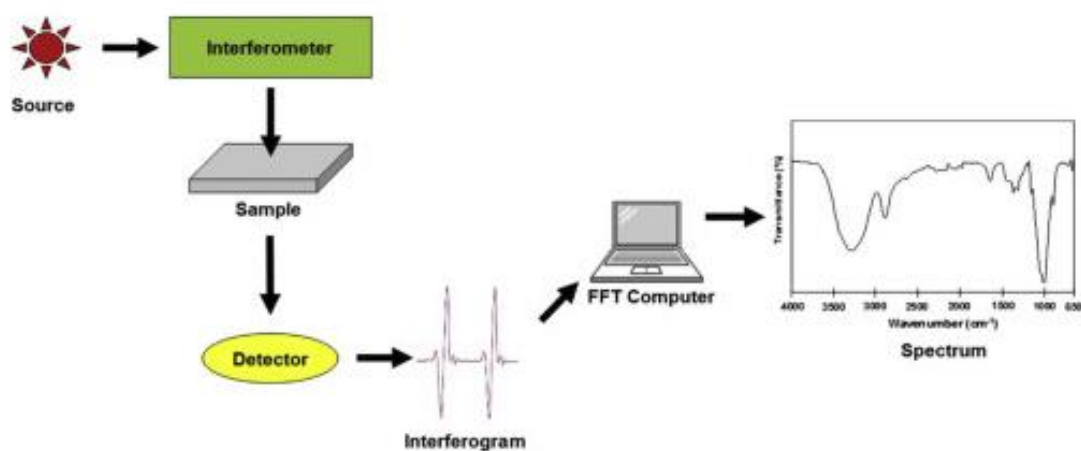


Fig 41. Block diagram of a FTIR spectrometer

FTIR spectra were obtained for samples of raw chitosan, methacrylated (MA) chitosan (before and after Cu<sup>2+</sup> adsorption) and methacrylated chitosan (MA) functionalized with Tannic Acid (before and after Cu<sup>2+</sup> adsorption). The interpretation of these spectra was based on previous works [54]. The comparison between spectra of raw chitosan and methacrylated chitosan can be useful to investigate if the methacrylation process correctly occurred (methacrylated chitosan shall present peaks related to the C=C double bond and the C=O double bond, which are not present in raw chitosan molecules).

## TGA – Thermogravimetric analysis

Thermogravimetric analysis or thermal gravimetric analysis (TGA) is a method of thermal analysis in which the mass of a sample is measured over time as the temperature changes. This measurement provides information about physical phenomena, such as phase transitions, absorption, adsorption-desorption, as well as chemical phenomena including chemisorption, thermal decomposition, and solid-gas reactions (e.g., oxidation or reduction).

Thermogravimetric analysis (TGA) is conducted on an instrument referred to as a thermogravimetric analyzer. A thermogravimetric analyzer continuously measures mass while the temperature of a sample is changed over time. Mass, temperature, and time are considered base measurements in thermogravimetric analysis while many additional measures may be derived from these three base measurements.

A typical thermogravimetric analyzer consists of a precision balance with a sample pan located inside a furnace with a programmable control temperature. The temperature is generally increased at constant rate (or for some applications the temperature is controlled for a constant mass loss) to incur a thermal reaction. The thermal reaction may occur under a variety of atmospheres including ambient air, vacuum, inert gas, oxidizing/reducing gases, corrosive gases, carburizing gases, vapors of liquids or "self-generated atmosphere"; as well as a variety of pressures including: a high vacuum, high pressure, constant pressure, or a controlled pressure.

The thermogravimetric data collected from a thermal reaction is compiled into a plot of mass or percentage of initial mass on the y axis versus either temperature or time on the x-axis. This plot, which is often smoothed, is referred to as a TGA curve. The first derivative of the TGA curve (the DTG curve) may be plotted to determine inflection points useful for in-depth interpretations as well as differential thermal analysis.

A TGA can be used for materials characterization through analysis of characteristic decomposition patterns. It is an especially useful technique for the study of polymeric materials, including thermoplastics, thermosets, elastomers, composites, plastic films, fibers, coatings, paints, and fuels.

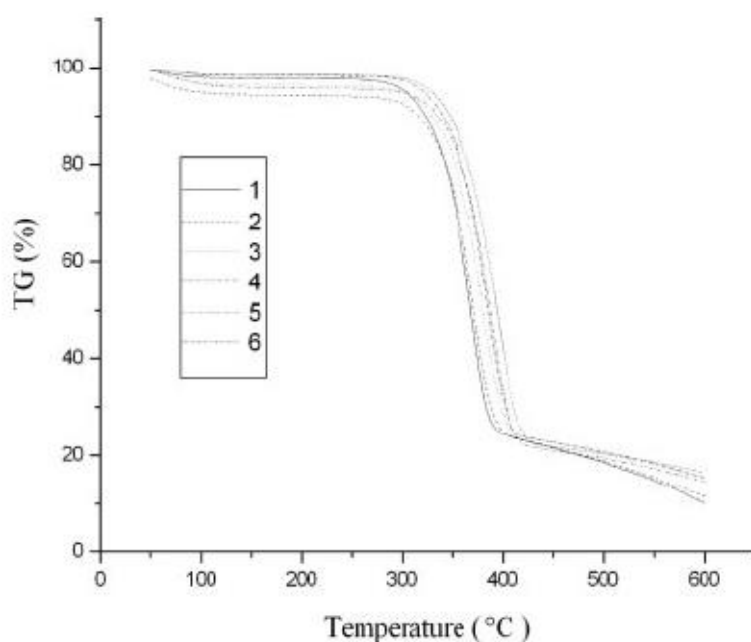


*Fig 42. Example of a TGA of chitosan samples at six different rates*

## DSC – Differential Scanning Calorimetry

The Differential scanning calorimetry (DSC) is a thermo-analytical technique in which the difference in the amount of heat required to increase the temperature of a sample and reference is measured as a function of temperature. Both the sample and reference are maintained at nearly the same temperature throughout the experiment. Generally, the temperature program for a DSC analysis is designed such that the sample holder temperature increases linearly as a function of time. The reference sample should have a well-defined heat capacity over the range of temperatures to be scanned.

The basic principle underlying this technique is that when the sample undergoes a physical transformation such as phase transitions, a different amount of heat will need to flow to it than the reference to maintain both at the same temperature. Whether less or more heat must flow to the sample depends on whether the process is exothermic or endothermic. For example, as a solid sample melts to a liquid, it will require more heat flowing to the sample to increase its temperature at the same rate as the reference. This is due to the absorption of heat by the sample as it undergoes the endothermic phase transition from solid to liquid. Likewise, as the sample undergoes exothermic processes (such as crystallization) less heat is required to raise the sample temperature. By observing the difference in heat flow between the sample and reference, differential scanning calorimeters measure the amount of heat absorbed or released during such transitions. DSC may also be used to observe more subtle physical changes, such as glass transitions. It is widely used in industrial settings as a quality control instrument due to its applicability in evaluating sample purity and for studying polymer curing.

The result of a DSC experiment is a curve of heat flux versus temperature or versus time. There are two different conventions: exothermic reactions in the sample shown with a positive or negative peak, depending on the kind of technology used in the experiment. This curve can be used to calculate enthalpies of transitions. This is done by integrating the peak corresponding to a given transition. It can be shown that the enthalpy of transition can be expressed using the following equation:

$$\Delta H = K * A$$

where  $\Delta H$  is the enthalpy of transition,  $K$  is the calorimetric constant, and  $A$  is the area under the curve. The calorimetric constant will vary from instrument to instrument and can be determined by analyzing a well-characterized sample with known enthalpies of transition.

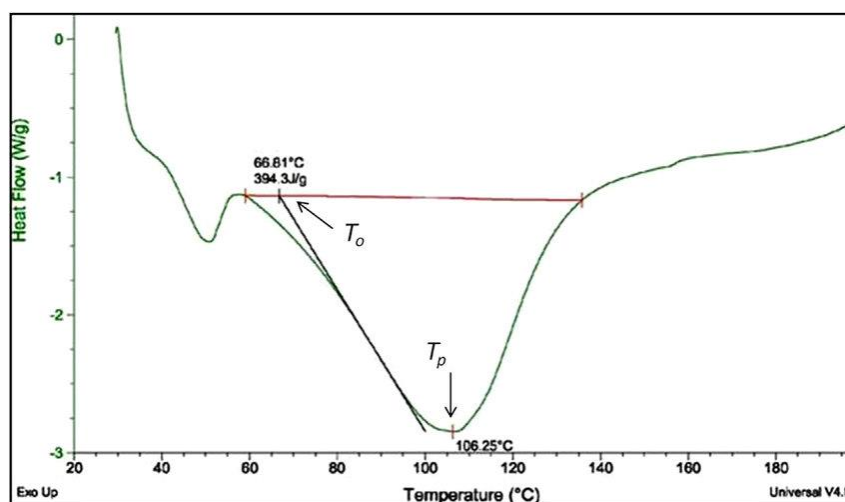


Fig 43. Example of a DSC thermogram showing a chitosan sample

## UV-Vis Spectroscopy

UV-visible spectrophotometry is the technique of adsorption (or reflectance) spectroscopy referring to part of the UV spectrum and the full visible region of the electromagnetic spectrum. Visible light is used, and the perceived color depends on the adsorption/reflectance in the visible range. This means that chemical species can be detected through this spectroscopic technique. Atoms/molecules undergo atomic transitions (from the ground state to the excited state) in the UV-visible range. In this case, it is easy to understand that adsorption spectroscopy is complementary to fluorescence spectroscopy, in which electrons decay from the excited state to the ground one.

UV-visible spectroscopy is used to determine the quantity of an analyte (i.e. transition metal ions, biological macromolecules, organic compounds), usually carried out in solutions; anyway, UV-visible spectroscopy is applicable to gases and solids too.

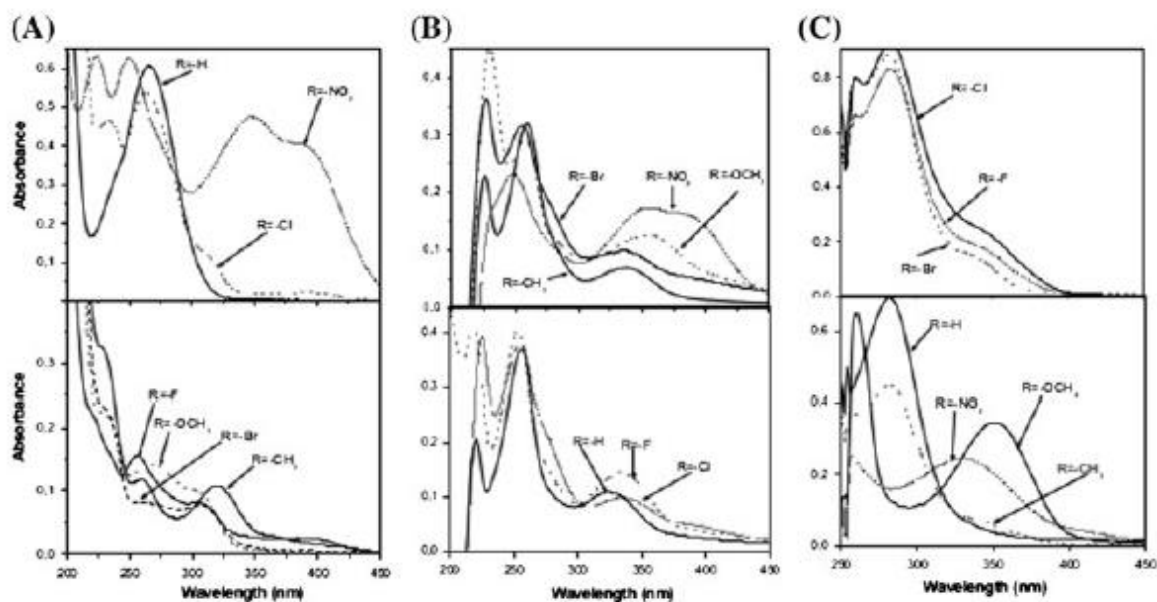


Fig 44. UV-Vis spectra of chitosan-metal complexes

## EDS-SEM (Energy Dispersive spectroscopy – Scanning electron microscopy)

In a SEM machine, the image is generated by the interaction of electrons with atoms of the sample at different depths; signals can be different: back-scattered electrons (BSE), secondary electrons (SE), absorbed current and cathodoluminescence (CL).

The energy of SEs is low (about 50 eV), so their mean free path is limited to few nanometers. In fact, BEs derive from the first nm of the sample, and mainly come from the impact area of the beam

Back-scattered electrons (BSE) are scattered elastically from the sample, they come from deeper regions of the sample: their energy is higher than the one of BEs, but the image resolution is lower. The intensity of BSEs signal is correlated with the atomic number (Z): this means that the distribution of different elements can be investigated along the sample.

X-rays are emitted when an incident electron undermines an inner shell electron, filling the vacant shell with a higher energy electron, and releasing energy. Energy-dispersive X-ray spectroscopy (EDS) can be used to identify elements and their abundance/distribution in the sample. SEM micrographs show a characteristic 3D appearance, useful to understand the structure of the sample. Energy-dispersive X-ray spectroscopy (EDS) is used to characterize the sample from a chemical/elemental point of view; the interaction occurs between the sample and an X-ray source. The working principle is that each atomic species has a unique atomic structure, so it possesses a unique set of peaks in the emission spectrum. An electron beam is focused on the sample: at rest, atoms are in an unexcited state. The incident beam causes the excitation of a ground state electron, ejecting it from the shell and generating a hole; at this point, a higher energy electron (from an outer shell) fills the lower hole, and the Energy difference between these two levels is released as X-rays.

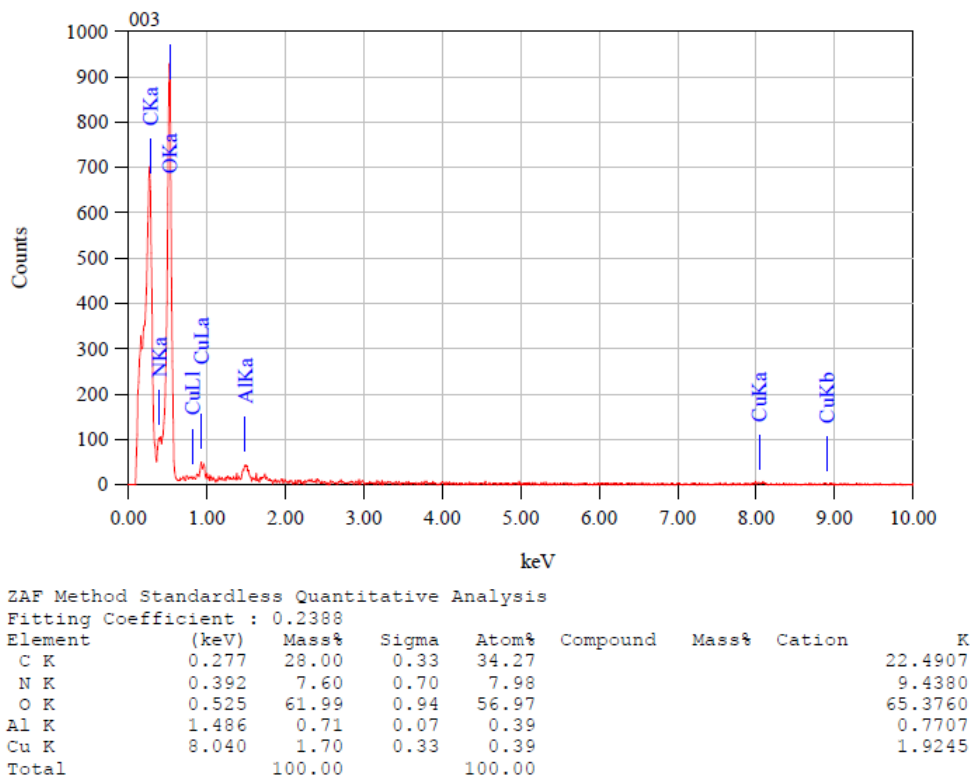


Fig 45. EDS spectrum of a chitosan sample

## 5 – RESULTS AND DISCUSSION

### 5.1 – FUNCTIONALIZATION OF CHITOSAN

As previously said, chitosan samples obtained by UV-curing were functionalized with polyphenols (in this case, Tannic Acid was chosen) to enhance the capability of removing heavy metal ions from wastewaters. Chitosan samples were allowed to dry after UV-curing, and then they were immersed in a solution at 15 mg/mL of Tannic Acid.

The capability of chitosan samples to restrain Tannic Acid was verified. Empirically, it can be shown that the sample changes its color from yellow to auburn, which is the typical color of a solution of Tannic Acid.

The presence of Tannic Acid in the sample can be however verified through a FTIR process. FTIR spectra of chitosan samples were obtained, and a FTIR process was carried out on Tannic Acid itself, to verify that the spectrum obtained in laboratory corresponds to the spectra which can be found in other works [55].

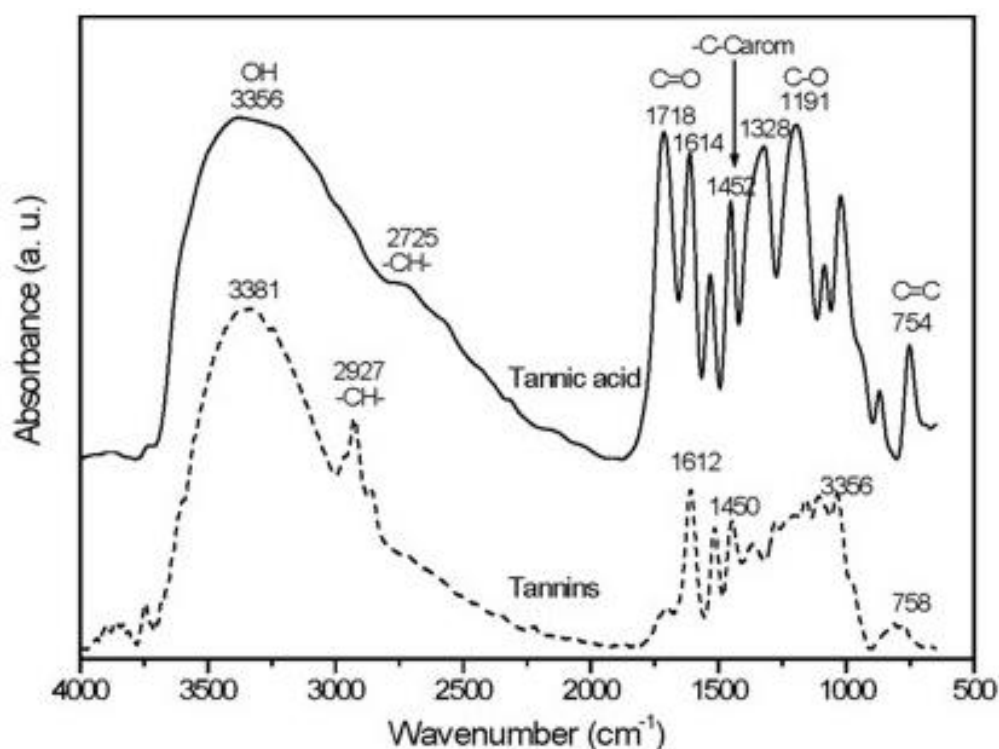


Fig 46. FTIR of Tannic Acid taken from literature

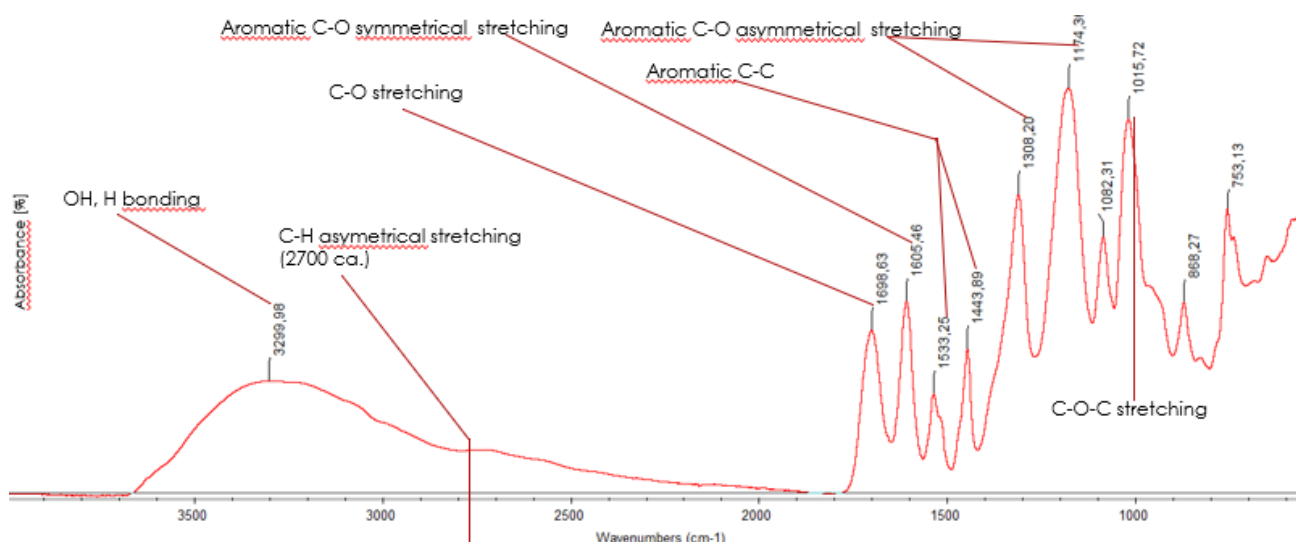


Fig 47. FTIR of Tannic Acid taken in laboratory

It was verified that the Tannic Acid used in this work was not affected by any kind of degradation, since the spectra match and the functional groups detected are the same.

Spectra of Tannic Acid and chitosan functionalized with Tannic Acid were compared, to investigate the presence of matching peaks and superimposable spectra, overall, for the tannic acid and the functionalized sample.

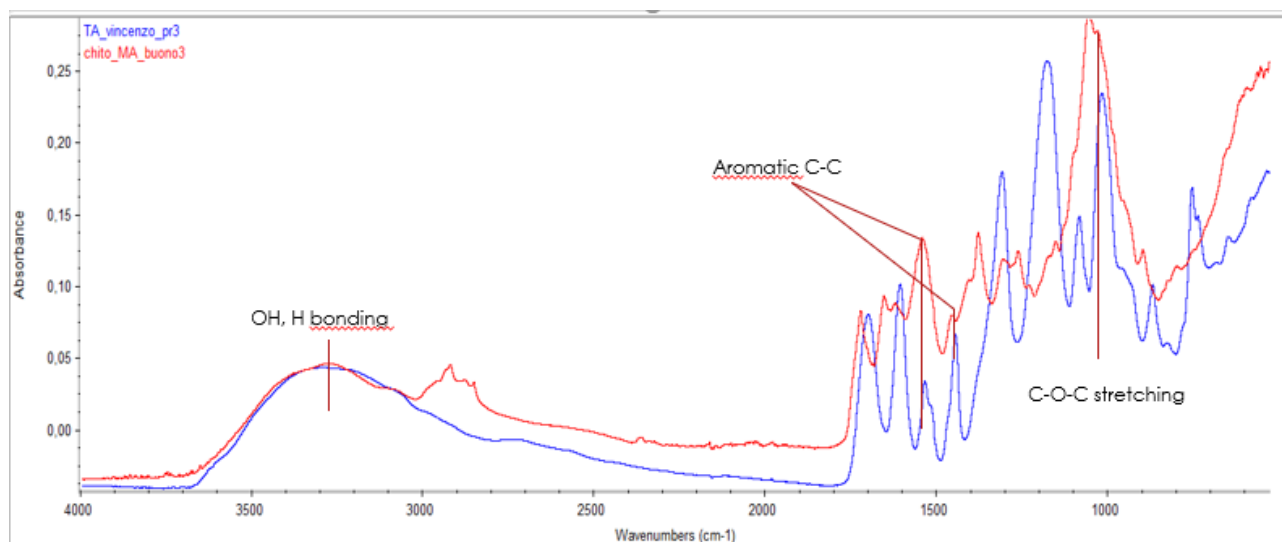
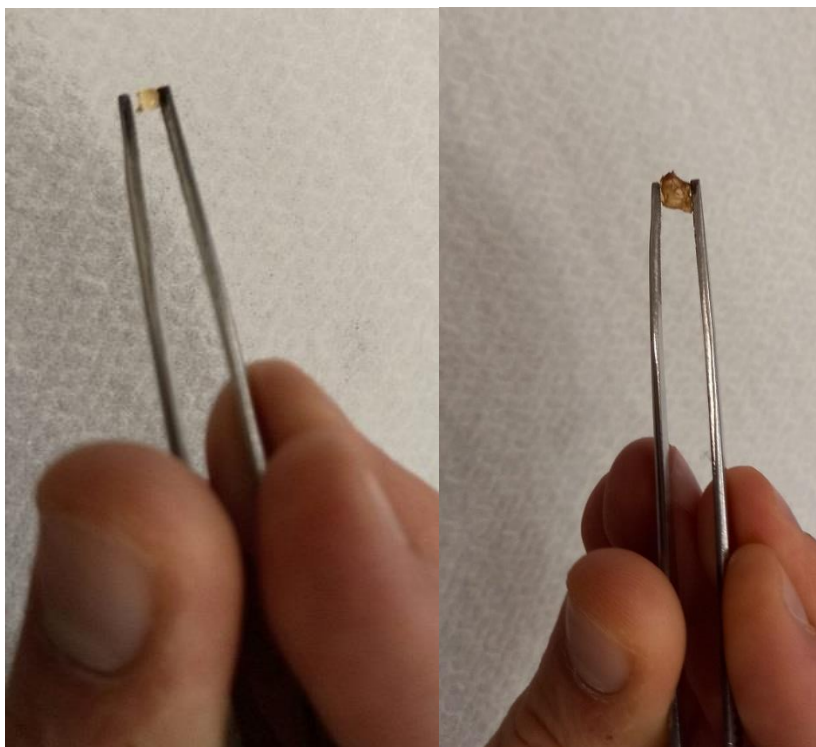


Fig 48. FTIR of tannic acid (blue) and a sample of chitosan functionalized with tannic acid (red); in this view, the curve for chitosan was upward shifted to be superimposed to Tannic Acid (TA) curve. The success of functionalization is visible as most of the peaks for TA are present even in chitosan's curve (red thin lines show the matching peaks, while some other peaks are lightly shifted)



*Fig 49. The change in color from yellow (left) to auburn (right) for a chitosan sample functionalized with Tannic Acid*

## 5.2 – PREPARATION AND CHARACTERIZATION OF CHITOSAN HYDROGELS

### Methacrylation process

A schematic process for methacrylation of raw chitosan is shown in *Figure 50*: amino groups of chitosan ( $-\text{NH}_2$ ) are involved in the methacrylation, while in methacrylic anhydride a bond is broken on the central oxygen atom; the amino group gets deprotonated (losing one hydrogen atom) and the resulting dangling bond is resolved by the Methacrylate functional group.

The free hydrogen radical binds to the reactive part of the methacrylic anhydride molecule to form Methacrylic Acid.

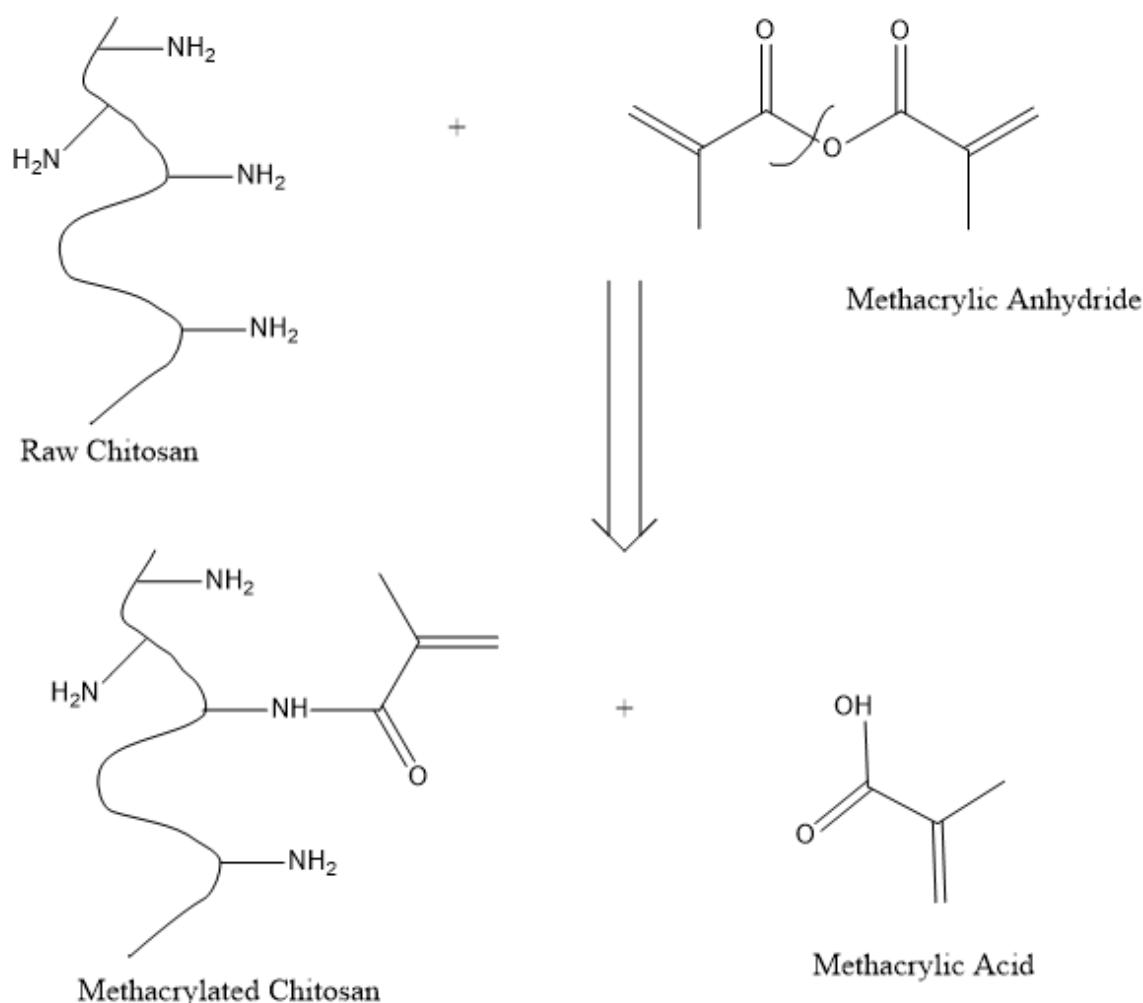


*Fig 50. Schematic representation of methacrylation process for chitosan (curve line on Methacrylic Anhydride indicates the bond which breaks)*

The success of the methacrylation process can be investigated by use of FTIR spectroscopy. What has to be verified is the presence of functional groups such as the  $\text{C}=\text{O}$  bond and the  $\text{C}=\text{C}$  bond (which were not present in raw chitosan). FTIR spectra of raw chitosan and methacrylated chitosan were compared in Figure 43, and methacrylated chitosan shows both the peaks for the  $\text{C}=\text{O}$  bond ( $1700\text{ cm}^{-1}$ ) and for the  $\text{C}=\text{C}$  bond ( $815\text{ cm}^{-1}$ ).

## FTIR – Fourier transform Infrared Spectroscopy

FTIR spectroscopic technique is used to investigate the chitosan samples and the occurrence of changes in their spectra, speaking about shifting and intensity of the peaks. Changes in the peaks of spectra can give useful information on which can be the preferential sites for Cu binding or can either give information on the binding mechanism.

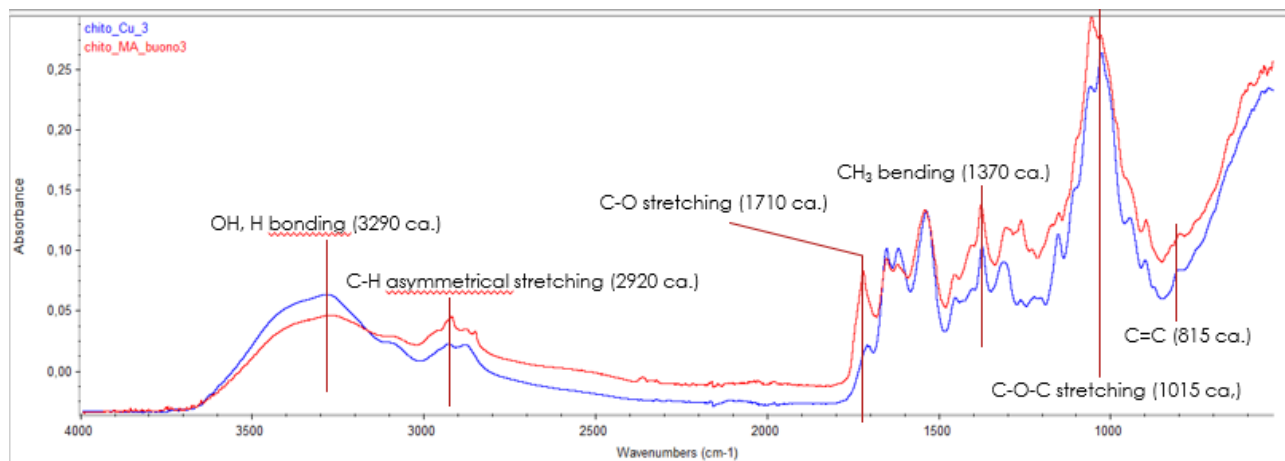


Fig 51. FTIR spectra for methacrylated chitosan hydrogels before (red) and after (blue) Cu(II) adsorption

The main peaks for methacrylated chitosan are shown in *Figure 51*. The same sample was investigated before and after Cu(II) adsorption. Particularly, this sample was immersed in a solution of Cu(II) ions, at a concentration equal to 10 ppm, for a time of four days (96 hours). The peaks result to be not shifted, while a change in intensity is visible for almost all peaks.

Significant changes of intensity can be seen for peaks at 1710 cm<sup>-1</sup> (attributed to C=O stretching) and at 815 cm<sup>-1</sup> (attributed to C=C). It can be hypothesized that these functional groups play a role in the chelation of Cu(II) ions.

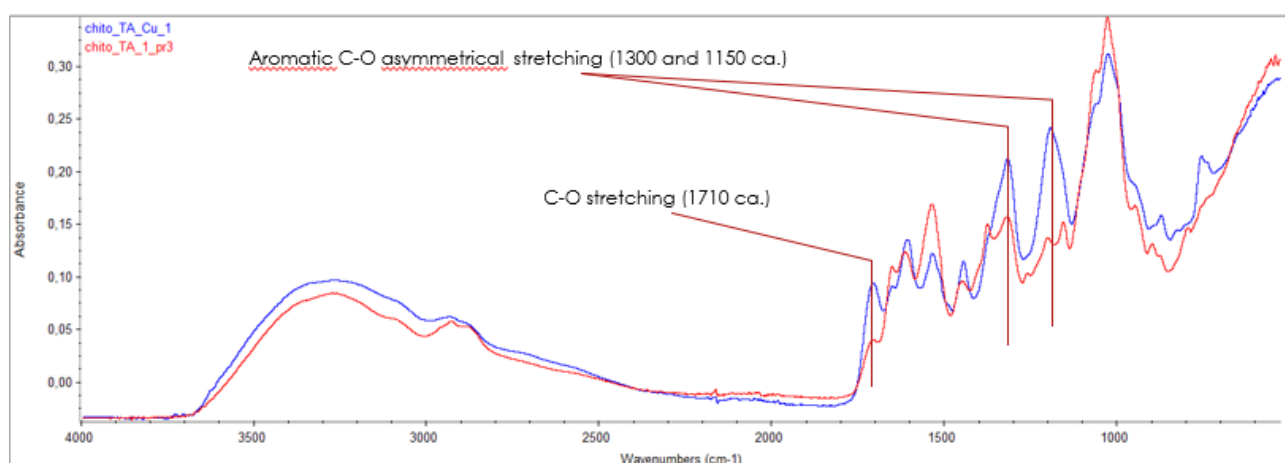
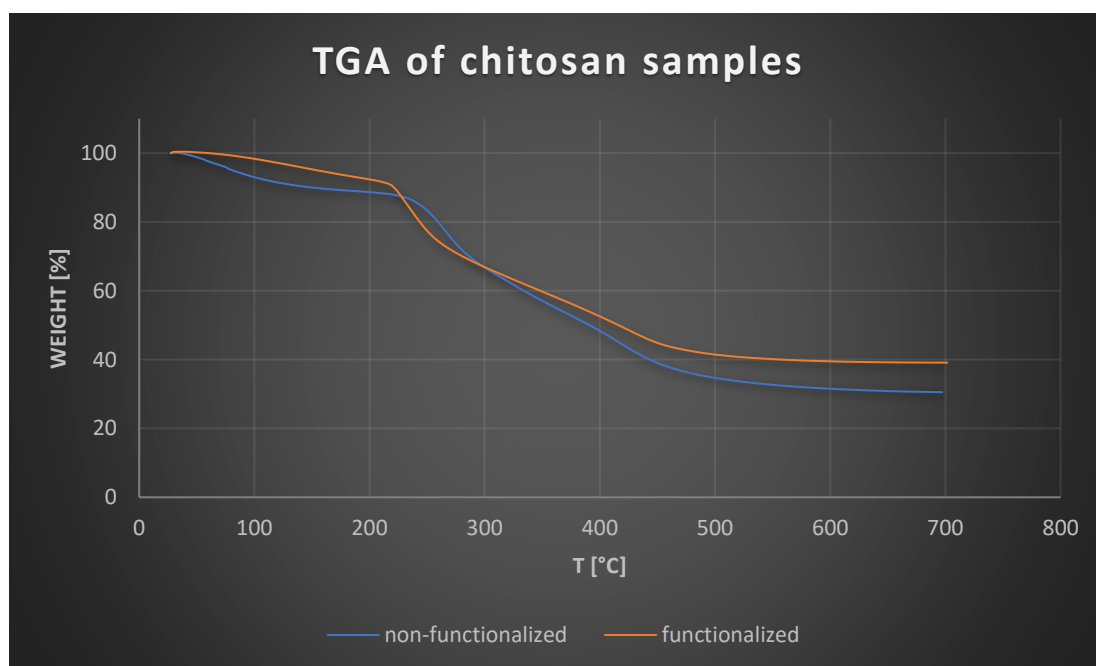


Fig 52. FTIR spectra for methacrylated chitosan hydrogels functionalized with Tannic Acid, before (red) and after (blue) Cu(II) adsorption

Similar considerations can be done for samples functionalized with Tannic Acid. In this case, difference in intensity can be seen in the peaks indicated in *Figure 52*, which are attributed to C-O stretching ( $1710\text{ cm}^{-1}$  ca.) and to aromatic C-O asymmetrical stretching ( $1300\text{ cm}^{-1}$  and  $1150\text{ cm}^{-1}$  ca.). The second and the third peak (at  $1300\text{ cm}^{-1}$  and  $1150\text{ cm}^{-1}$ ) are attributed to the chemical structure of Tannic Acid, so it reasonable to think that Tannic Acid plays a relevant role in the sequestration of Cu(II) ions from the solution.

## TGA – Thermogravimetric analysis

TGA was conducted on both samples of functionalized chitosan and non-functionalized chitosan, and the result is shown in *Figure 53*. No interaction with atmosphere is desired, so the analysis was conducted in Nitrogen atmosphere. Sample's weight must be comprehended between 4 mg and 8 mg. Samples are posed into Alumina crucibles (which do not undergo degradation until 1000 °C) and then the method is chosen on the software. Method used is called "TGA 25-700 N<sub>2</sub>", meaning that the sample is going to be heated from room T to 700 °C in N<sub>2</sub> atmosphere.



*Fig 53. TGA of chitosan samples, non-functionalized (blue) and functionalized with Tannic Acid (orange)*

Both curves show only one weight-loss step (around 250 °C), so it's reasonable to think that thermal degradation of the chitosan samples conducted in N<sub>2</sub> atmosphere is a simple one-step reaction. Also, the samples were dry, so it makes sense that no weight loss is detected at 100 °C (a non-completely dried sample would show the loss of its residual water content at this temperature). For both samples, no further weight losses can be clearly detected right after 450 °C, and the residue is equal to 40% for functionalized chitosan, while it is around 30% for non-functionalized chitosan: the difference in the residue is easily explained because of the presence of Tannins.

## DSC – Differential Scanning Calorimetry

DSC was conducted on both samples of functionalized chitosan and non-functionalized chitosan, and the result is shown in *Figure 54*. Sample's weight must be comprehended between 4 mg and 8 mg, as for the TGA analysis. The sample is posed into an Aluminum crucible, and then into the machine (the reference sample is an empty crucible). The process occurs in Nitrogen atmosphere, through four temperature steps:

- ramp from 25 °C to 200 °C
- ramp from 200 °C to 25 °C
- maintaining at 25 °C
- ramp from 25 °C to 200 °C

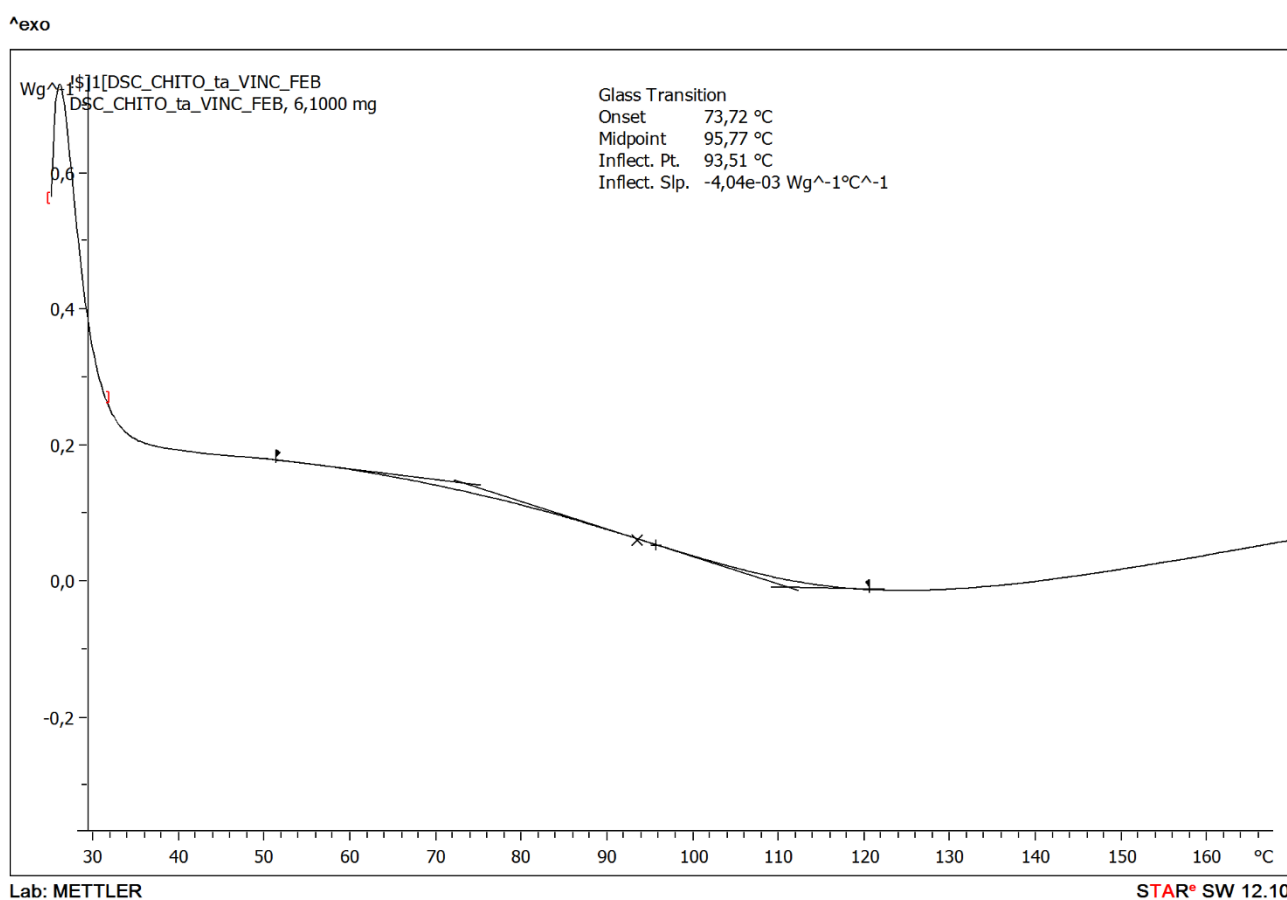


*Fig 54. DSC of a functionalized chitosan sample*

The maximum temperature of 200 °C was selected to avoid a possible degradation of chitosan samples. It is reasonable the melting of water does not appear, since the samples were dried before all the characterization processes. Another peak can be detected at around 70 °C (precisely, at 73,72 °C) and according to some authors [56] this peak is related to chitosan's melting. The second peak, detected around 110 °C, is supposed to be chitosan's  $T_g$ .

## UV-Vis Spectroscopy

UV-Vis spectroscopy was carried out in order to investigate the presence of an effective bond between the hydrogels and the Cu(II) ions and the formation of the relative complex. UV-Vis spectra were taken for four samples, as indicated in *Figure 55*: two samples of non-functionalized chitosan after 96h in bath, one in only ultrapure water and the other in a solution 10 ppm of Cu(II) ions; two samples of functionalized chitosan (with TA) after 96h in bath, one only in ultrapure water and the other in a solution 10 ppm of Cu(II) ions. Analysis was carried out between 200 nm and 1000 nm.

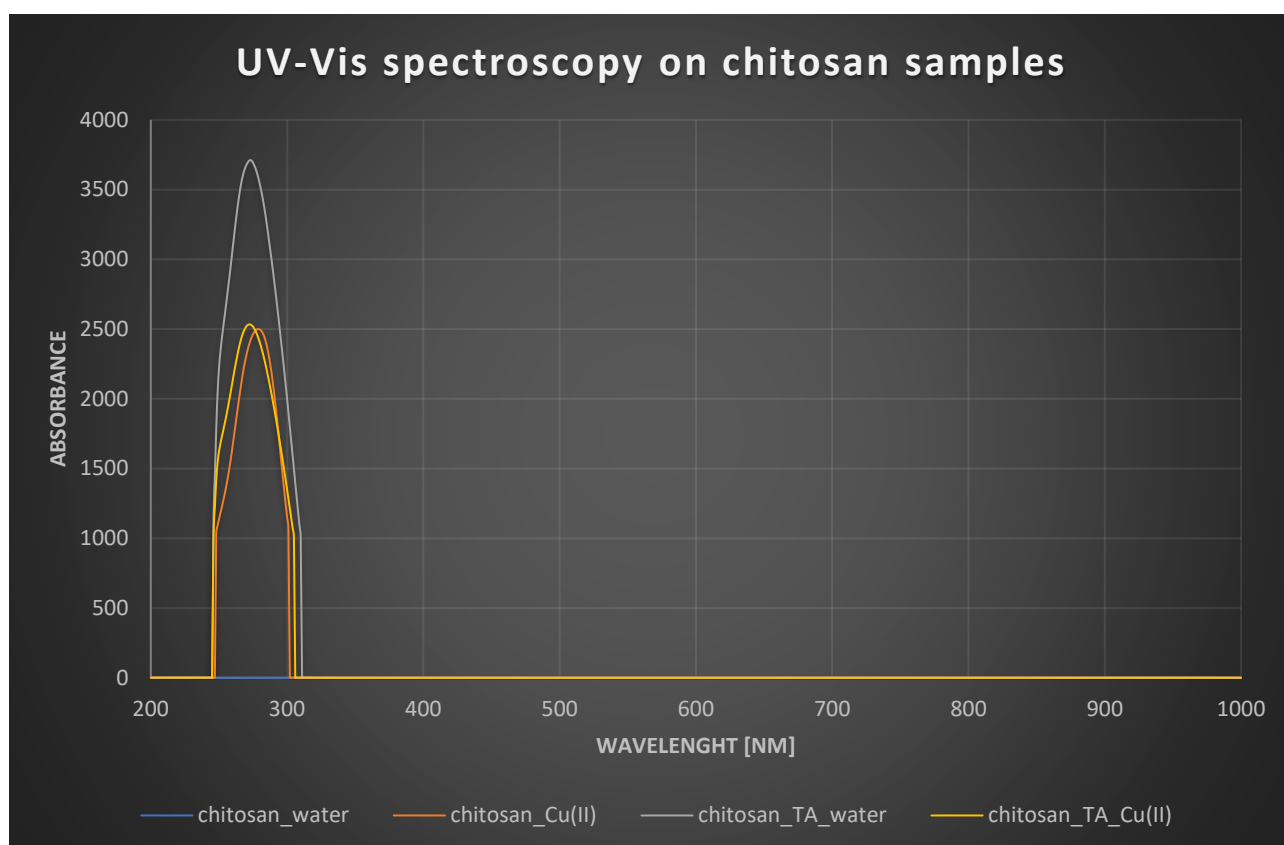


*Fig 55. UV-Vis spectroscopy on solutions which contained chitosan samples, functionalized and non-functionalized; comparison was made between ultrapure water (milliQ) only and a solution of Cu(II) ions*

It is clearly visible that the spectrum of chitosan in water gave no response. As far as regarding the resting three samples, a single peak is present at around a wavelength of 280 nm, and this happens both for samples which chelated Cu(II) ions and the sample which didn't (*grey curve*).

The peaks are not fully coincident as one can see: in curves referring to functionalized samples, 280 nm is the typical wavelength attributed to Tannic Acid [55] while for the sample of non-functionalized chitosan in a solution of 10 ppm of Cu(II) ions the peak is very lightly shifted on the right (*orange curve*). According to some authors [57], the peak of the complex between chitosan and Cu(II) is located between 200 nm and 300 nm, but no precise evidence was found about this study. The peak at around 281 nm could be attributed to the formation of a chitosan-Cu complex, but further investigation needs to be done on UV-Vis spectra regarding this chitosan-metal complex.

## EDS-SEM (Energy Dispersive spectroscopy – Scanning electron microscopy)

EDS analysis were performed on samples of chitosan (both functionalized and non-functionalized) to investigate the effective presence of Copper after the samples were left in a solution of 10 ppm of Cu(II) ions for 96h.

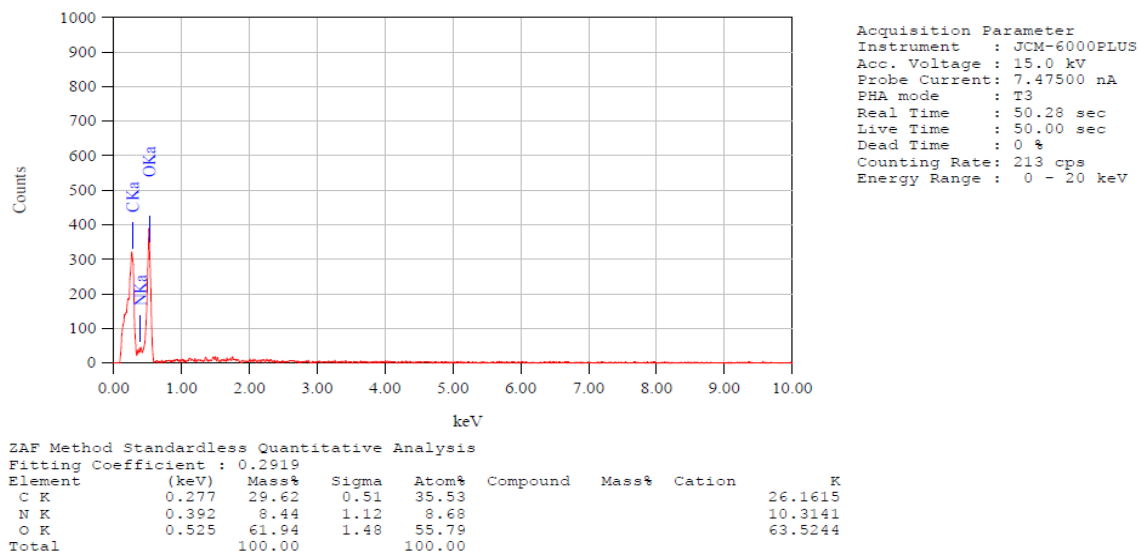


Fig 56. EDS analysis on a sample of chitosan functionalized with TA

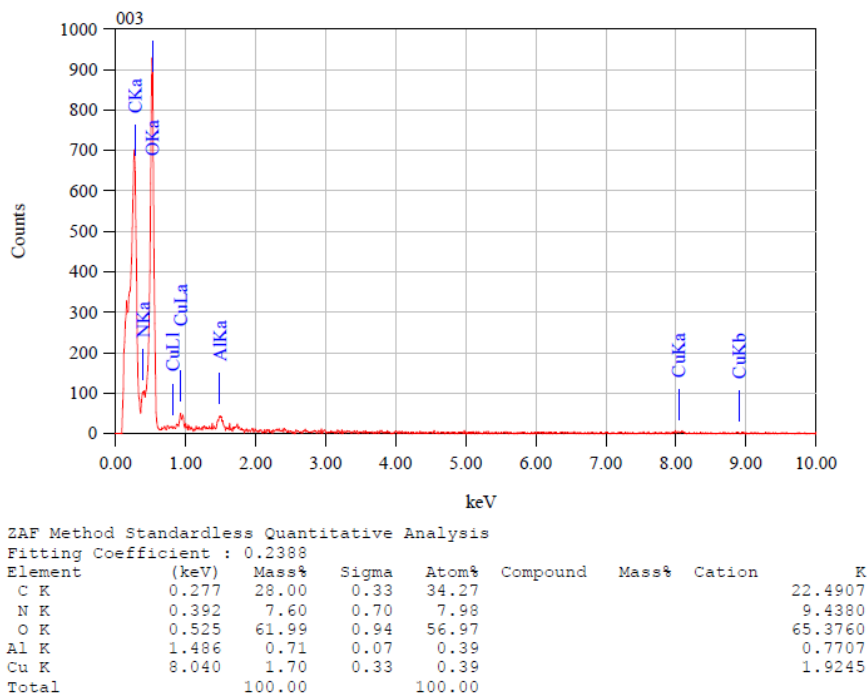


Fig 57. EDS analysis on a chitosan sample functionalized with TA and left in a solution of 10 ppm of Cu(II) ions for 96h

In a functionalized sample (*Figure 56*) only Nitrogen, Carbon and Oxygen are detected (Hydrogen is not detectable by EDS analysis), while for the sample which stayed in bath for 96h in a solution of Cu(II) ions (*Figure 57*) the presence of Copper is detected, along with Aluminum (this latter is thought to be a contamination occurred in some part of the hydrogel's preparation process).

### 5.3 – STUDY ON COPPER REMOVAL

Chitosan hydrogels (functionalized with polyphenols) were synthesized to remove heavy metal ions from wastewaters. In this study, removal of Cu(II) is chosen to be investigated.

Hydrogel samples (both functionalized and non-functionalized) are immersed in a solution of Cu(II) ions. The volume of solution in which the hydrogel is immersed is calculated by knowing the weight of each sample (which is not predictable), to maintain a precise ratio “weight of sample : volume of liquid”, chosen to be equal to “7 mg : 10 mL”.

The starting solution is obtained by adding CuSO<sub>4</sub> (anhydrous) to ultrapure water, which will give Cu<sup>2+</sup> and SO<sub>4</sub><sup>2-</sup> ions. Two studies are conducted: a kinetic study and an Isotherm study.

#### Kinetic study

Samples of chitosan hydrogel are immersed in a solution of Cu(II) ions, at a given Cu(II) concentration (10 mg/L). The change in concentration is checked at precise time intervals and the analysis ends when the concentration becomes constant so that a plateau is reached. The kinetic curve is obtained for both samples of functionalized and non-functionalized hydrogels.

The study of Cu(II) concentration is carried out by using a Copper Spectrophotometer.



*Fig 58. Portable spectrophotometer*

Spectrophotometers are used to measure absorbance, at various wavelengths. It can be used in UV, visible and IR region of the electromagnetic spectrum. Light that falls on a colored solution can be absorbed or transmitted. A colored solution selectively transmits only one color, which is its own color [58].

A beam of incident light with intensity  $I_0$  passes through a solution; part of incident light is reflected ( $I_r$ ), part is absorbed ( $I_a$ ) and rest is transmitted ( $I_t$ ):

$$I_0 = I_r + I_a + I_t$$

In photometers ( $I_r$ ) is eliminated and it is sufficient to determine the ( $I_a$ ). For this purpose ( $I_r$ ) is kept constant (by using cells with the same properties). ( $I_0$ ) and ( $I_t$ ) are measured.

The mathematical relationship between the amount of light absorbed and the concentration of the substance can be shown by the two fundamental laws of photometry on which the Spectrophotometer is based.

$$\text{Log}_{10} I_0 / I_t = a_s b c$$

$b$  is kept constant by applying Cuvette or standard cell then,

$$\text{Log}_{10} I_0 / I_t = a_s c$$

The absorbency index  $a_s$  is defined as

$$a_s = A/cl$$

where:

- $c$  = concentration of the absorbing material (in g/L)
- $l$  = distance traveled by the light in solution (in cm)

Samples are immersed in a solution at a Concentration of 10 ppm of Cu(II) ions and the concentration is checked at precise time intervals until a plateau (in terms of adsorption) is reached for each sample. The whole experiment is conducted at room temperature. It is observed that no plateau is reached: the amount of adsorbate Cu(II) ions reaches a maximum value and then decreases. This behavior can be attributed to several reasons, the main one being adsorption/desorption phenomena of Cu(II) ions returning from the surface of the sample to the solution bath. In these experiments, the pH of the solution was monitored to remain between 6 and 8 in order to respect the imposed conditions for the Spectrophotometer analysis.

The results of Kinetic analysis are shown in *Figure 59 and Figure 60*. The calculation of " $Q_t$ " is made as follows:

$$Q_t = \frac{(C_0 - C_t) * V}{m}$$

Where " $Q_t$ " is the amount of adsorbate at time " $t$ ", " $C_0$ " and " $C_t$ " are the concentrations at the beginning of the experiment and at a defined time " $t$ ", respectively. " $V$ " is the volume of the solution in which the sample is immersed and " $m$ " is the mass of the sample itself.

## **Isothermal study**

Six different samples of chitosan hydrogels functionalized with Tannic Acid are immersed in solutions at different Cu(II) ions concentrations (5 mg/L, 10 mg/L, 20 mg/L, 50 mg/L, 75 mg/L and 100 mg/L), and the same ratio of 7:10 (weight of sample : volume of solution) is respected for all samples. Cuvettes containing samples are put to stir at room temperature for a time of four days (96 hours), and this time was chosen accordingly to literature [59]. The experiment was carried out only on functionalized chitosan samples because it was observed that non-functionalized chitosan (Kinetic experiment) is capable of capturing a very low amount of Cu(II) ions, while far better results are obtained for functionalized chitosan, so it was chosen to use these samples to remove Copper at higher initial concentrations of Cu(II) ions in the solution.

For this Isothermal study, the same Copper Spectrophotometer is used, taking into account that multiple dilutions are mandatory in order not to overcome the upper detection limit of the instrument (which is equal to 1,5 mg/L), and the instrument's Cuvettes must contain a precise amount of solution (10 mL).

The calculation of “ $Q_e$ ” is made as follows:

$$Q_e = \frac{(C_0 - C_e) * V}{m}$$

Where “ $Q_e$ ” is the amount of adsorbate at equilibrium, “ $C_0$ ” and “ $C_e$ ” are the concentrations at the beginning of the experiment and at equilibrium at 96 hours, respectively. “ $V$ ” is the volume of the solution in which the sample was immersed and “ $m$ ” is the mass of the sample itself. The results are shown in *Figure 61*.

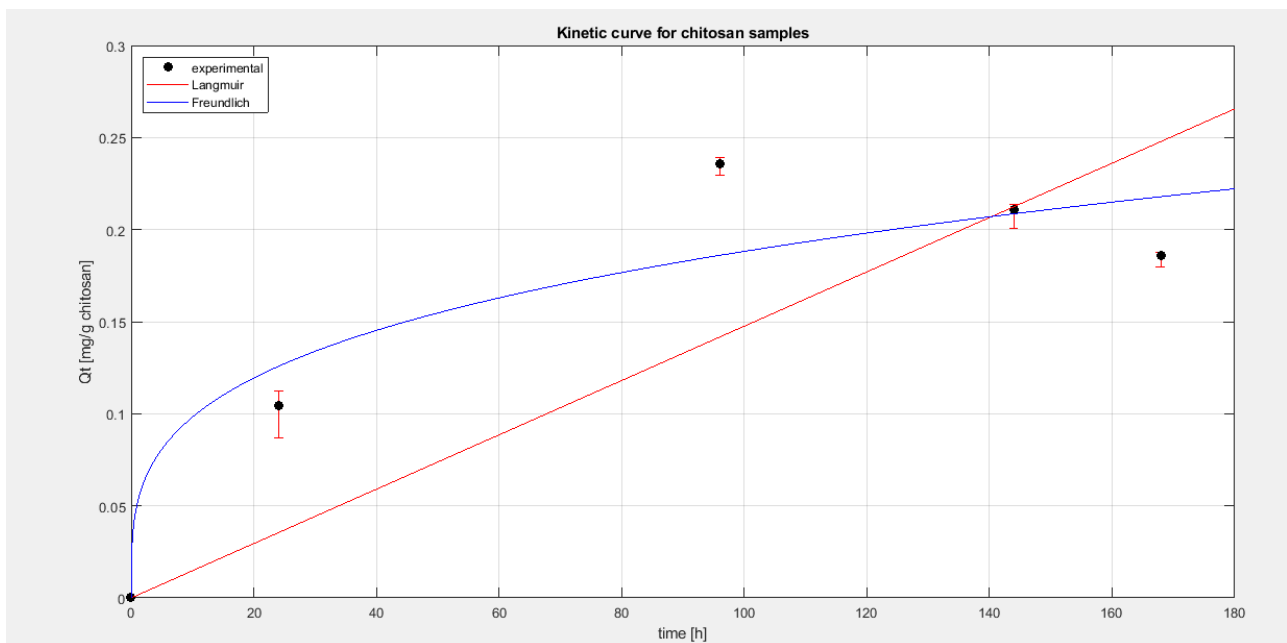


*Figure 59 – Adsorption curve for chitosan in a solution of 10 mg/L of Cu(II)*

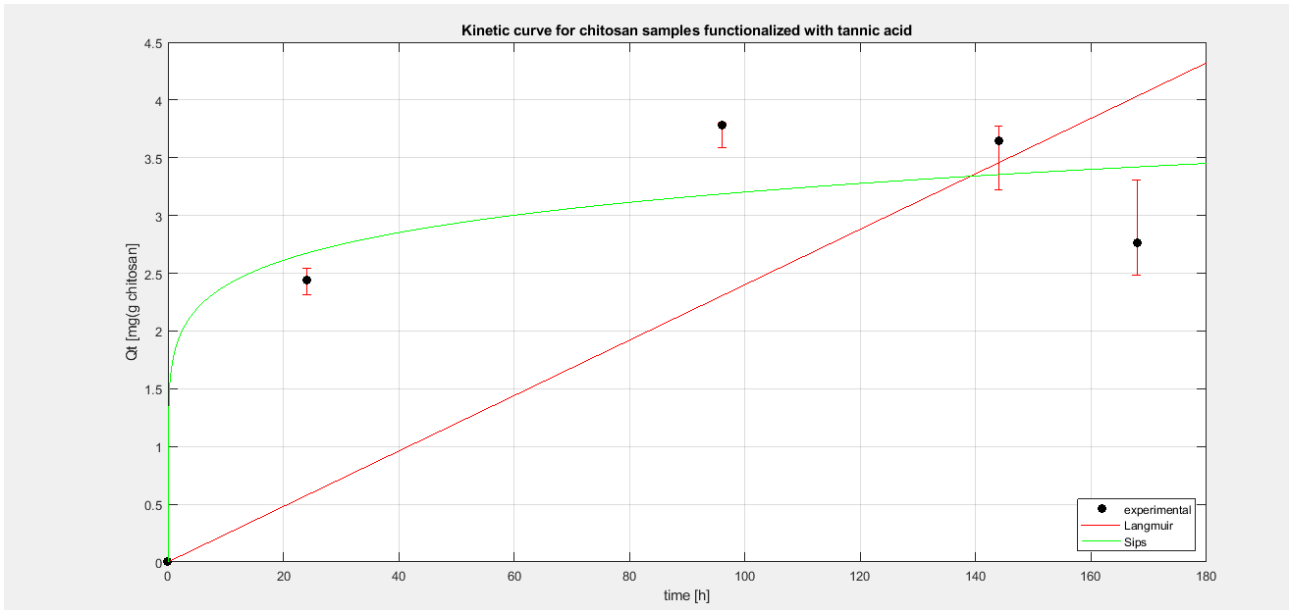


Figure 60 – Adsorption curve for chitosan functionalized with Tannic Acid, in a solution of 10 mg/L of Cu(II)

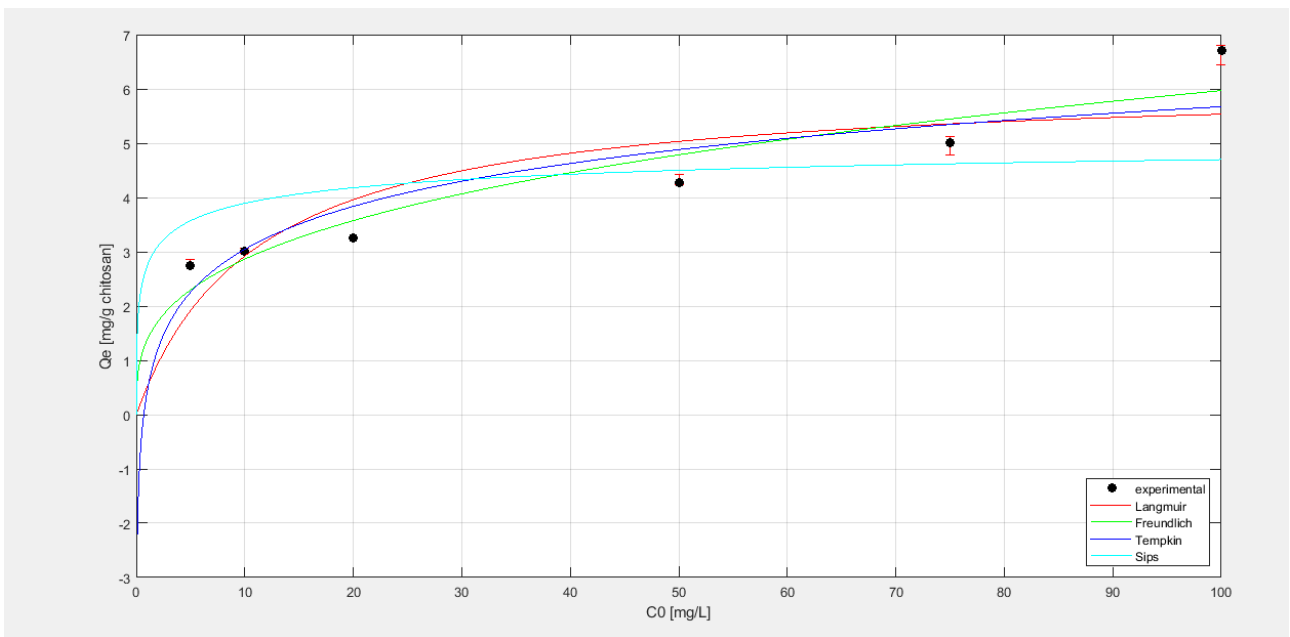


Figure 61 – Adsorption curve for chitosan functionalized with Tannic Acid, at six different initial concentrations of Cu(II) ions – Isothermal study

Comparing the kinetic curves (*Figures 59 and 60*) it is clearly visible that the uptake capacity for functionalized chitosan is quite higher than the one of original chitosan. Particularly, the highest uptake for original chitosan was equal to 0,24 mg/g of chitosan, while for the functionalized samples, the highest uptake was equal to 3,75 mg/g of chitosan.

This is the reason why the following experiment (the Isothermal study) was conducted only on functionalized samples.

The curves were fitted with adsorption models of Langmuir, Freundlich, Tempkin and Sips. It is visible, from all curves (*Figures 59, 60 and 61*) that none of the models proposed accurately fits the curves. The behavior of the experimental curves is the following:

- Kinetic curve: a plateau is never reached, while a maximum is reached and then the adsorbed quantity decreases; this may be indicative of some sort of desorption mechanism. It may be interesting to see what happens to adsorption values for longer times.
- Isothermal curve: values are always increasing with a relatively small slope and, again, no plateau is reached. In this case, it may be interesting to see what happens for higher initial Cu(II) ions concentrations.

## 6 – CONCLUSIONS

In this study, chitosan hydrogels were prepared with the aim of capturing heavy metal ions from wastewaters.

Raw chitosan was methacrylated by use of methacrylic anhydride. Methacrylated chitosan was purified in cellulose membranes and then lyophilized. Lyophilized chitosan is analyzed on FTIR to verify that a correct methacrylation process occurred. The detection of functional groups like the double bond C=C and the double bond C=O reveals that methacrylation process occurred correctly [60].

The methacrylated chitosan was solubilized in acid solution (water and acetic acid) and added with the photoinitiator Irgacure 2959, to be UV-cured. After curing process, chitosan hydrogels are obtained. and these latter are then dried under the adsorption hood to be successively characterized.

First of all, a swelling test was performed on chitosan samples: results are shown in *Table 11* and *Figure 62*.

Time [min]	Sample 1 [mg]	Sample 2 [mg]	Sample 3 [mg]
0	1,6	2	2,4
5	23	23	32
10	59	35	40
15	31	26	36
20	30	23	28
40	34	30	34
60	34	32	29
90	41	26	40
120	30	28	26
180	22	35	32
240	20	24	31
300	21	32	31
360	22	36	39
420	25	33	30
480	25	33	30

*Tab 11. Swelling test for three chitosan hydrogels*

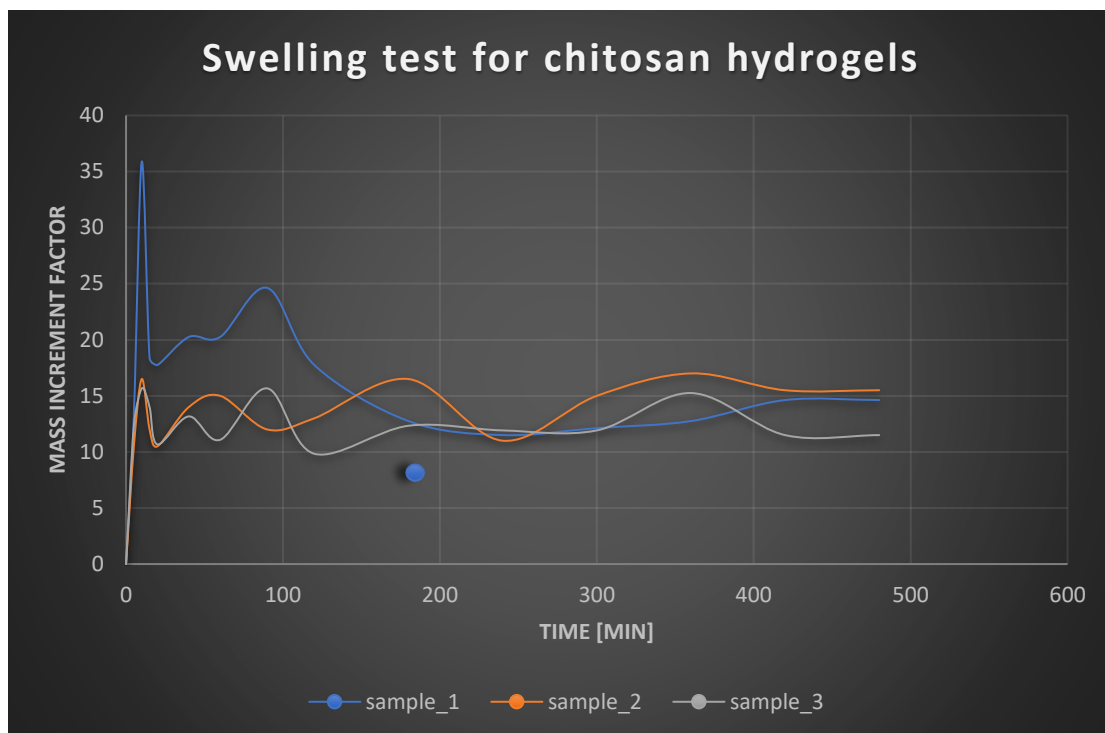


Fig 62. Swelling test for three chitosan hydrogels; the non-dimensional value indicated as “mass increase factor” is calculated as follows:  $\frac{\text{weight at } t_i - \text{weight at } t_0}{\text{weight at } t_0}$

Some of the dried chitosan hydrogels are functionalized with a polyphenol, Tannic Acid, to enhance their capability in capturing heavy metal ions from wastewaters. Polyphenols are well known for their chelating ability towards metal ions. Functionalization occurred by immersing the chitosan samples in little wells filled with a solution of water and Tannic Acid, at a concentration of 15 mg/mL of Tannic Acid (chosen according to literature, [61]). These samples are let at a temperature of 37°C for three hours, and they are successively dried out in the adsorption hood.

Samples are then characterized. Functionalized samples are analyzed on FTIR to compare their spectra with the spectrum of Tannic Acid and verify if the functionalization occurred correctly. The spectra match and the functionalized samples show a marked change in color, from the original light yellow to a strong auburn (corresponding to the color of tannic acid).

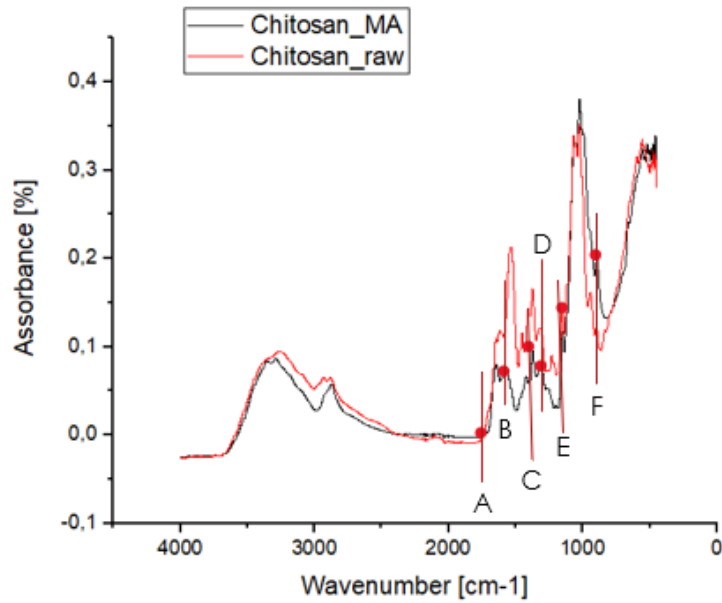


Fig 63. FTIR spectra of raw chitosan and methacrylated chitosan. The most important peaks are shown in the graph: A) C=O stretching at  $1700\text{ cm}^{-1}$  B) Stretching of Amide I at  $1590\text{ cm}^{-1}$  C) CH<sub>2</sub> bending at  $1420\text{ cm}^{-1}$  D) CH<sub>3</sub> bending at  $1370\text{ cm}^{-1}$  E) C-O stretching at  $1066\text{ cm}^{-1}$  F) C=C stretching at  $815\text{ cm}^{-1}$ .

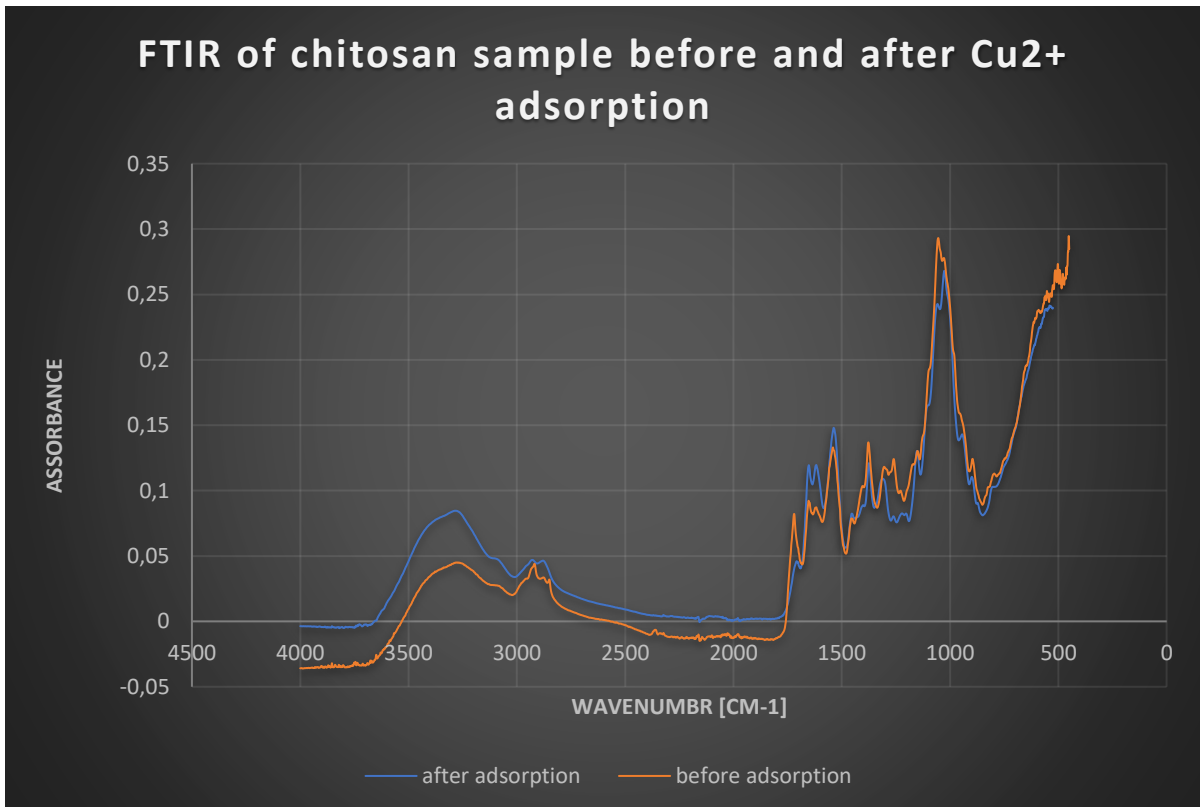


Fig 64. FTIR spectra of methacrylated chitosan before (orange) and after (blue)  $\text{Cu}^{2+}$  adsorption

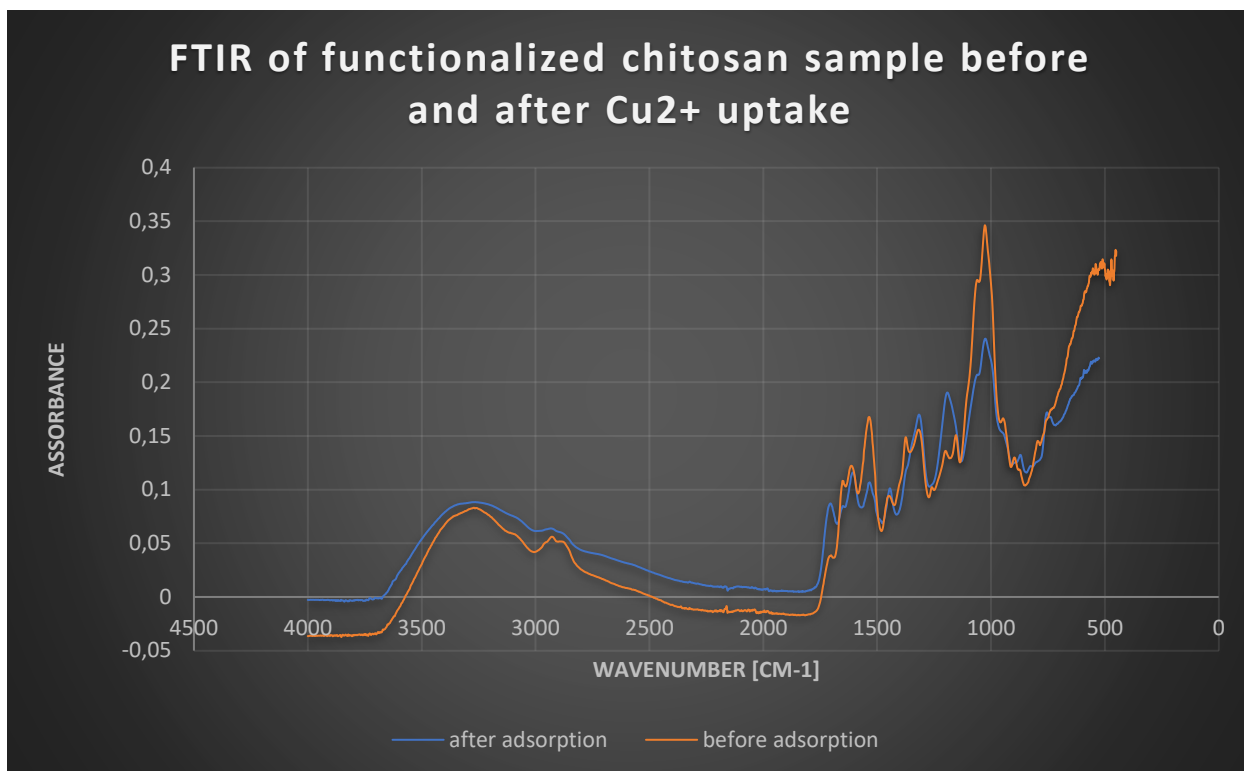


Fig 65. FTIR spectra of methacrylated chitosan (functionalized with TA) before (orange) and after (blue)  $\text{Cu}^{2+}$  adsorption

TGA analysis show a simple, one-step weight loss for both functionalized and non-functionalized samples, and functionalized samples show a slightly higher residue: this is due to the presence of tannins.

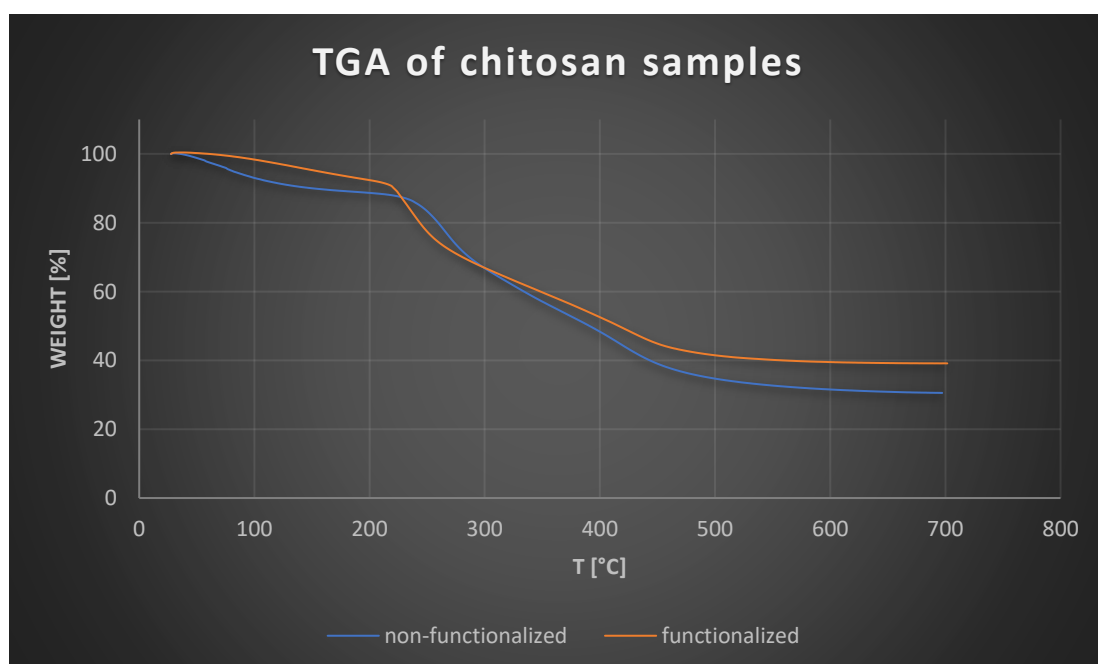
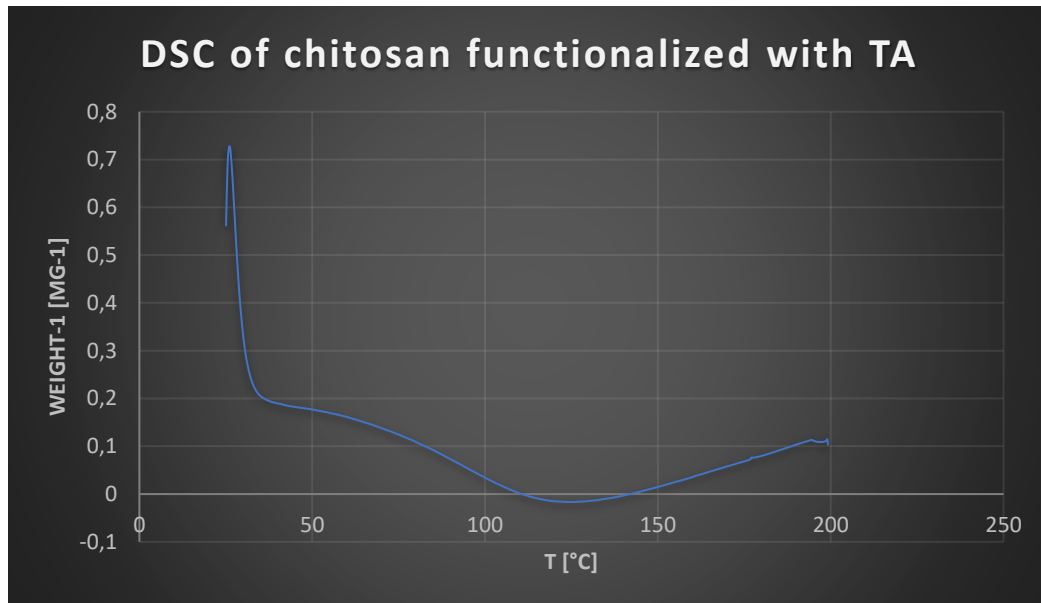


Fig 66. TGA of chitosan samples, non-functionalized (blue) and functionalized with Tannic Acid (orange)

DSC analysis show a melting peak for chitosan at 72 °C ca. and a peak which is supposed to be related to the  $T_g$  of the material around 110 °C ca., these results are found in other works [56]. Results of the DSC analysis are shown in *Figure 67*.



*Fig 67. DSC of a chitosan sample functionalized with Tannic Acid*

UV-Vis spectra were obtained by analyzing the solutions in which the samples were immersed to capture Copper ions. A peak related to the presence of tannic acid is present, and this reveals that a certain amount of material is released in the solution: this negatively affects the capturing of ions, of course. A lightly shifted peak (to the right) can be attributed to the formation of a complex between Cu(II) and chitosan (according to literature [57] this peak should be located between 200 nm and 300 nm), but no more accurate information were found to support this hypothesis; further investigation shall be done on UV-Vis spectra for chitosan samples after the complexation of Cu(II) ions. Results of UV-Vis spectra are shown in *Figure 68*.

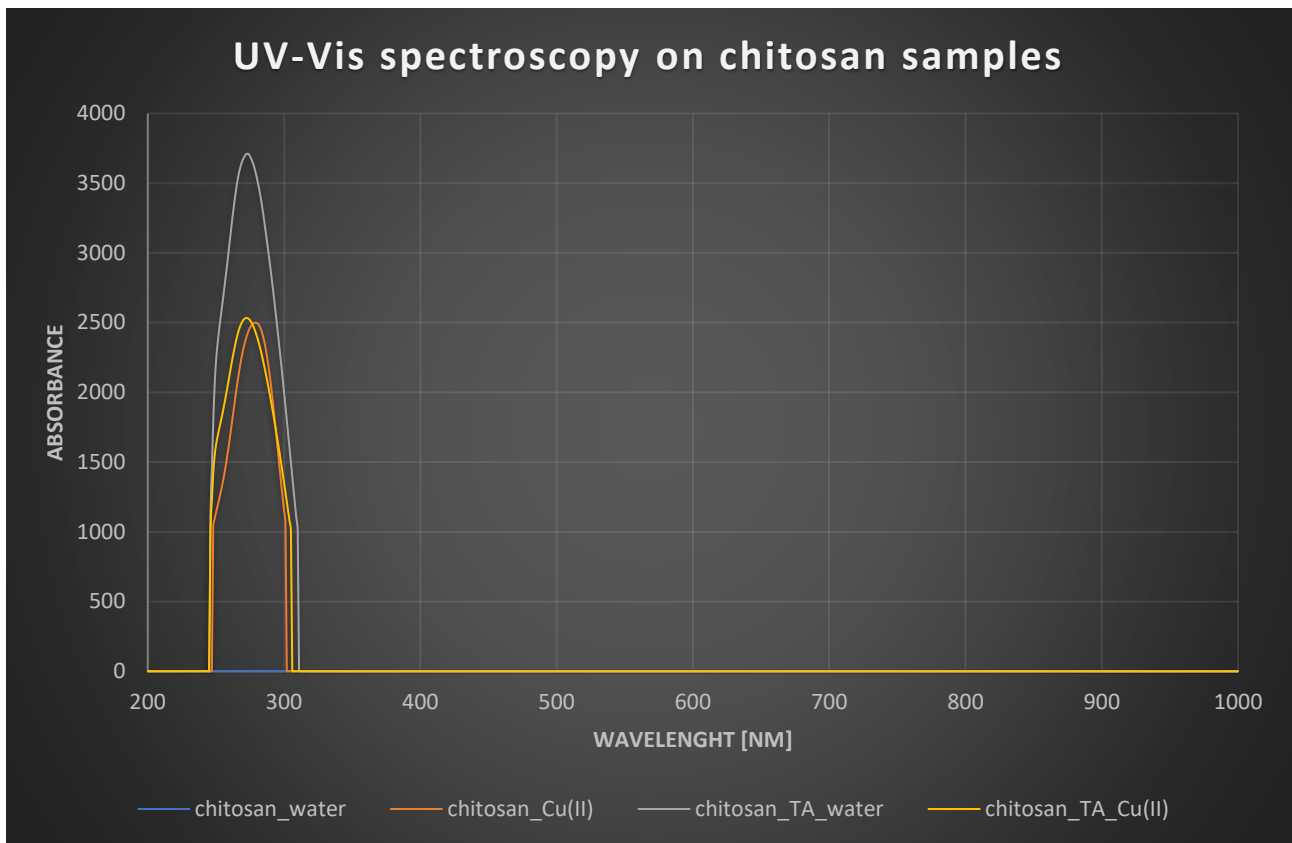


Fig 68. UV-Vis spectroscopy on solutions which contained chitosan samples, functionalized and non-functionalized; comparison was made between ultrapure water (milliQ) only and a solution of Cu(II) ions

EDS-SEM analysis was conducted on samples to verify the effective presence of Copper, which was actually detected, differently from samples which were immersed in water, which show only Oxygen, Nitrogen and Carbon.

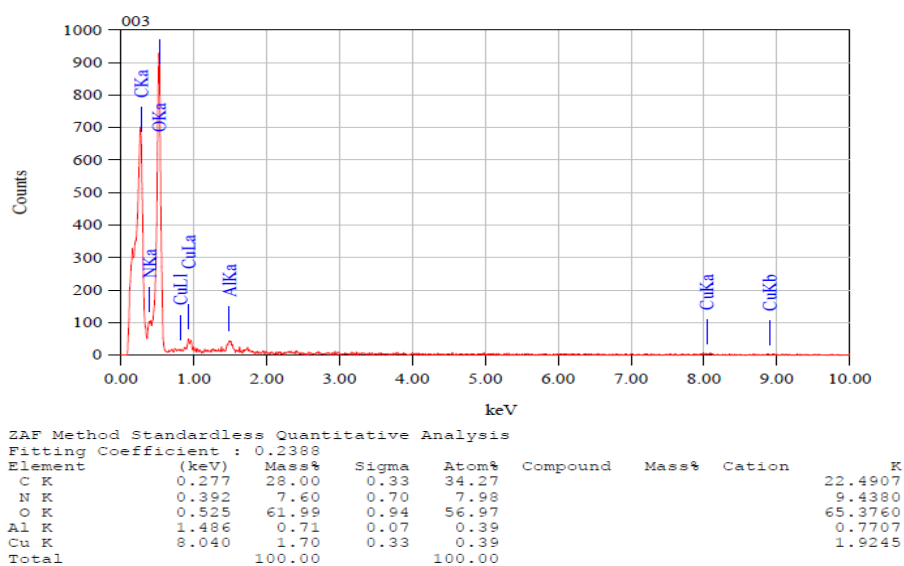
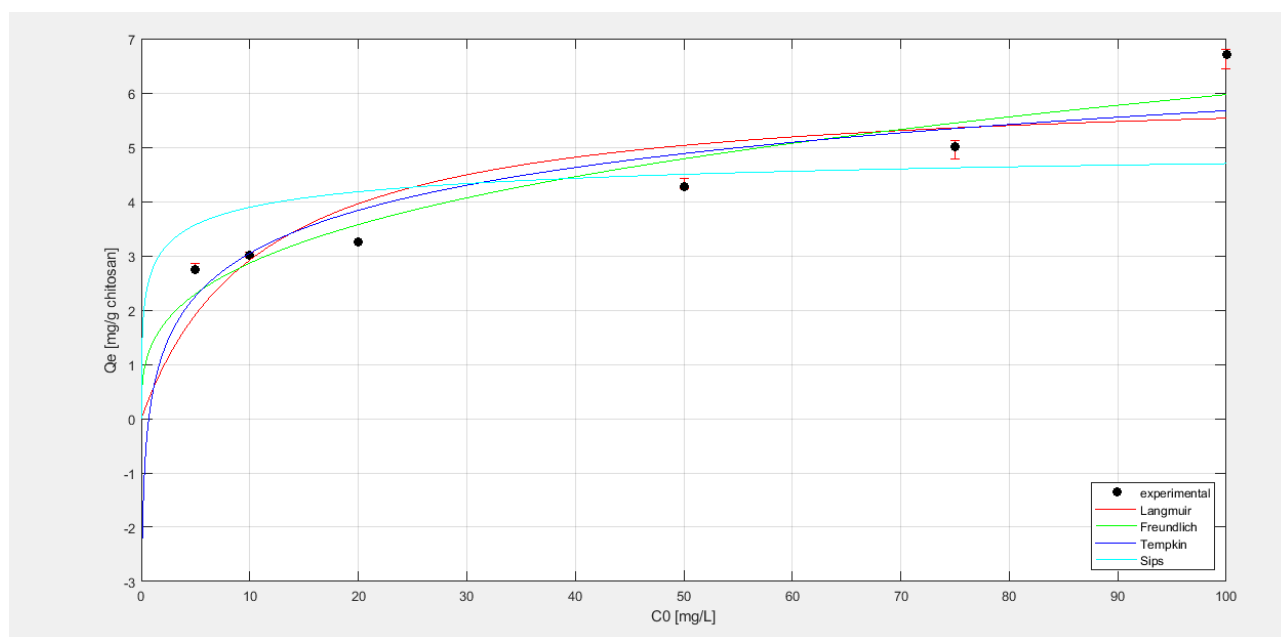


Fig 69. EDS analysis on a chitosan sample functionalized with TA and left in a solution of 10 ppm of Cu(II) ions for 96h

The capture of Cu(II) ions was conducted with two experiments: a kinetic experiment, carried out by monitoring the concentration of Cu(II) ions in the solution at precise time intervals, and a isothermal experiment, carried out by monitoring the change in concentration after 96h for six different samples, each of which was immersed in a solution of Cu(II) ions at different initial concentration of Cu(II) ions. The Kinetic curve shows an initial adsorption of Cu(II) ions for both functionalized and non-functionalized chitosan hydrogels, but after some hours, the amount of adsorbate ions decreases: this induces to think that some sort of desorption process takes place. The Isothermal curve (*Figure 70*) shows a constantly increasing adsorbed amount with a small slope, not actually reaching a plateau within 96 hours (as predicted in literature, [59]).



*Figure 70 – Adsorption curve for chitosan functionalized with Tannic Acid, at six different initial concentrations of Cu(II) ions – Isothermal study*

The adsorption process is influenced by several factors, such as pH, temperature, metal ion's initial concentration, and more. In these experiments, pH was maintained between 6 and 8 to respect the indication about the usage of the Copper Spectrophotometer, and all experiments were carried out at room temperature. The same ratio of 7:10 (milligrams of sample per milliliters of solution) was respected in each adsorption study; however, the weight of dried hydrogels is not easily controllable, making their weight to range from 5 mg to 10 mg. One more problem which can occur is related to the dilution of Cu(II) solutions: the limit of 1,5 mg/L for the Copper Spectrophotometer must be respected, and this implies that all solutions used in this study had to be diluted (in some cases, multiple dilutions were needed); it's easy to understand that a dilution implies an error (which may be due to defects in the instruments, or lack of experience in the operator), and multiple dilutions make this error to be multiplied.

Further studies have to be conducted on the adsorption of Cu(II) ions from chitosan hydrogels: the influence of a more defined shape and weight of samples should be considered; the duration of the experiment can be increased to verify if (and when) a plateau is reached; the influence of pH and temperature should be taken into account, as for the concentration of tannic acid in water in the chitosan's functionalization step.

## 7 – BIBLIOGRAPHY

[1] - Wikipedia

[2] - <https://www.allevi3d.com/photocuring-basics/>

[3] - C. Peniche-Covas, L.W. Alvarez, W. Arguelles-Monal, Adsorption of mercuric ions by chitosan, *J. Appl. Polym. Sci.* 46 (1992) 1147–1150

[4] - E. Lopes, F. dos Anjos, E. Vieira, A. Cestari, An alternative Avrami equation to evaluate kinetic parameters of the interaction of Hg (II) with thin chitosan membranes, *J. Colloid Interf. Sci.* 263 (2003) 542–547.

[5] - E. Taboada, G. Cabrera, G. Cardenas, Retention capacity of chitosan for copper and mercury ions, *J. Chile Chem. Soc.* 48 (2003) 7–12.

[6] - E. Guibal, Heterogeneous catalysis on chitosan-based materials: a review, *Prog. Polym. Sci.* 30 (2005) 71–109.

[7] - E.P. Kunkoro, J. Roussy, E. Guibal, Mercury recovery by polymer-enhanced ultrafiltration: comparison of chitosan and poly(ethylenimine) used as macroligand, *Sep. Sci. Technol.* 40 (2005) 659–684.

[8] - A. Gamage, F. Shahidi, Use of chitosan for the removal of metal ion contaminants and proteins from water, *Food Chem.* 104 (2007) 989–996.

[9] - M. Benavente, Adsorption of metallic ions onto chitosan: equilibrium and kinetic studies, Licentiate Thesis, Royal Institute of Technology, Department of Chemical Engineering and Technology, Stockholm, Sweden, 2008

[10] - Choong Jeon, Wolfgang H. Holl, Chemical modification of chitosan and equilibrium study for mercury ion removal, Institute of Technical Chemistry, Forschungszentrum Karlsruhe, Section WGT, P.O. Box 3640, Karlsruhe D-76021, Germany

[11] - Ludovico Pontoni, Massimiliano Fabbricino, Use of chitosan and chitosan-derivatives to remove arsenic from aqueous solutions—a mini review, University of Naples Federico II, Department of Hydraulics Geotechnics and Environmental Engineering, Via Claudio 21, 80125 Naples, Italy

[12] - Li Jin and Renbi Bai\*, Mechanisms of Lead Adsorption on Chitosan/PVA Hydrogel Beads, Department of Chemical and Environmental Engineering, National University of Singapore, 10 Kent Ridge Crescent, Singapore 119260

[13] - Rodrigo S. Vieira <sup>a</sup>, Mona Lisa M. Oliveira <sup>b</sup>, Eric Guibal<sup>c</sup>, Enrique Rodríguez-Castellón <sup>b</sup>, Marisa M. Beppu, Copper, mercury and chromium adsorption on natural and crosslinked chitosan films: An XPS investigation of mechanism, <sup>a</sup> Departamento de Termofluidodinâmica, Faculdade de Engenharia Química, Universidade Estadual de Campinas, Caixa Postal 6066, Barão Geraldo, CEP 13081-970, Campinas, SP, Brazil <sup>b</sup> Departamento de Química Inorgânica, Cristalografía y Mineralogía, Facultad de Ciencias, Unidad Asociada del Instituto de Catálisis y Petroleoquímica, CSIC, Universidad de Málaga, Campus de Teatinos, 29071 Málaga, Spain <sup>c</sup> Ecole des Mines d'Alès, Laboratoire Génie de l'Environnement Industriel, 6 Avenue de Clavières, F-30319 Ales Cedex, France

- [14] - L. Dambies, C. Guimon, S. Yiacoumi, E. Guibal, Characterization of metal ion interactions with chitosan by X-ray photoelectron spectroscopy, *Colloids Surf. A: Physicochem. Eng. Aspects* 177 (2001) 203–214.
- [15] - Kadirvelu, K., Kavipriya, M., Karthika, C., Radhika, M., Vennilamani, N., Pattabhi, S., 2003. Utilization of various agricultural wastes for activated carbon preparation and application for the removal of dyes and metal ions from aqueous solutions. *Bioresour. Technol.* 87, 129–132.
- [16] - Williams, C.J., Aderhold, D., Edyvean, G.J., 1998. Comparison between biosorbents for the removal of metal ions from aqueous solutions. *Water Res.* 32, 216–224.
- [17] - Namasivayam, C., Sangeetha, D., 2006. Recycling of agricultural solid waste, coirpith: removal of anions, heavy metals, organics and dyes from water by adsorption onto ZnCl<sub>2</sub> activated coirpith carbon. *J. Hazard. Mater. B* 135, 449–452.
- [18] - Bailey, S.E., Olin, T.J., Bricka, R.M., Adrian, D.D., 1999. A review of potentially low-cost sorbents for heavy metals. *Water Res.* 33, 2469–2479.
- [19] - Gaballah, I., Goy, D., Allain, E., Kilbertus, G., Thauront, J., 1997. Recovery of copper through decontamination of synthetic solutions using modified barks. *Met. Metall. Trans. B* 28, 13-23
- [20] - Nakajima, A., Sakaguchi, T., 1990. Recovery and removal of uranium by using plant wastes. *Biomass* 21, 55–63.
- [21] - Haslam, E. *Plant Polyphenols, Vegetable Tannins Revisited*; Cambridge University Press: Cambridge, U.K., 1989.
- [22] - Haslam, E. Plant polyphenols (syn. vegetable tannins) and chemical defenses a reappraisal. *J. Chem. Ecol.* 1988, 14, 1789-1805
- [23] - Scalbert, A. Antimicrobial properties of tannins. *Phytochemistry* 1991, 30, 3875-3883
- [24] – Kennedy, J. A.; Powell, K. J. Polyphenol interactions with aluminium(III) and iron(III): their possible involvement in the podzolization process. *Aust. J. Chem.* 1985, 38, 879-888.
- [25] – Powell, H. K. J.; Rate, A. W. Aluminium-tannin equilibria: a potentiometric study. *Aust. J. Chem.* 1987, 40, 2015-2022.
- [26] – Slabbert, N. P. Mimosa-Al tannagessan alternative to chrome tanning. *J. Am. Leather Chem. Assoc.* 1981, 76, 231-244.
- [27] - Okuda, T.; Mori, K.; Shiota, M.; Ida, K. Effect of the interaction of tannins with coexisting substances. II. Reduction of heavy metal ions and solubilization of precipitates. *Yakugaku Zasshi* 1982, 102, 735-742.
- [28] – Mila, I.; Scalbert, A. Tannin antimicrobial properties through iron deprivation: a new hypothesis. *Acta Hort.* 1994, 381, 749-755.

- [29] - Scalbert, A.; Monties, B.; Janin, G. Tannins in wood: comparison of different estimation methods. *J. Agric. Food Chem.* 1989, 37, 1324-1329.
- [30] – Sampat, S. S.; Vora, J. C. Influence of colloids on the corrosion of 3S aluminium in low flow velocity water. *Indian J. Technol.* 1975, 13, 476.
- [31] – Seavell, A. J. Anticorrosive properties of mimosa (wattle) tannin. *J. Oil Col. Chem. Assoc.* 1978, 61, 439-462.
- [32] – Chang, C. W.; Anderson, J. U. Flocculation of clays and soils by organic compounds. *Soil Sci. Soc. Am. Proc.* 1968, 32, 23-27.
- [33] – Randall, J. M.; Bermann, R. L.; Garrett, V.; Waiss, A. C. J. Use of bark to remove heavy metal ions from waste solutions. *For. Prod. J.* 1974, 24, 80-84
- [34] – Meunier, L.; Vaney, C. *La Tannerie*; Gauthier-Villars: Paris, 1903.
- [35] – Grimshaw, J. Phenolic aralkylamines, monohydric alcohols, monocarbaldehydes, monoketones and monocarboxylic acids. In *Rodd's Chemistry*, 2nd ed.; Coffey, S., Ed.; Elsevier: Amsterdam, 1976; pp 141-202
- [36] - Gray, V. E. The acidity of wood. *J. Inst. Wood Sci.* 1958, 1, 58-64
- [37] - Aplincourt, M.; Bee, A.; Gerard, C.; Hugel, R. P.; Njomgang, R.; Prudhomme, J.-C. Modelling of the interactions of metal cations with soil organic matter. Part 3. Thermodynamic stability of copper(II) and iron(III) complexes with 3,4- dihydroxybenzoic acid. *J. Chem. Res. (S)* 1987, 398-399.
- [38] – W.M. Lee, US Patent 6,276,372 (2000).
- [39] – W. Zhang, Q. Zhang, F.B. Ma, J.G. Zhu, J. Guizhou, Univ. Technol. *Nat. Sci. Ed.* 29 (2000), 70–74.
- [40] – Z.H. Zhang, C.M. Zhong, J.L. Huang, Q. Qing, H. Xu, CN Patent 1,887,842 (2007).
- [41] – M.J. Hynes, M.O. Coinceanainn, *J. Inorg. Biochem.* 85 (2001) 131–142.
- [42] – S.A. Kazmi, M.S. Qureshi, Z. Maqsood, *Inorg. Chim. Acta* 137 (1987) 151–154.
- [43] - H.K.J. Powell, M.C. Taylor, *Aust. J. Chem.* 35 (1982) 739–756.
- [44] – Kochian, L. V.; Pineros, M. A.; Liu, J. P.; Magalhaes, J. V. Plant adaptation to acid soils: The molecular basis for crop aluminum ̀resistance. *Annu. Rev. Plant Biol.* 2015, 66, 571–598.
- [45] – von Uexkull, H. R.; Mutert, E. Global extent, development and economic impact of acid soils. *Plant Soil* 1995, 171, 1–15.
- [46] – Poschenrieder, C.; Gunse, B.; Corrales, I.; Barcelo, J. A glance into aluminum toxicity and resistance in plants. *Sci. Total Environ.* 2008, 400, 356–368.

- [47] – Tolra, R. P.; Poschenrieder, C.; Luppi, B.; Barcelo, J. Aluminium-induced changes in the profiles of both organic acids and phenolic substances underlie Al tolerance in *Rumex acetosa* L. *Environ. Exp. Bot.* 2005, 54, 231–238.
- [48] – Ofei-Manu, P.; Wagatsuma, T.; Ishikawa, S.; Tawarayama, K. The plasma membrane strength of the root-tip cells and root phenolic compounds are correlated with Al tolerance in several common woody plants. *Soil Sci. Plant Nutr.* 2001, 47, 359–375.
- [49] – Ikka, T.; Ogawa, T.; Li, D.; Hiradate, S.; Morita, A. Effect of aluminum on metabolism of organic acids and chemical forms of aluminum in root tips of *Eucalyptus camaldulensis* Dehnh. *Phytochemistry* 2013, 94, 142–147.
- [50] – Niemetz, R.; Gross, G. G. Oxidation of pentagalloylglucose to the ellagitannin, tellimagrandin II, by a phenol oxidase from *Tellima grandiflora* leaves. *Phytochemistry* 2003, 62, 301–306.
- [51] - Salminen, J.-P.; Karonen, M. Chemical ecology of tannins and other phenolics: We need a change in approach. *Funct. Ecol.* 2011, 25, 325–338.
- [52] – Likussar, W.; Boltz, D. F. Theory of continuous variations plots and a new method for spectrophotometric determination of extraction and formation constants. *Anal. Chem.* 1971, 43, 1265–1272.
- [53] - Tahara, K.; Hashida, K.; Otsuka, Y.; Ohara, S.; Kojima, K.; Shinohara, K. Identification of a hydrolyzable tannin, oenothetin B, as an aluminum-detoxifying ligand in a highly aluminum-resistant tree, *Eucalyptus camaldulensis*. *Plant Physiol.* 2014, 164, 683–693.
- [54] - S. Mekahlia a, B. Bouzid b, Chitosan-Copper (II) complex as antibacterial agent: synthesis, characterization and coordinating bond- activity correlation study, a Département de chimie, Faculté des sciences, Université Saad Dahlab de Blida, BP 270-09000, Blida. Algérie. b Département de chimie industrielle, Faculté des sciences de l'ingénieur, Université Saad Dahlab de Blida, BP 270-09000, Blida. Algérie.
- [55] - Arianna Riccia, Kenneth J. Olejarb, Giuseppina P. Parpinelloa, Paul A. Kilmartinb & Andrea Versaria a Department of Agricultural and Food Sciences, University of Bologna, Piazza Goidanich, 60, 47521 Cesena (FC), Italy. b Department of Chemistry, The University of Auckland, Private Bag 92019, Auckland, New Zealand., Application of Fourier Transform Infrared (FTIR) Spectroscopy in the Characterization of Tannins
- [56] - Khalid, M. N., Agnely, F., Yagoubi, N., Grossiord, J. L., & Courrazze, G. (2002). Water state characterization, swelling behavior, thermal and mechanical properties of chitosan-based networks. *European Journal of Pharmaceutical Sciences*, 15, 425–432
- [57] - Claudia A. Caroa, Gerardo Cabelloa, Esteban Landaetab, Jerónimo Péreza, Miguelina Gonzáleza, José H. Zagalc & Luis Lilloa a Facultad de Ciencias, Departamento de Ciencias Básicas, Universidad del Bío-Bío, Chillán, Chile b Facultad de Química, Departamento de Química Inorgánica 2, Pontificia Universidad Católica de Chile, Santiago, Chile c Facultad de Química y Biología, Departamento de Química de los Materiales, Universidad de Santiago de Chile, Santiago, Chile, Preparation, spectroscopic, and electrochemical characterization of metal(II) complexes with Schiff base ligands derived from chitosan: correlations of redox potentials with Hammett parameters

[58] - <https://paramedicsworld.com/biochemistry-practicals/demonstration-of-spectrophotometer-principle-components-working-applications/medical-paramedical-studynotes>

[59] - Zofia Modrzejewskaa,, Grzegorz Rogackia, Witold Sujkaa, Roman Zarzyckib a Lodz University of Technology Faculty of Process and Environmental Engineering, 90-924 Lodz, Wolczanska 213, Poland b Higher Vocational State School of President Stanislaw Wojciechowski in Kalisz, 62-800 Kalisz Nowy Swiat 4, Poland, Sorption of copper by chitosan hydrogel: Kinetics and equilibrium

[60] - Zhaoxuan Feng, Minna Hakkarainen, Hansjörg Grützmacher, Annalisa Chiappone, and Marco Sangermano, Photocrosslinked Chitosan Hydrogels Reinforced with Chitosan-Derived Nano-Graphene Oxide

[61] - Hailong Fan, Jiahui Wang, Qiuya Zhang, and Zhaoxia Jin, Department of Chemistry, Renmin University of China, No. 59 Zhongguancun Street, Haidian District, Beijing 100872, P. R. China, Tannic Acid-Based Multifunctional Hydrogels with Facile Adjustable Adhesion and Cohesion Contributed by Polyphenol Supramolecular Chemistry

## 8 – RINGRAZIAMENTI

Ringrazio i miei genitori e tutta la mia famiglia, per avermi sempre sostenuto nel mio percorso e nella mia scelta. Ringrazio il professor Marco Sangermano, la professoressa Silvia Maria Spriano, Sara Ferraris, Camilla Noè e Rossella Sesia per avermi supportato e affiancato nel mio lavoro di Tesi Magistrale. Ringrazio tutti i miei amici, e tutti coloro che in questi anni hanno condiviso con me questo percorso universitario.